BUKS2018

Large-amplitude prominence oscillations: observations & numerical simulations

Qingmin Zhang

zhangqm@pmo.ac.cn

Purple Mountain Observatory

Y. N. Su, Z. J. Ning, H. S. Ji, D. Li
(Purple Mountain Observatory)
P. F. Chen (Nanjing University)
C. Xia (Yunnan University)
R. Keppens (KU Leuven)
T. Li (National Astronomical Observatories)
R. S. Zheng (Shandong University)

La Laguna, Tenerife, Spain, from 3 to 7 September, 2018

Outline

- background
- *Part 1:* **Longitudinal oscillations of an active region prominence**
  (Zhang et al. 2012 A&A 542, A52)
- *Part 2:* **Parameter survey of longitudinal prominence oscillation simulations**
  (Zhang et al. 2013 A&A 554, A124)
- *Part 3:* **Large-amplitude Longitudinal Filament oscillations with Mass Drainage**
  (Zhang et al. 2017 ApJ 842, 27)
- *Part 4:* **Simultaneous Transverse and Longitudinal Oscillations in a Quiescent Prominence Triggered by a Coronal Jet**
  (Zhang et al. 2017 ApJ 851, 47)
- *Part 5:* **Vertical Oscillation of a Coronal Cavity Triggered by an EUV Wave**
  (Zhang & Ji 2018 ApJ 860, 113)
- summary and outlook

filament/prominence

thin, dark threads along PIL
Ca II H, Ha and EUV wavelengths
QR, AR, Polar crown filament
suspended by magnetic tension force
sheared arcade or magnetic flux rope
normal polarity or inverse polarity
chirality: sinistral or dextral
(Mackay et al. 2010;
Labrosse et al. 2010; Parenti 2014)

T: 0.01 MK
n_e: 1.0e+11 cm^(-3)

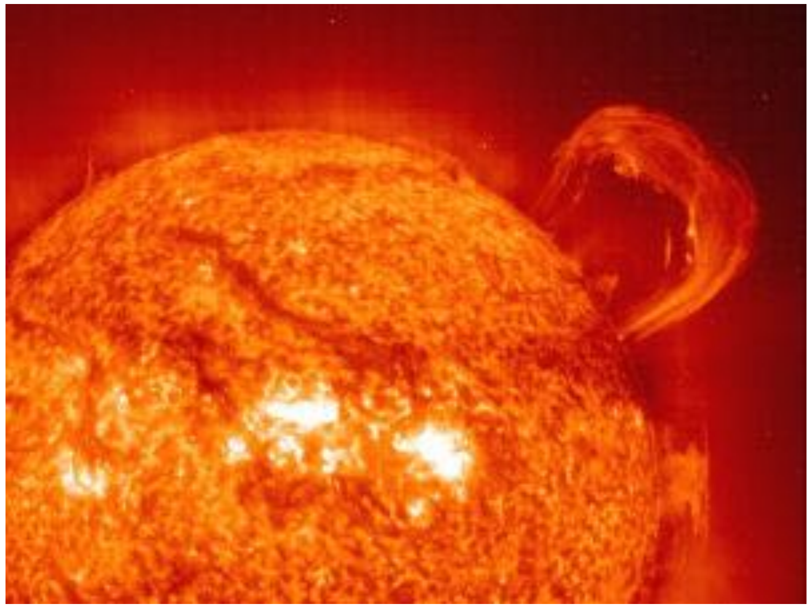

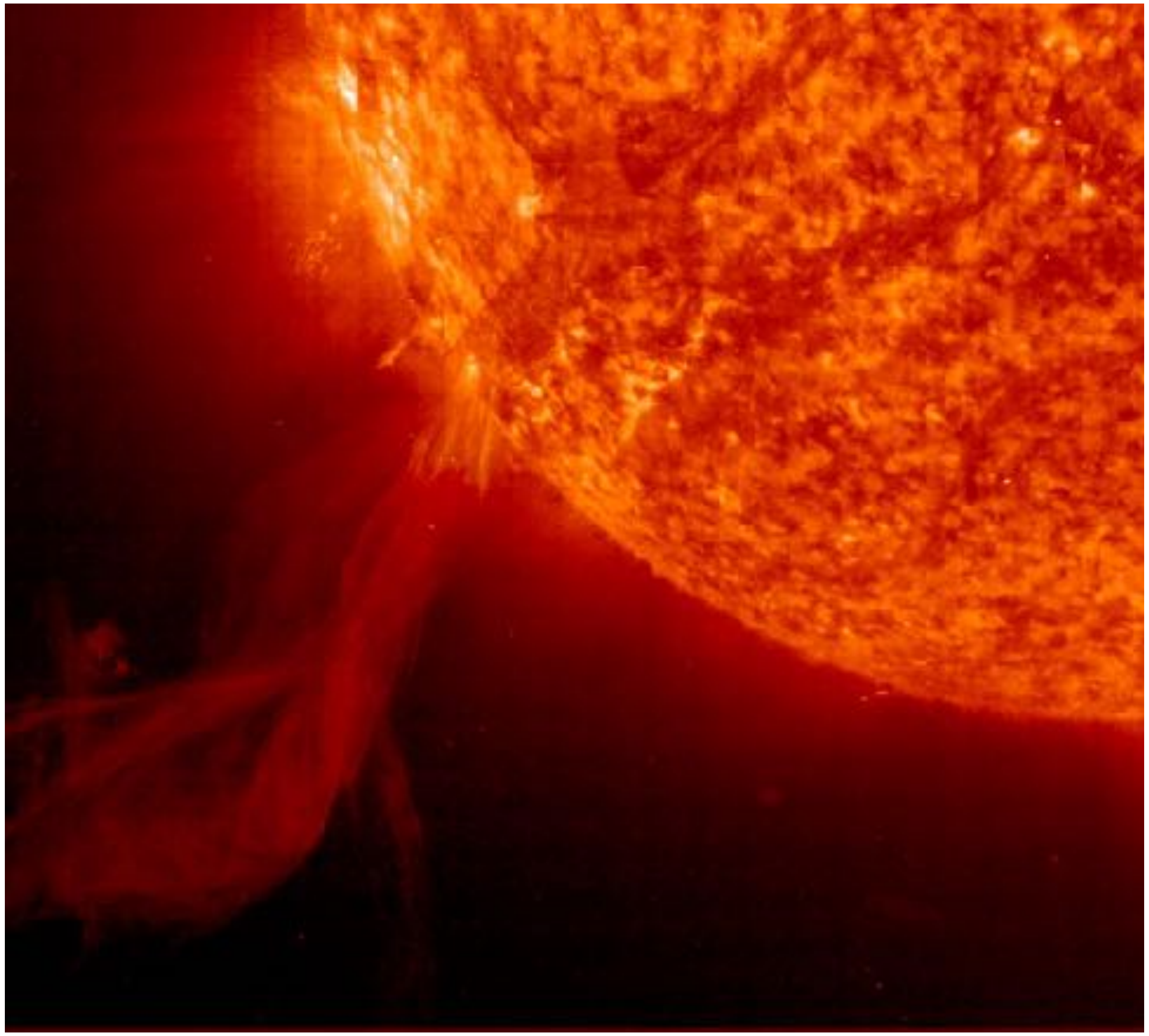

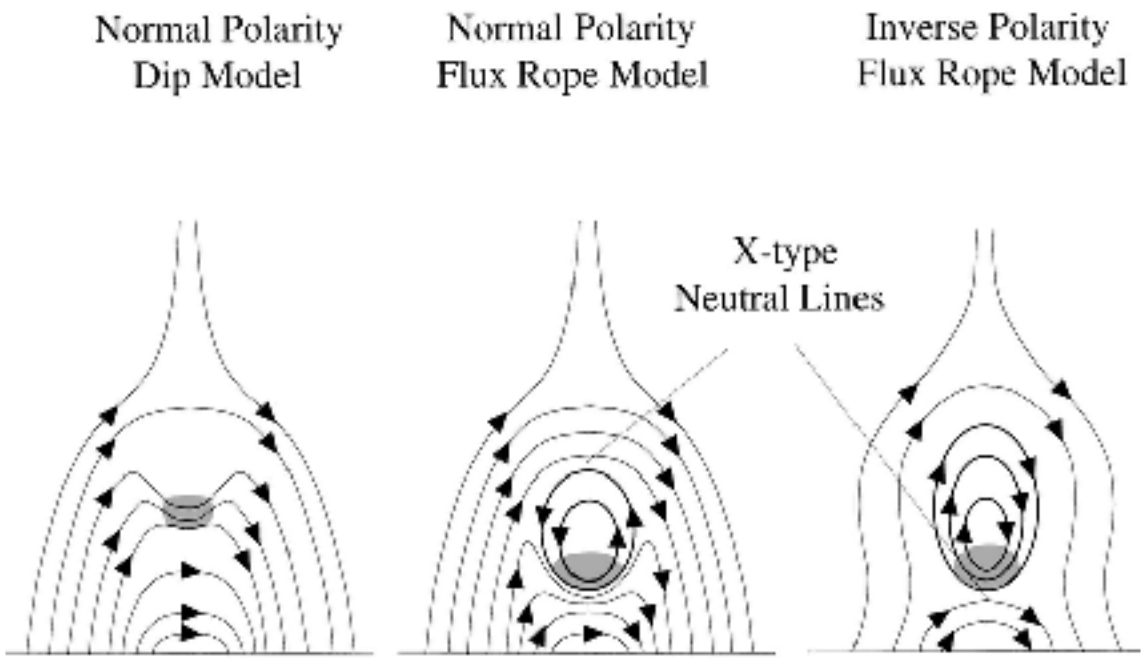

filament oscillation in different directions

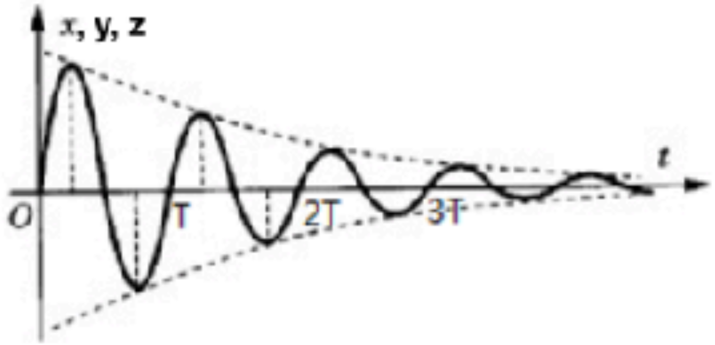

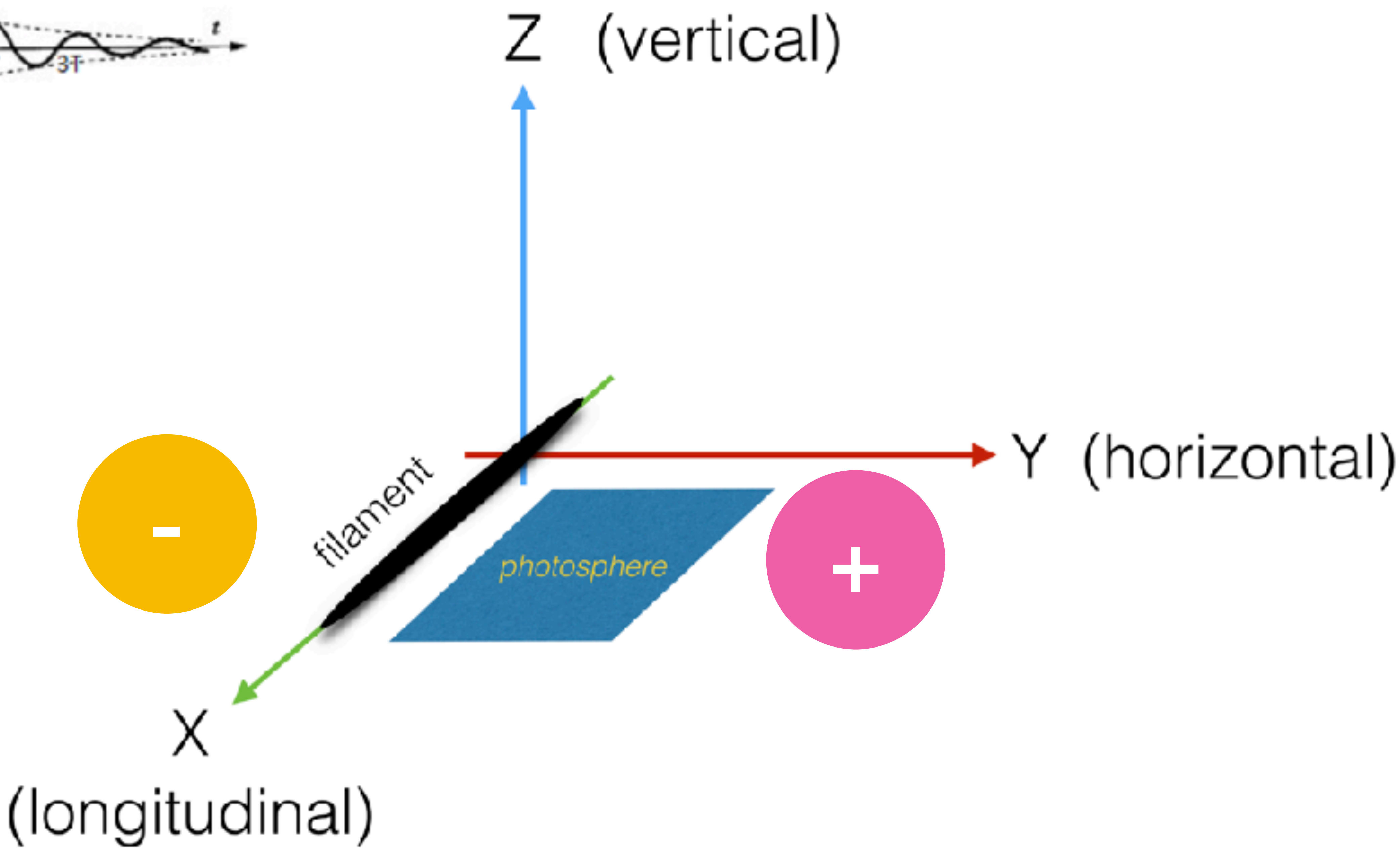

vertical filament oscillation

Ramsey & Smith 1966

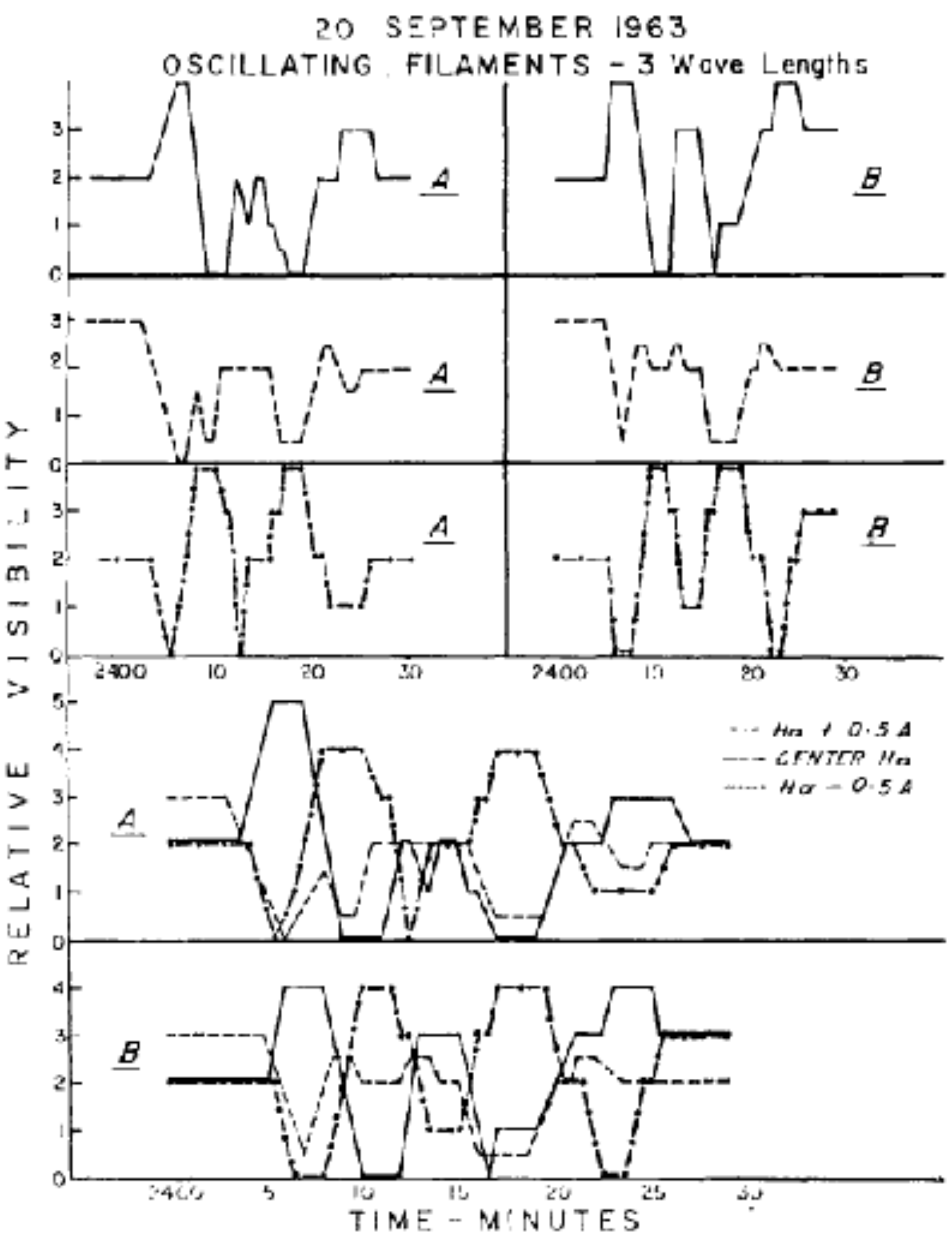

"winking filament"

Eto et al. 2002

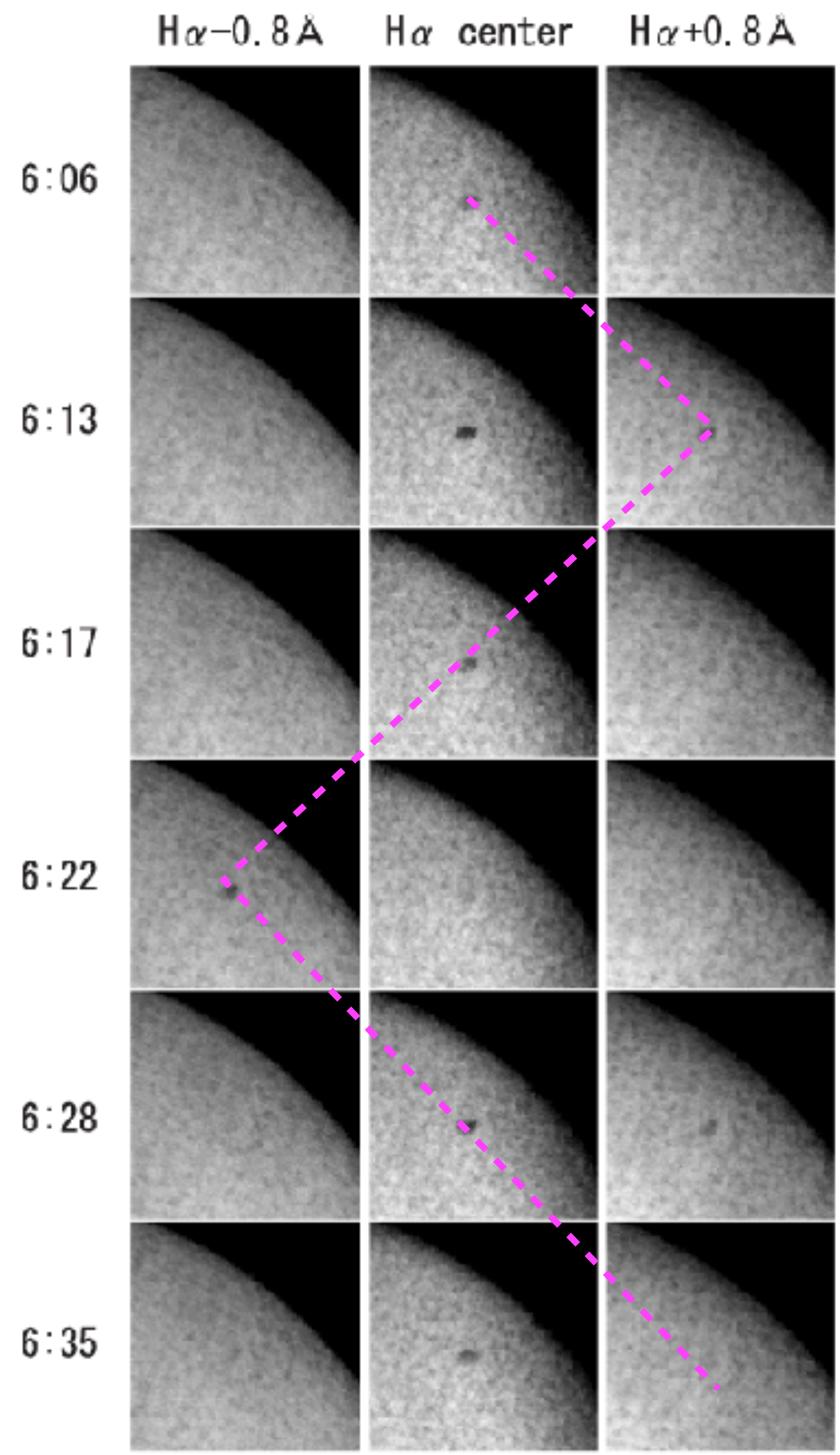

vertical filament oscillation

Ramsey & Smith 1966

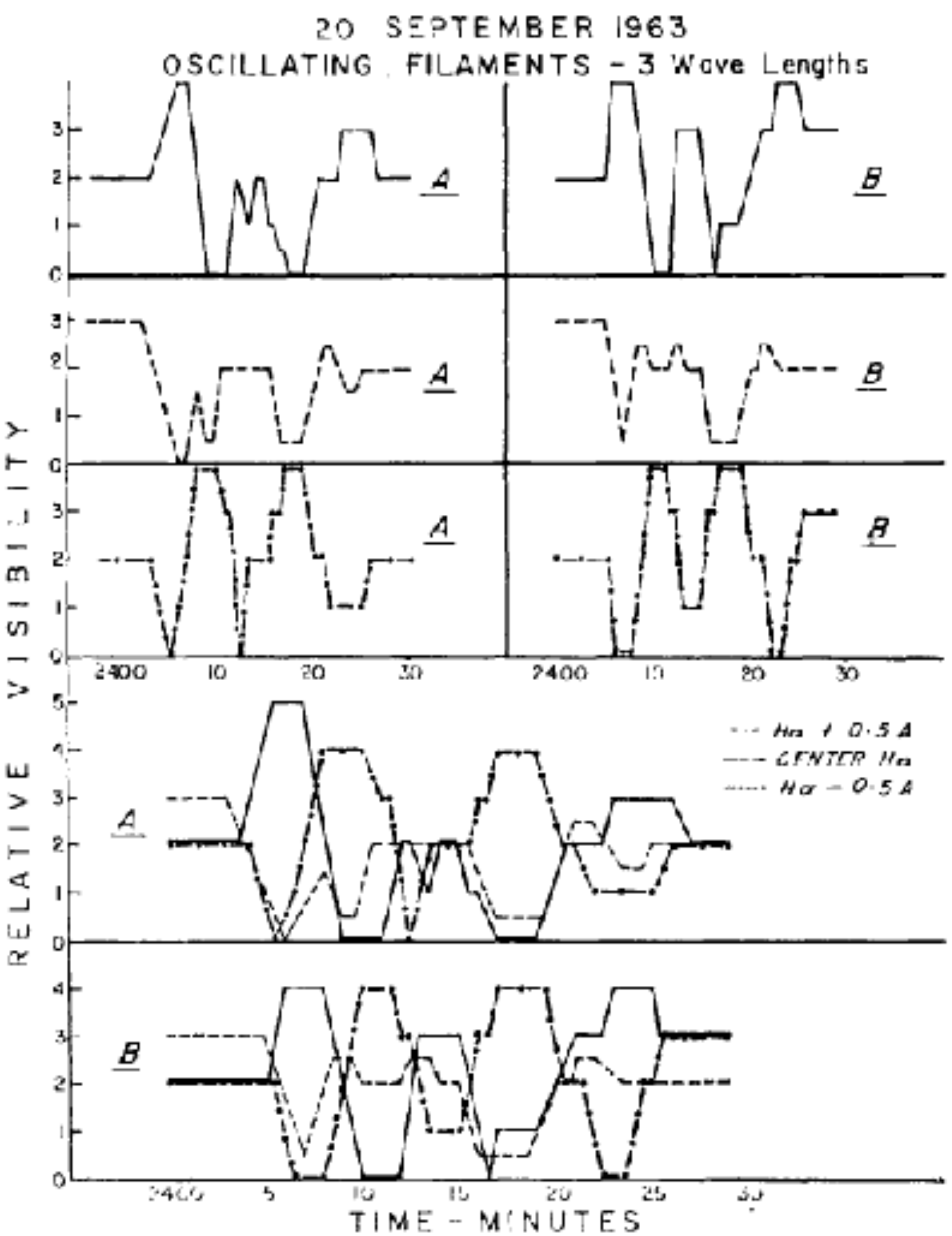

"winking filament"

Eto et al. 2002

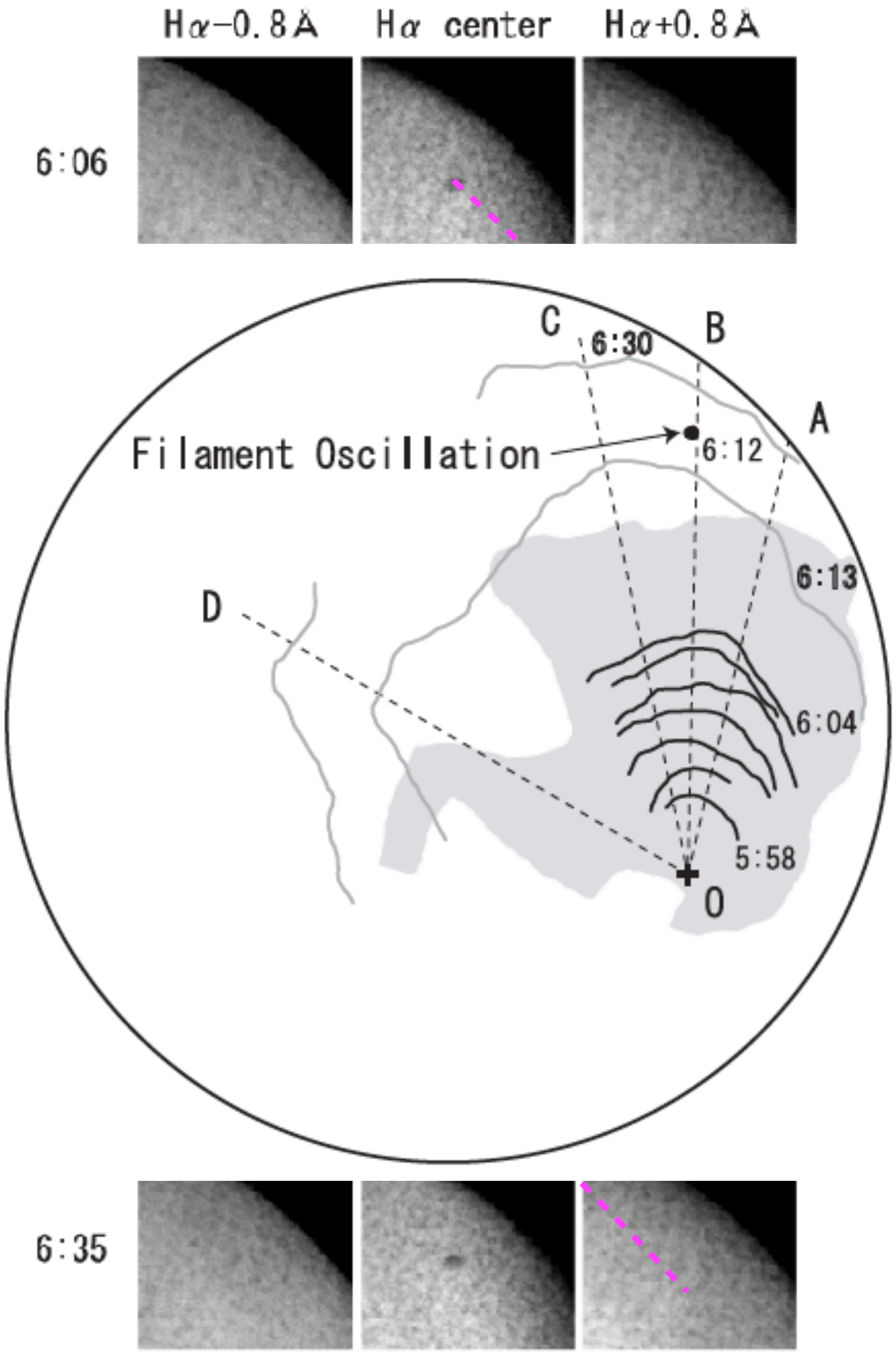

vertical filament oscillation

Ramsey & Smith 1966

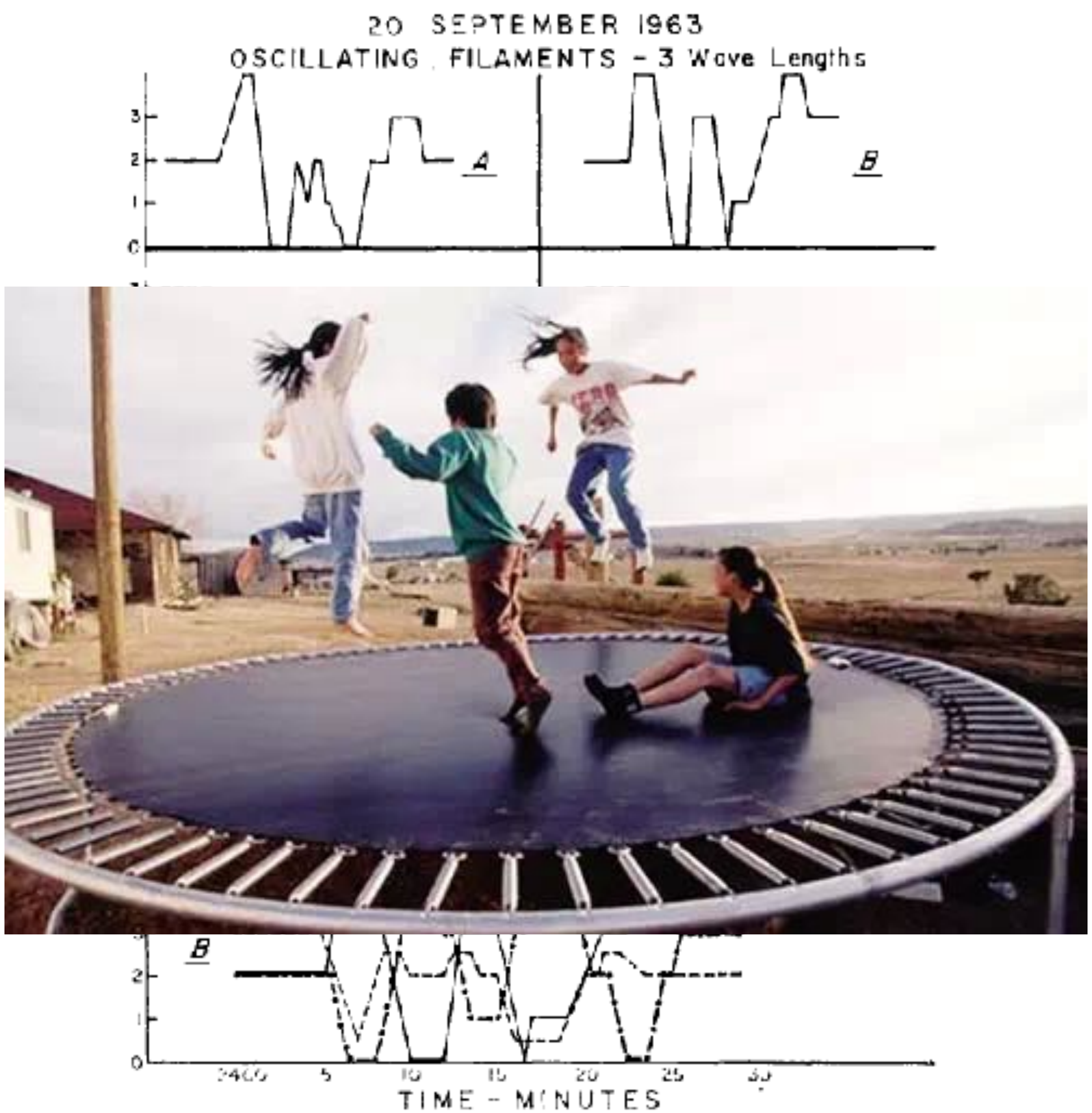

“winking filament”

Eto et al. 2002

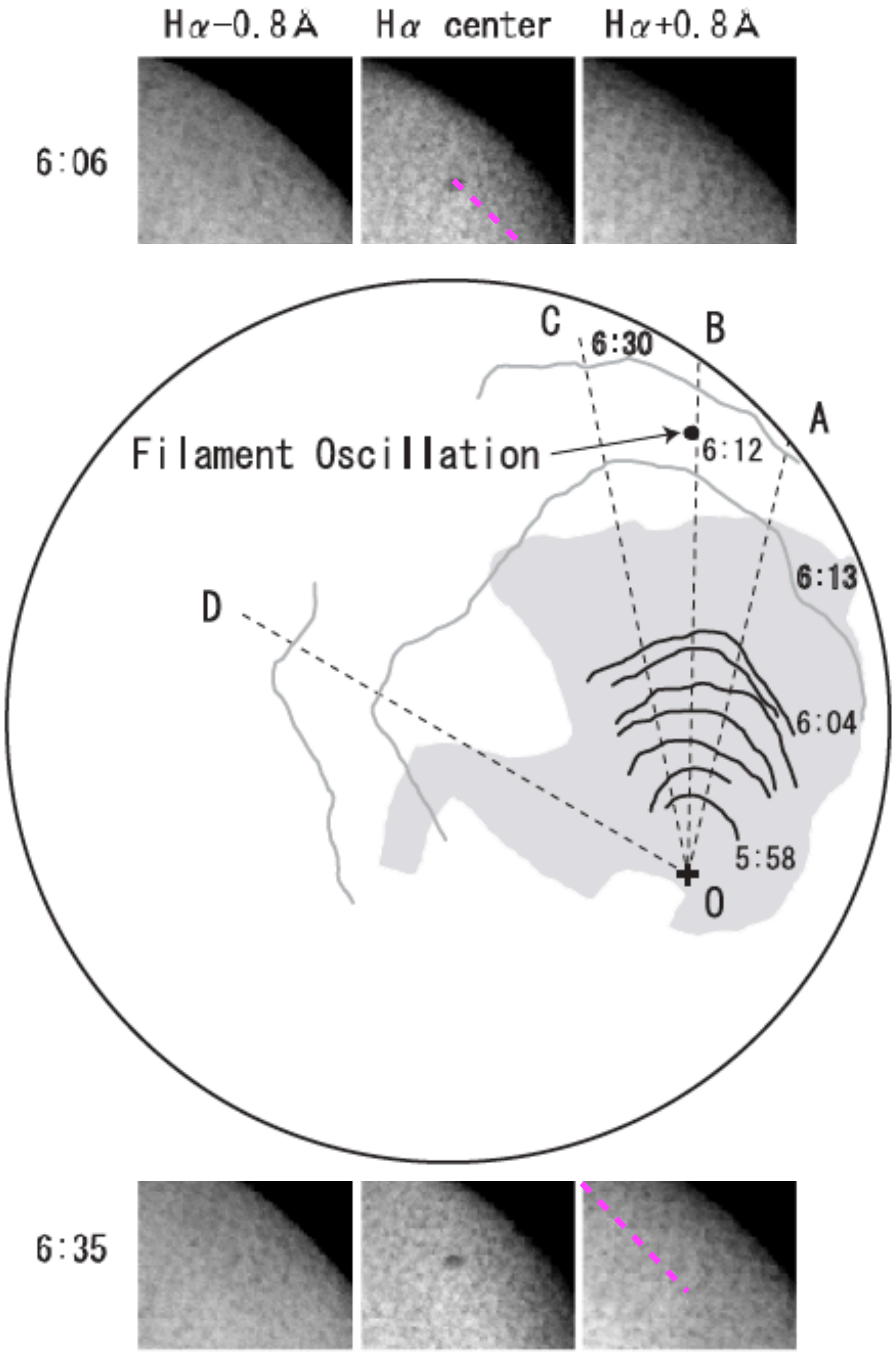

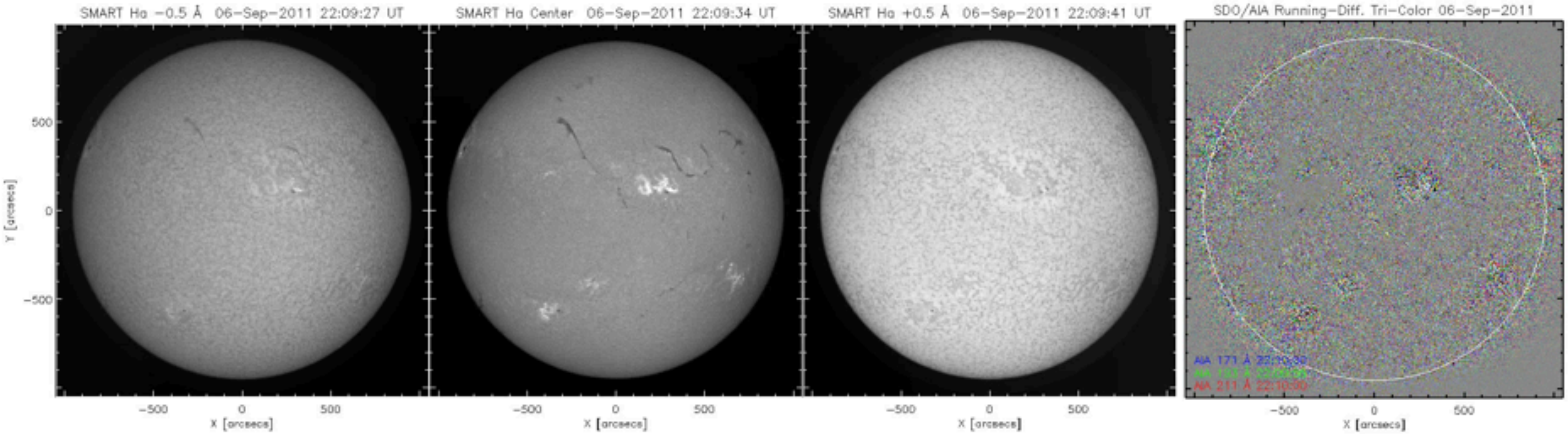

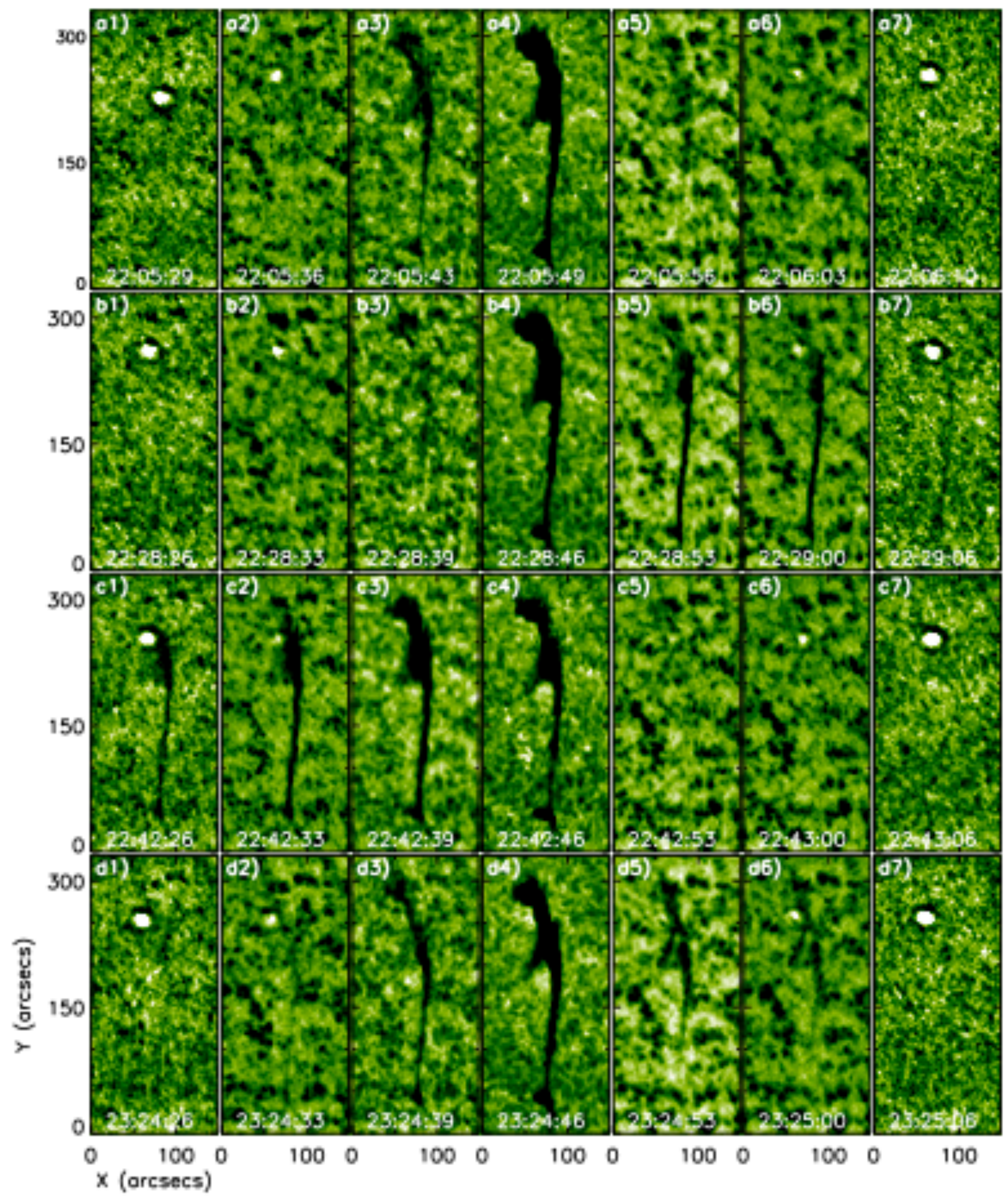

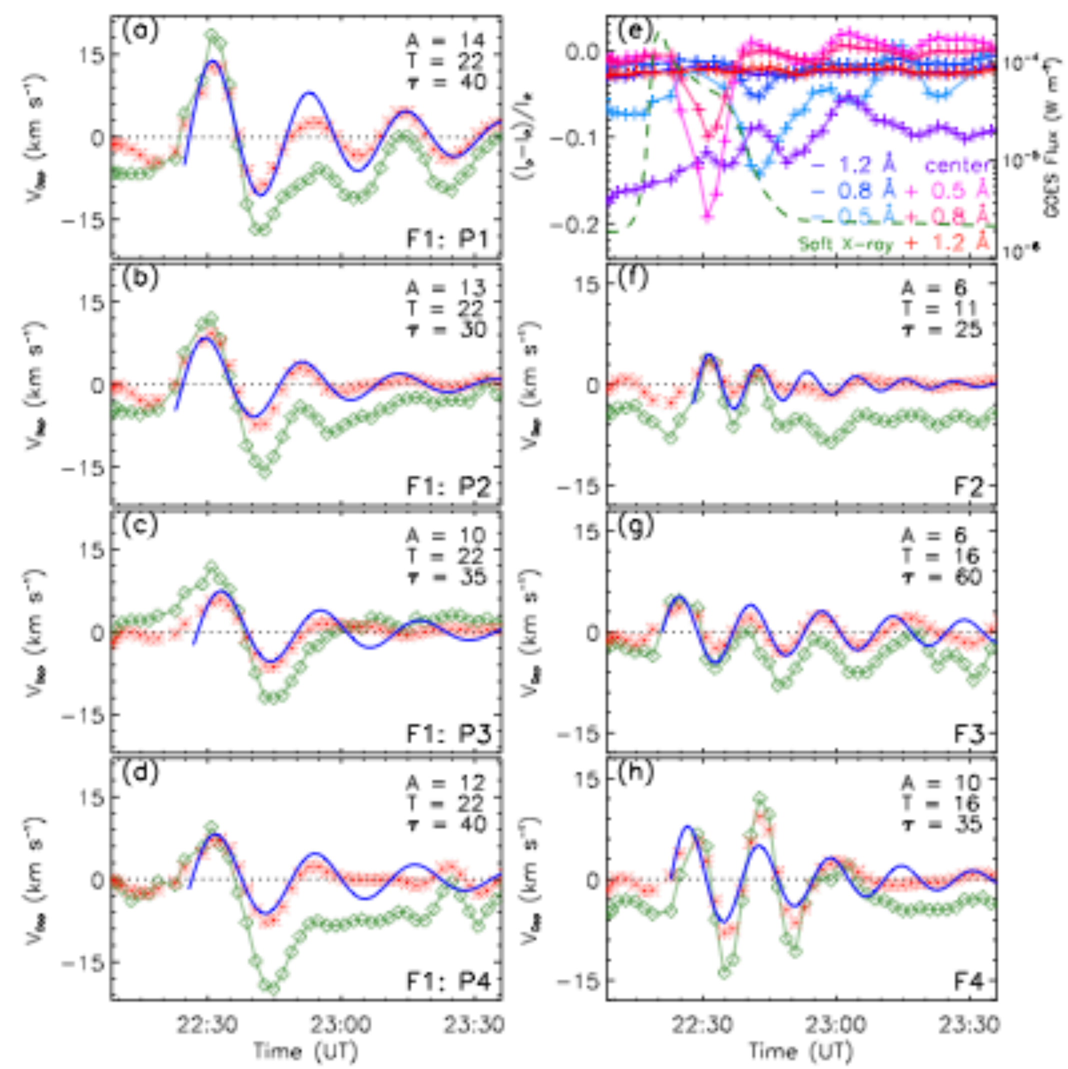

Consecutive filament oscillations caused by an EUV wave.==>EUV waves can be a good agent for trigger sympathetic solar activities **Shen et al. 2014a**

horizontal filament oscillation

Isobe & Tripathi 2006

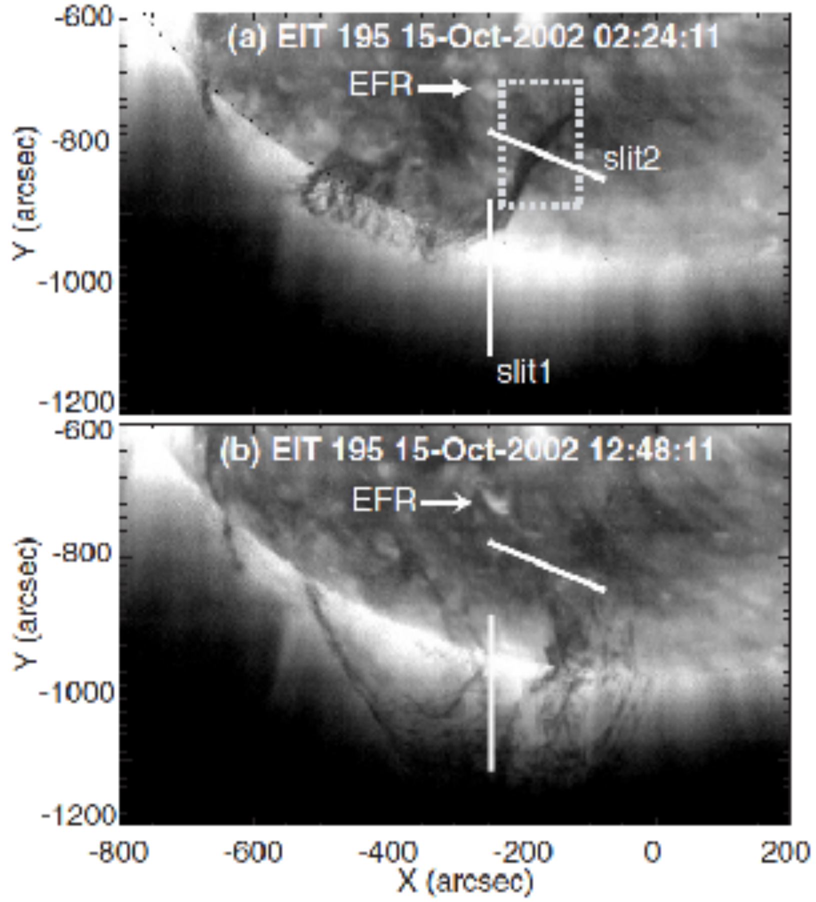

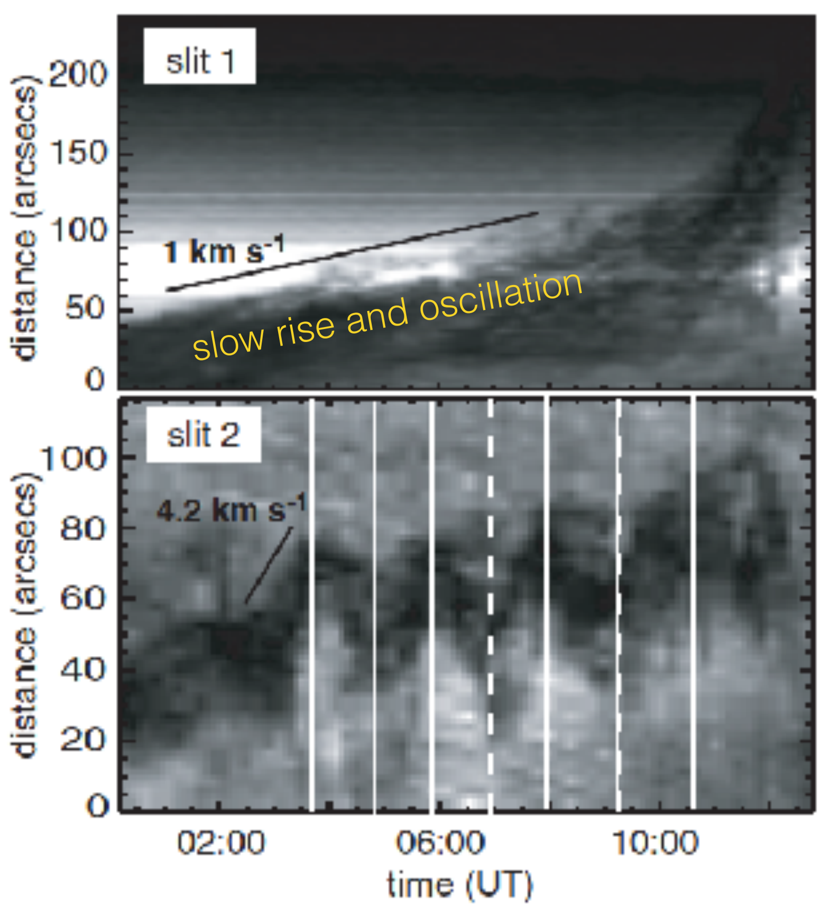

Chen et al. 2008

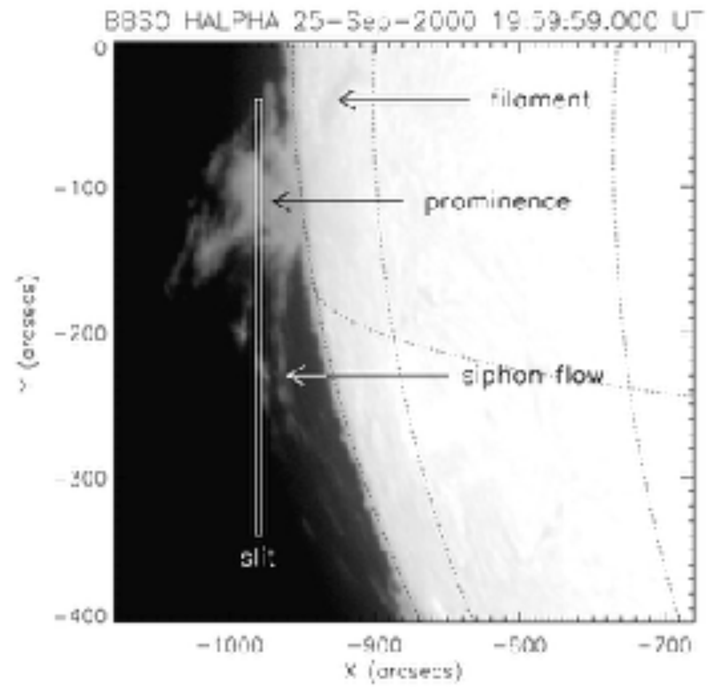

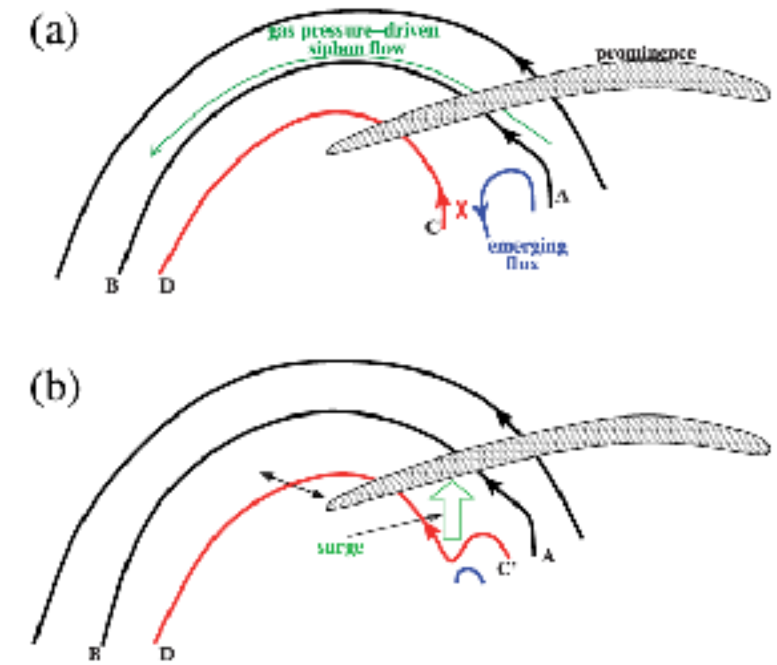

SOHO/SUMER

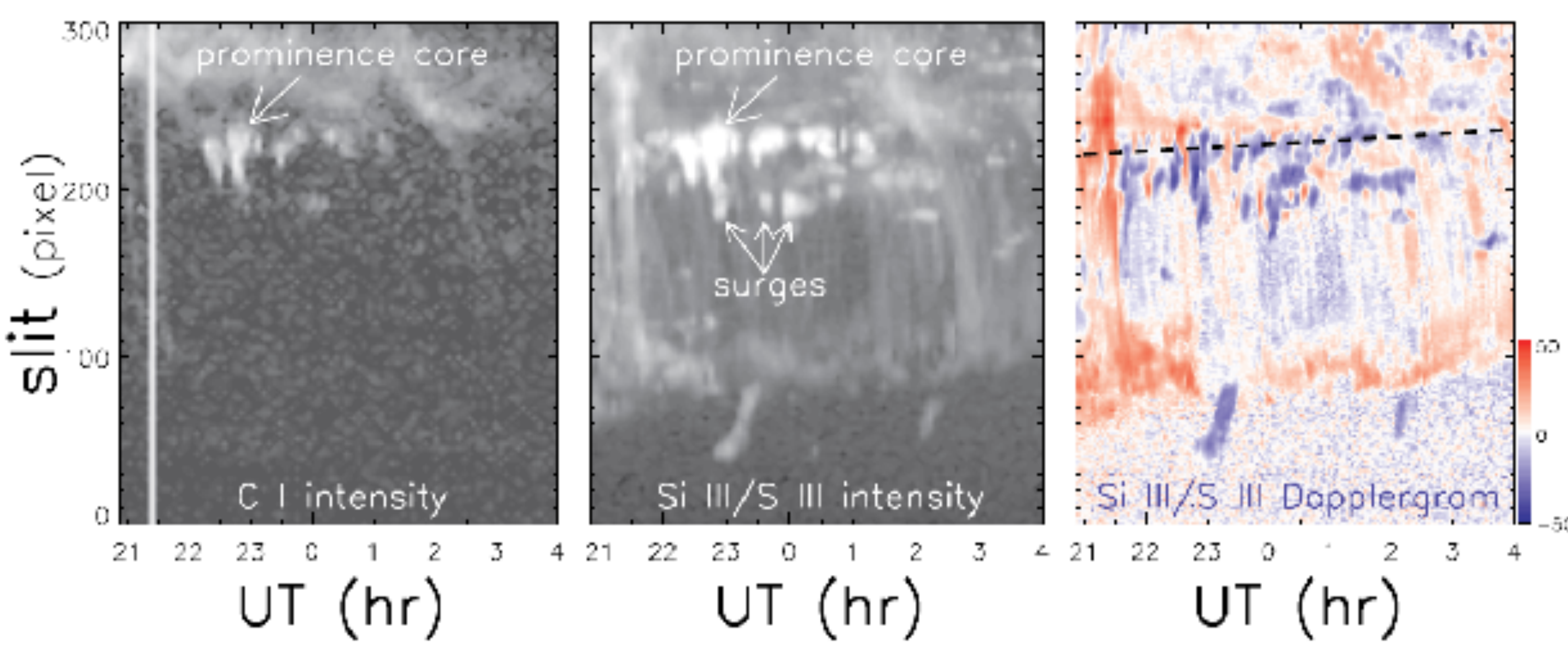

Isobe & Tripathi 2006

horizontal filament oscillation

Chen et al. 2008

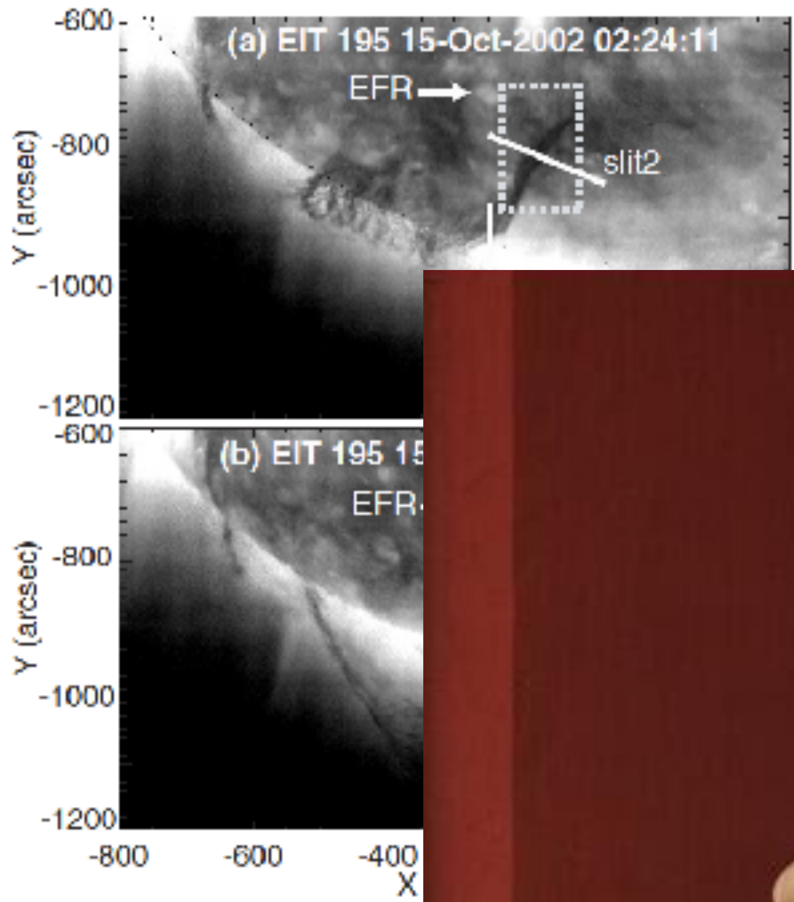

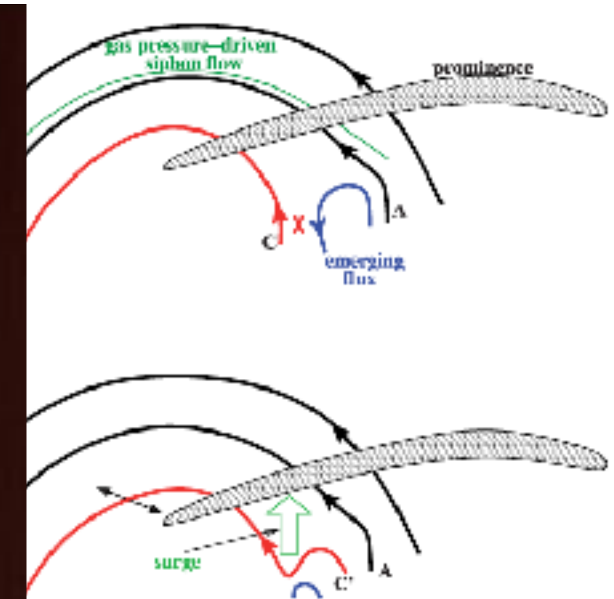

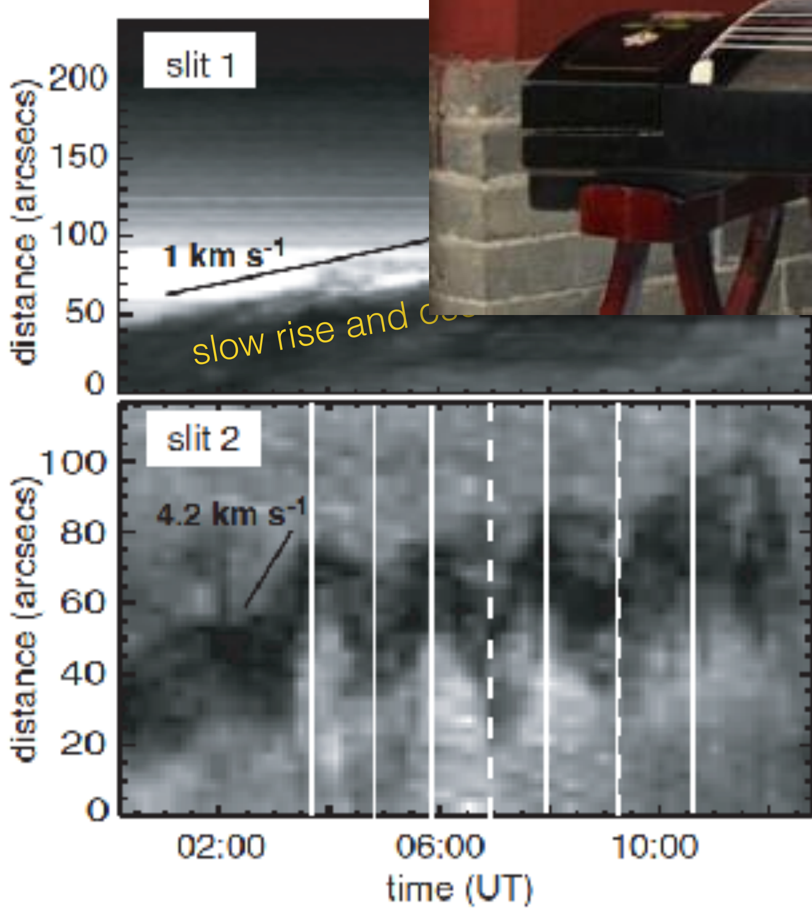

SOHO/SUMER

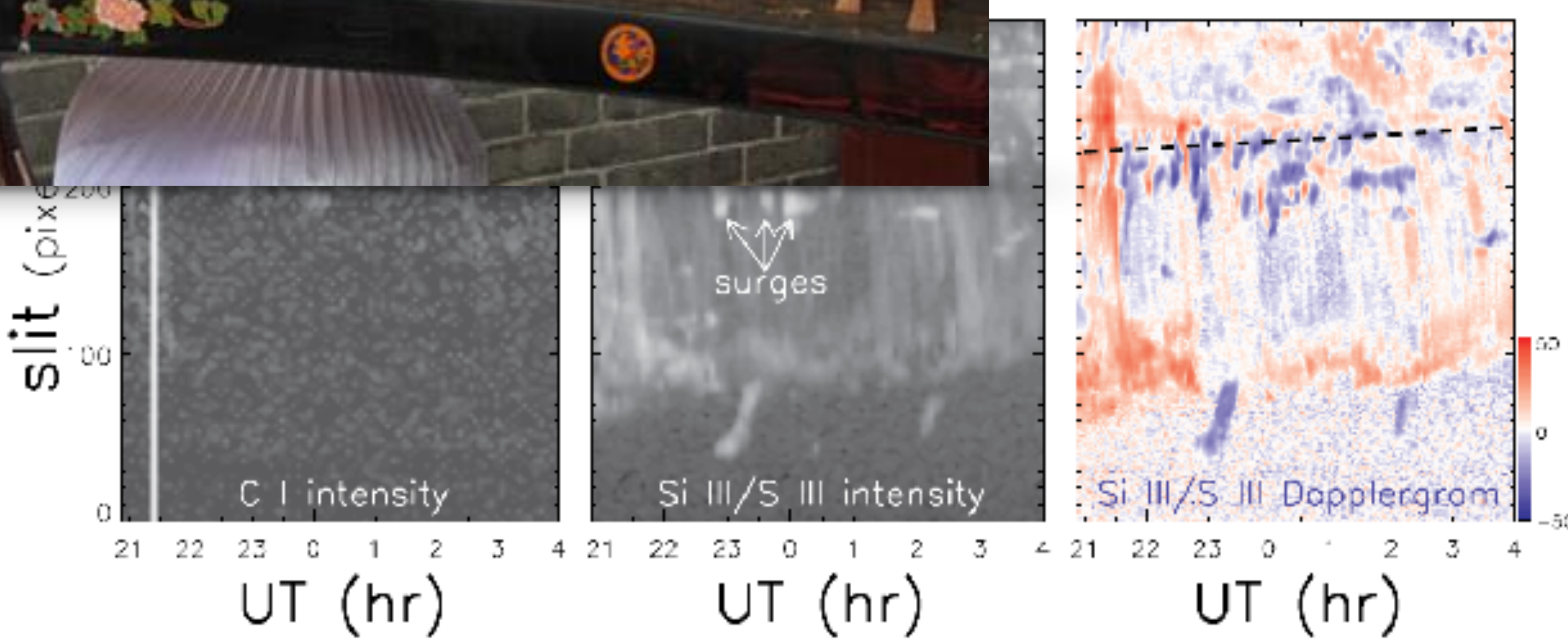

longitudinal filament oscillation

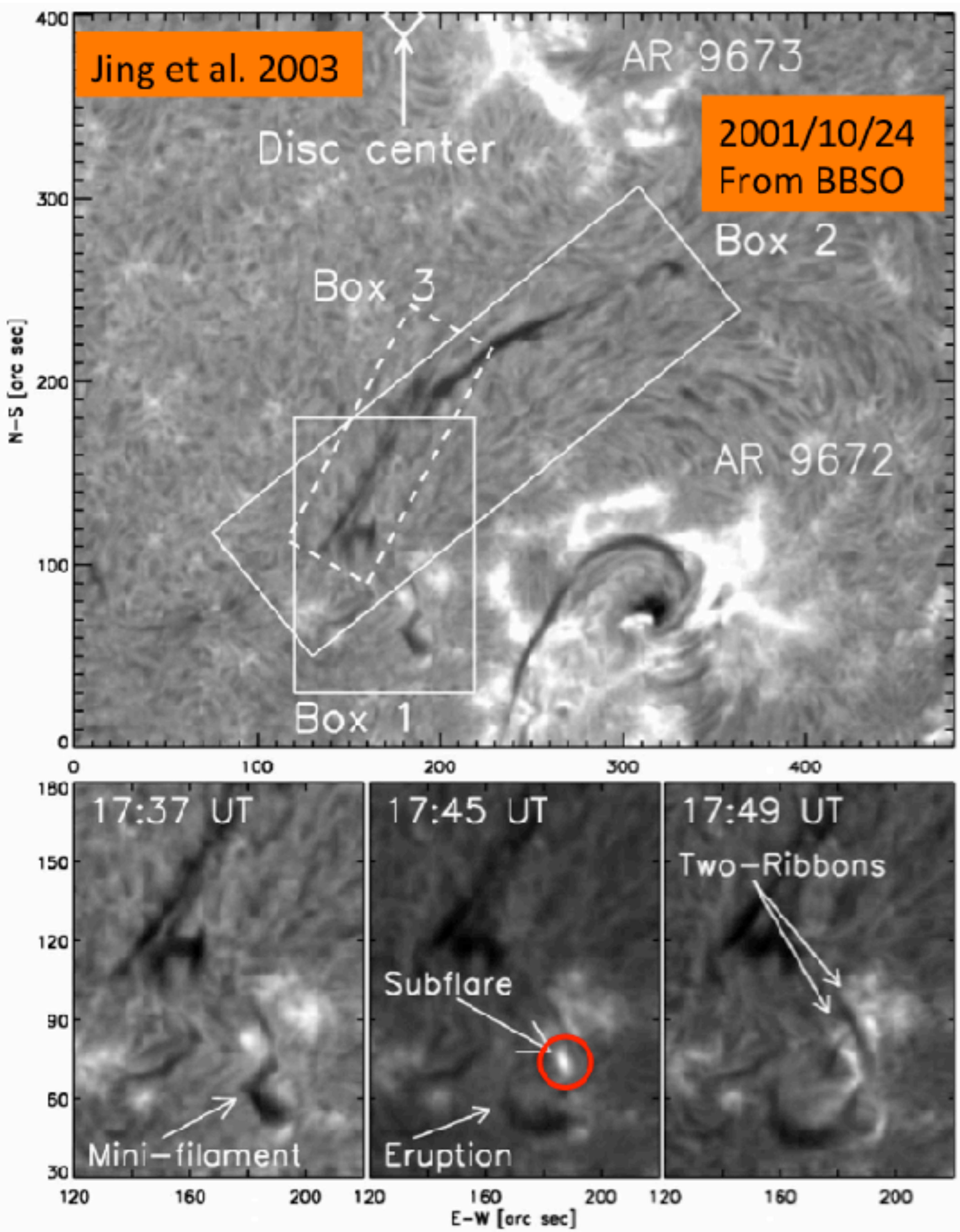

Large-amplitude, damping, longitudinal filament oscillation triggered by subflare

P~80 min
Tau~210 min
V_0~92 km/s

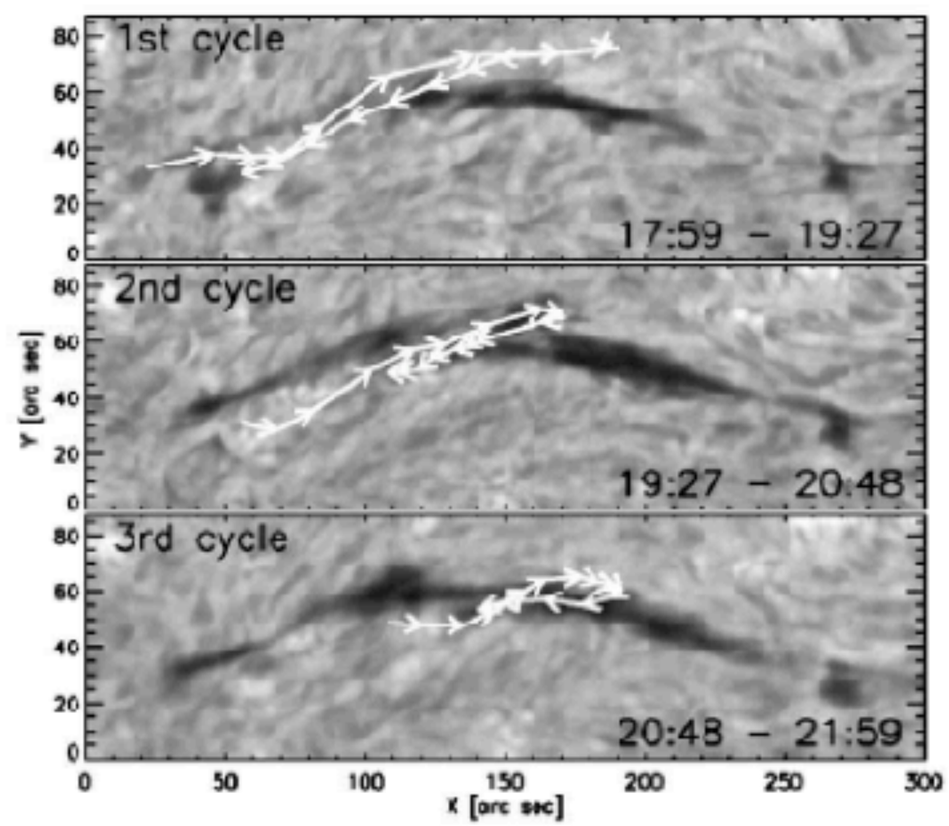

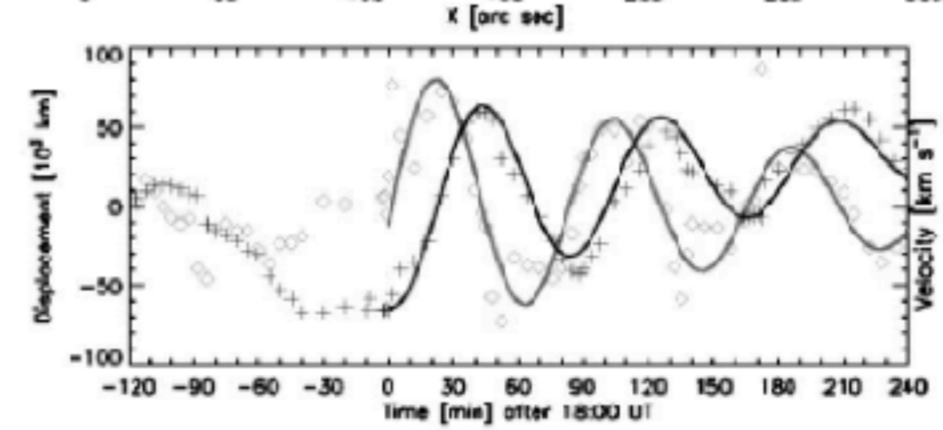

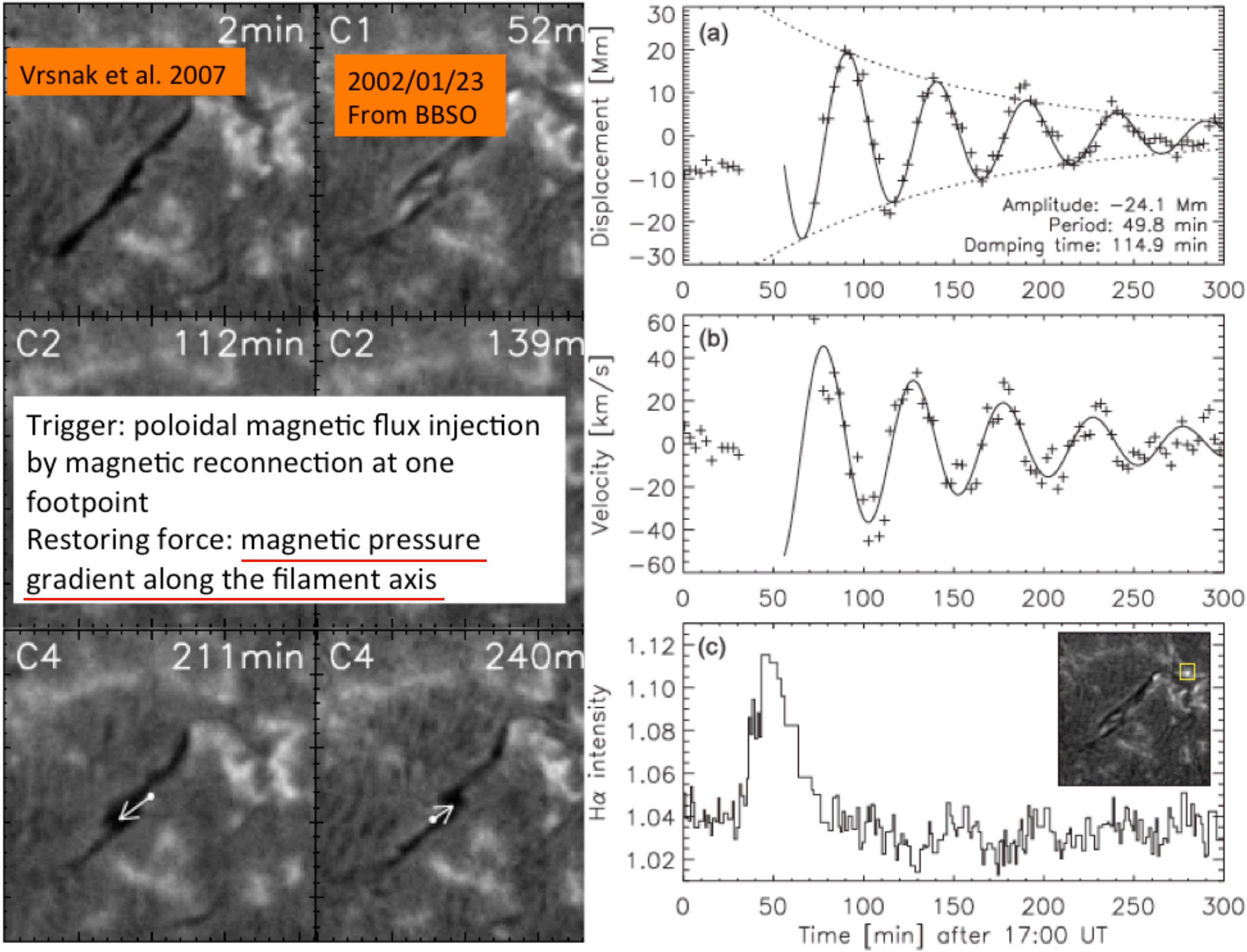

Vrsnak et al. 2007
2002/01/23
From BBSO
2min
C1 52m
C2 112min
C2 139m
C4 211min
C4 240m
Trigger: poloidal magnetic flux injection by magnetic reconnection at one footpoint
Restoring force: magnetic pressure gradient along the filament axis
(a)
Displacement [Mm]
Amplitude: −24.1 Mm
Period: 49.8 min
Damping time: 114.9 min
(b)
Velocity [km/s]
(c)
Hα intensity
Time [min] after 17:00 UT

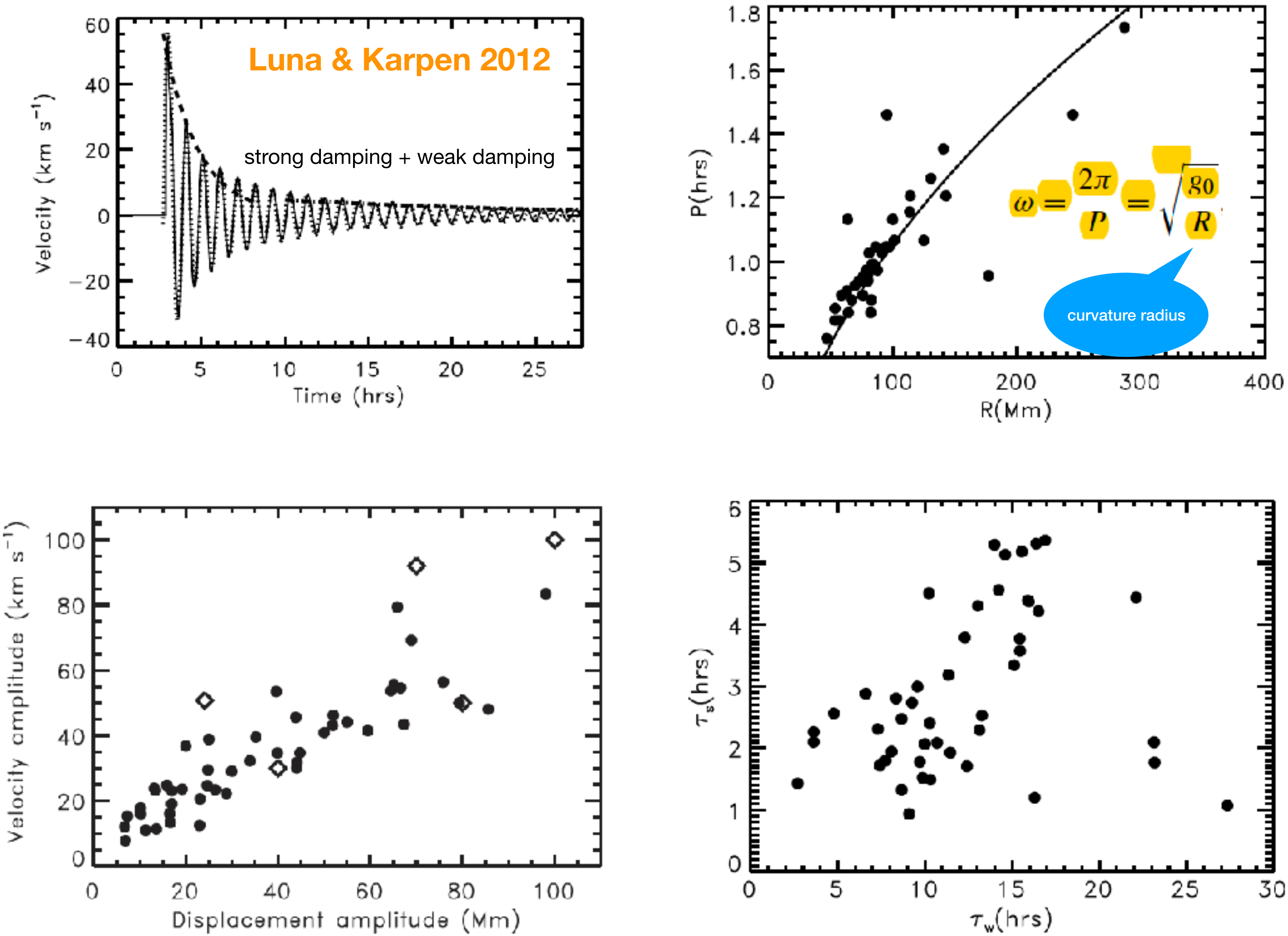
Luna & Karpen 2012
strong damping + weak damping
Velocity (km s^{-1})
Time (hrs)
P(hrs)
R(Mm)
$\omega = \frac{2\pi}{P} = \sqrt{\frac{g_0}{R}}$
curvature radius
Velocity amplitude (km s^{-1})
Displacement amplitude (Mm)
τ_s(hrs)
τ_w(hrs)

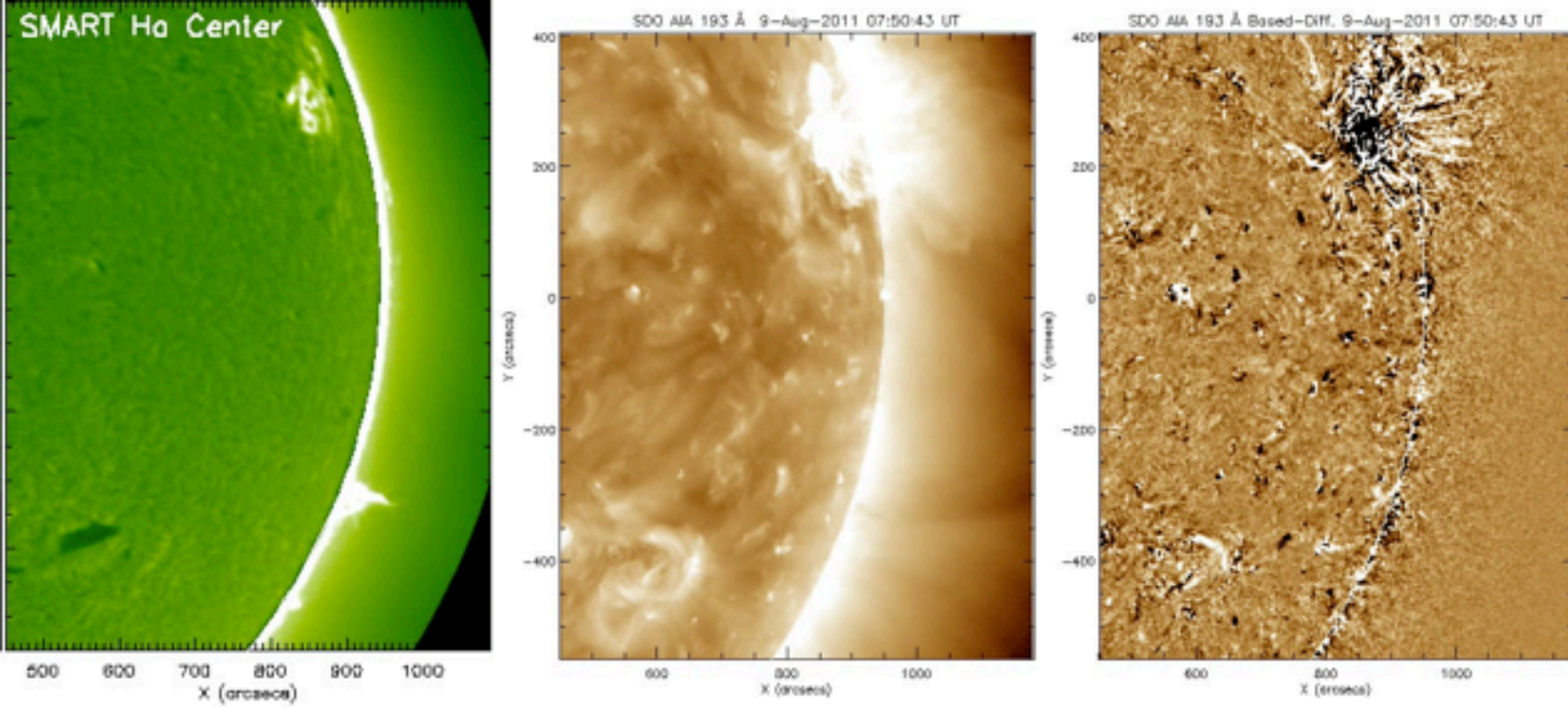

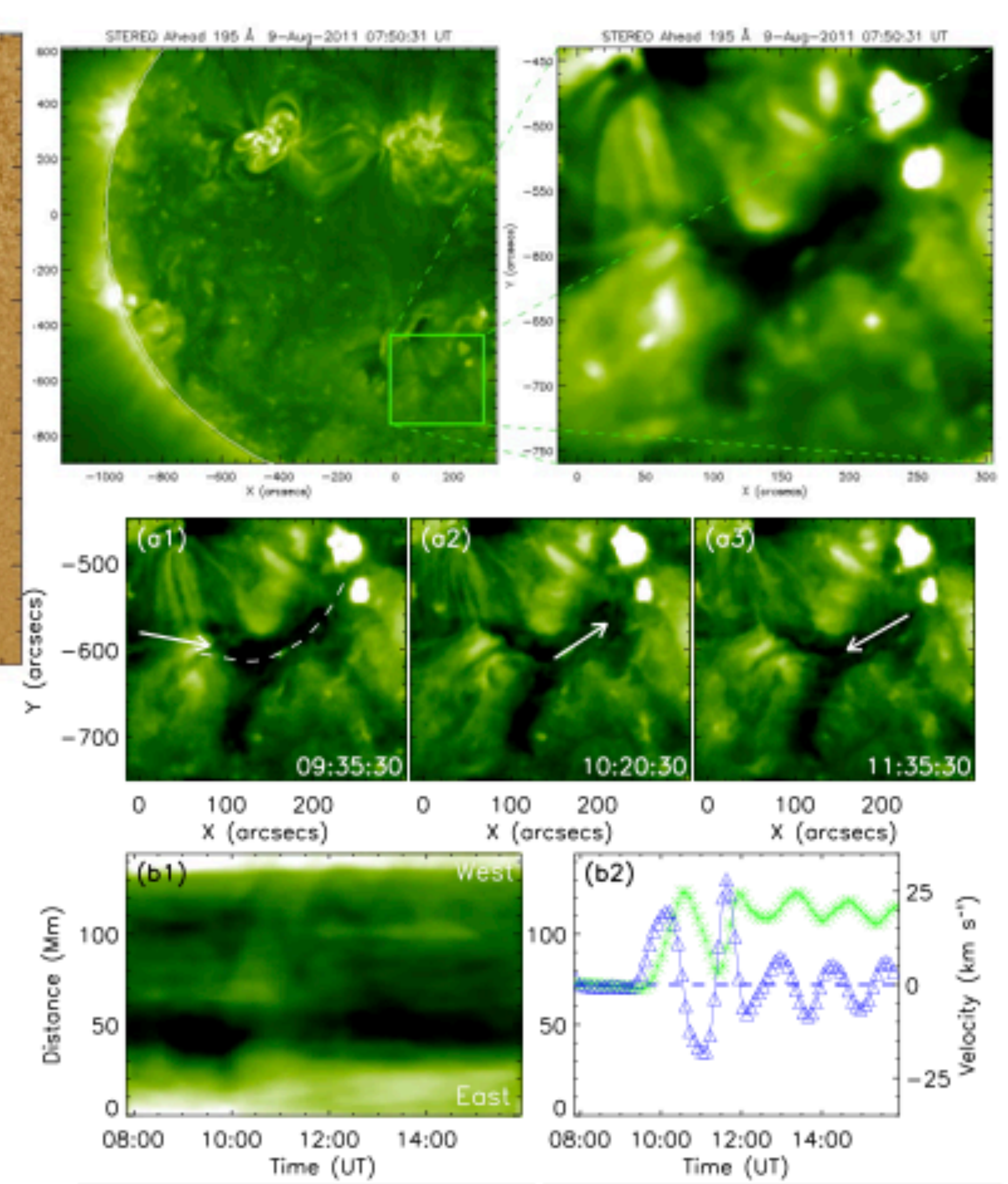

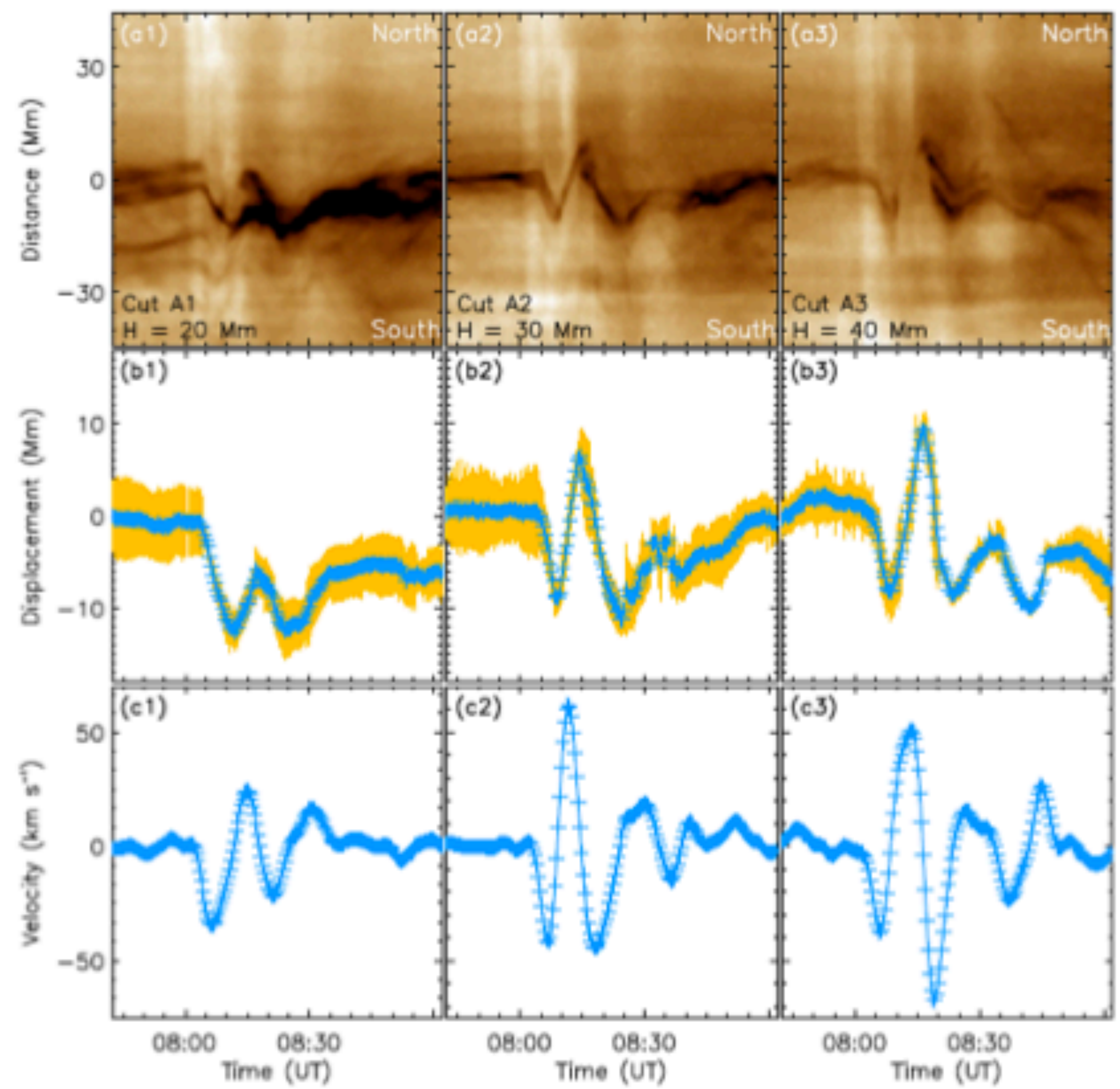

Different filament oscillation modes caused by a single shock wave, mainly depend on the interaction angle between the incoming wave and the filament axis.

Shen et al. 2014b

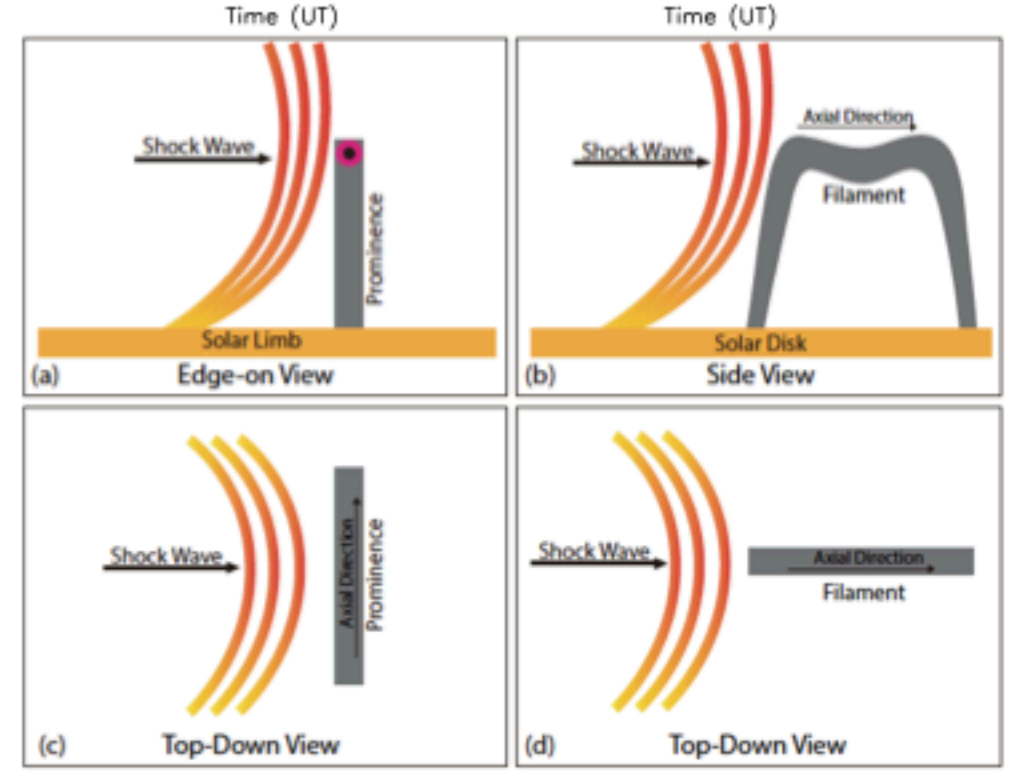

Part 1 longitudinal oscillations of an active region prominence

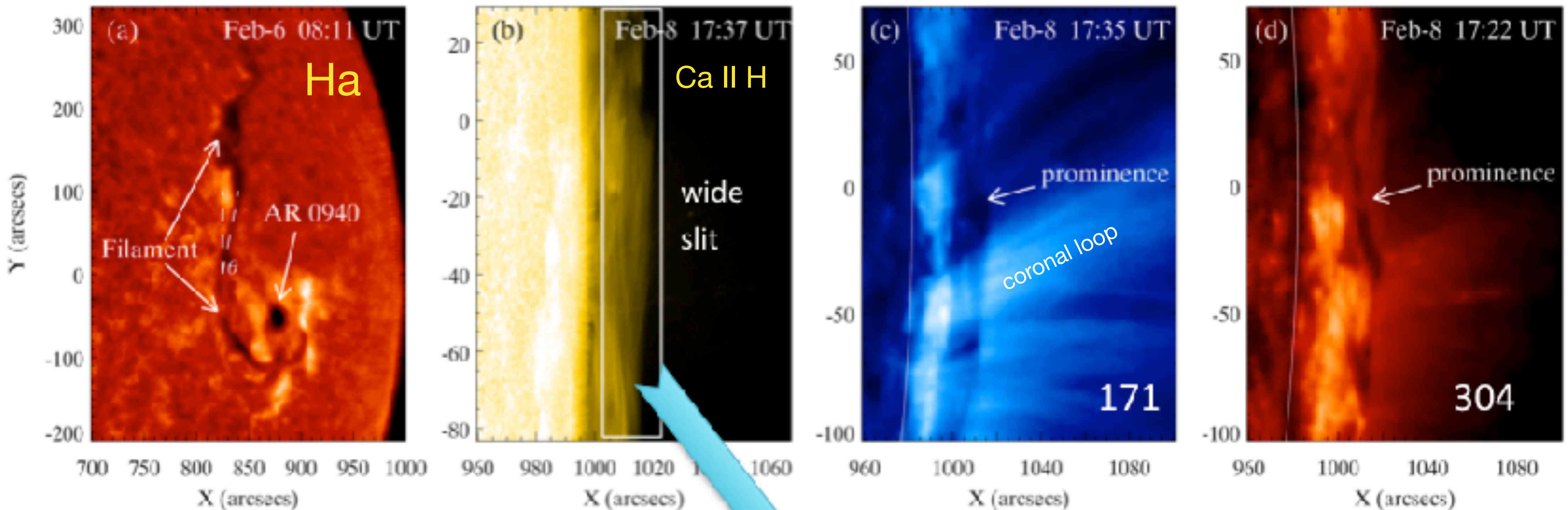

2007 Feb. 6 – 8
AR 10940

Kanzelhohe solar observatory Ha
SOT/FG Ca II H
STEREO-A/EUVI
STEREO-A/COR1
SOHO/LASCO

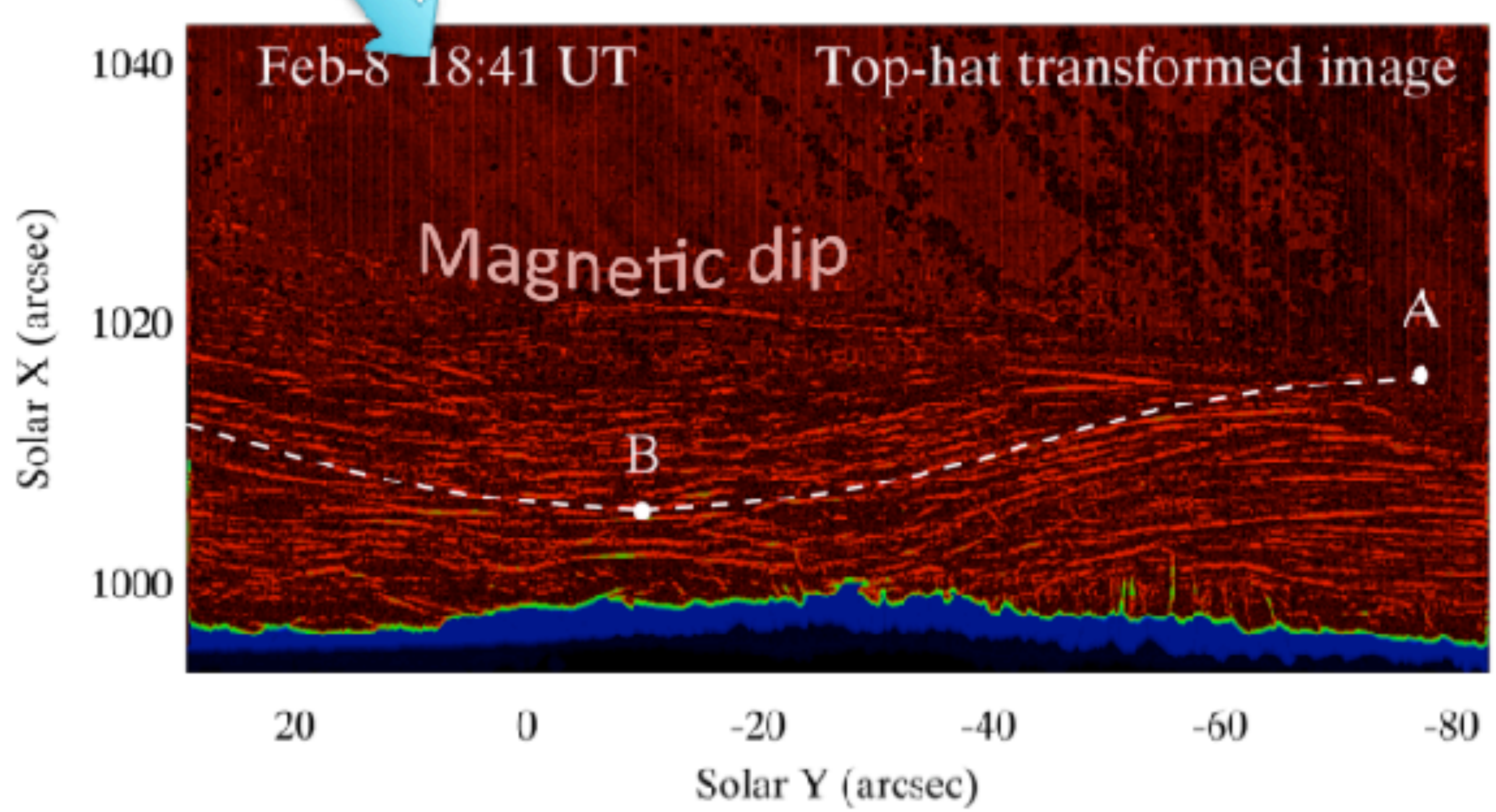

2012 A&A 542, A52

$$y = A\sin\left(\frac{2\pi}{P}t + \phi\right)e^{-t/\tau} + y_0, A = 24\ \text{Mm}, \phi = -\pi/2, P = 52\ \text{min}, \tau = 133\ \text{min}$$

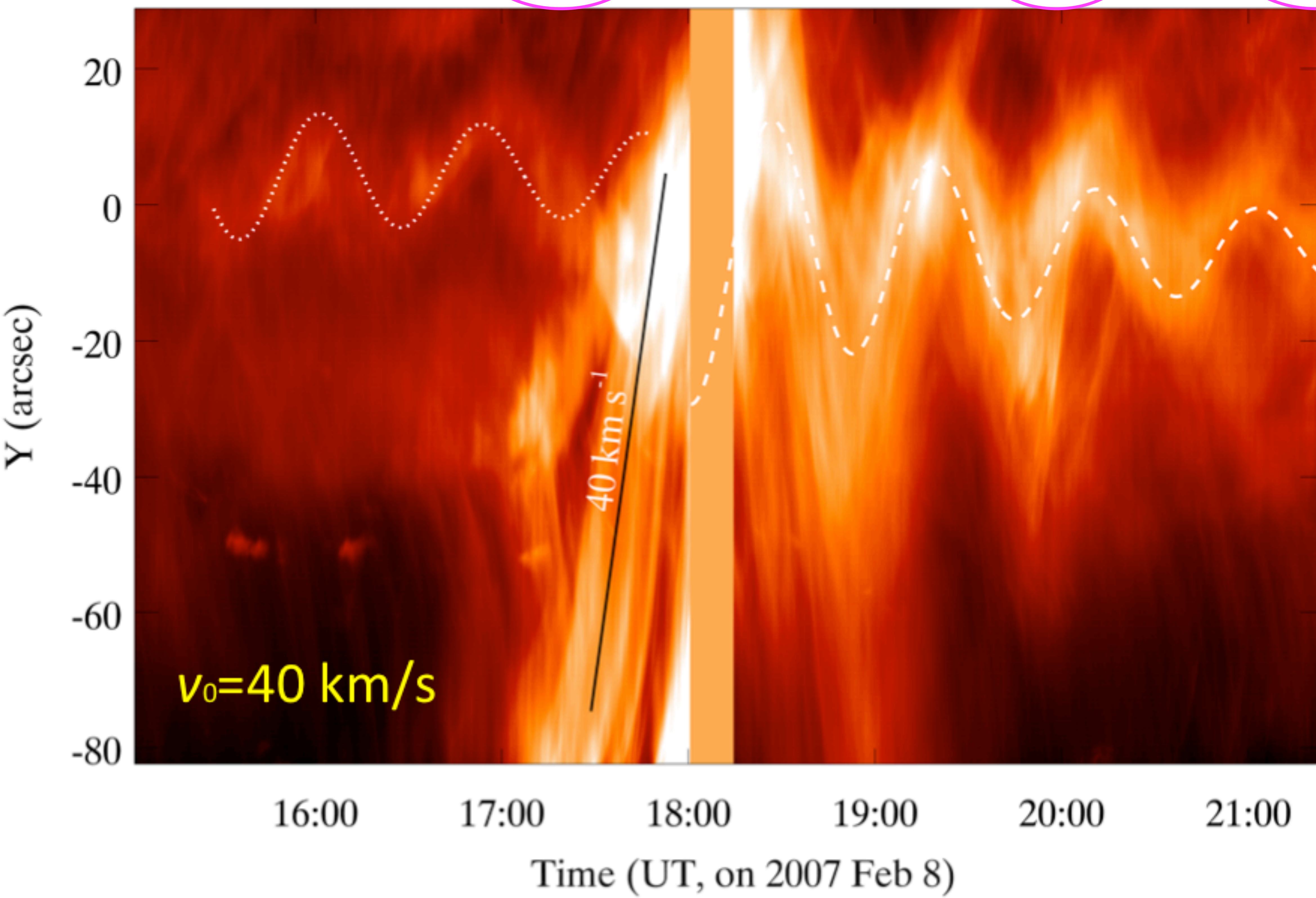

Possible partial prominence eruption in running-difference images

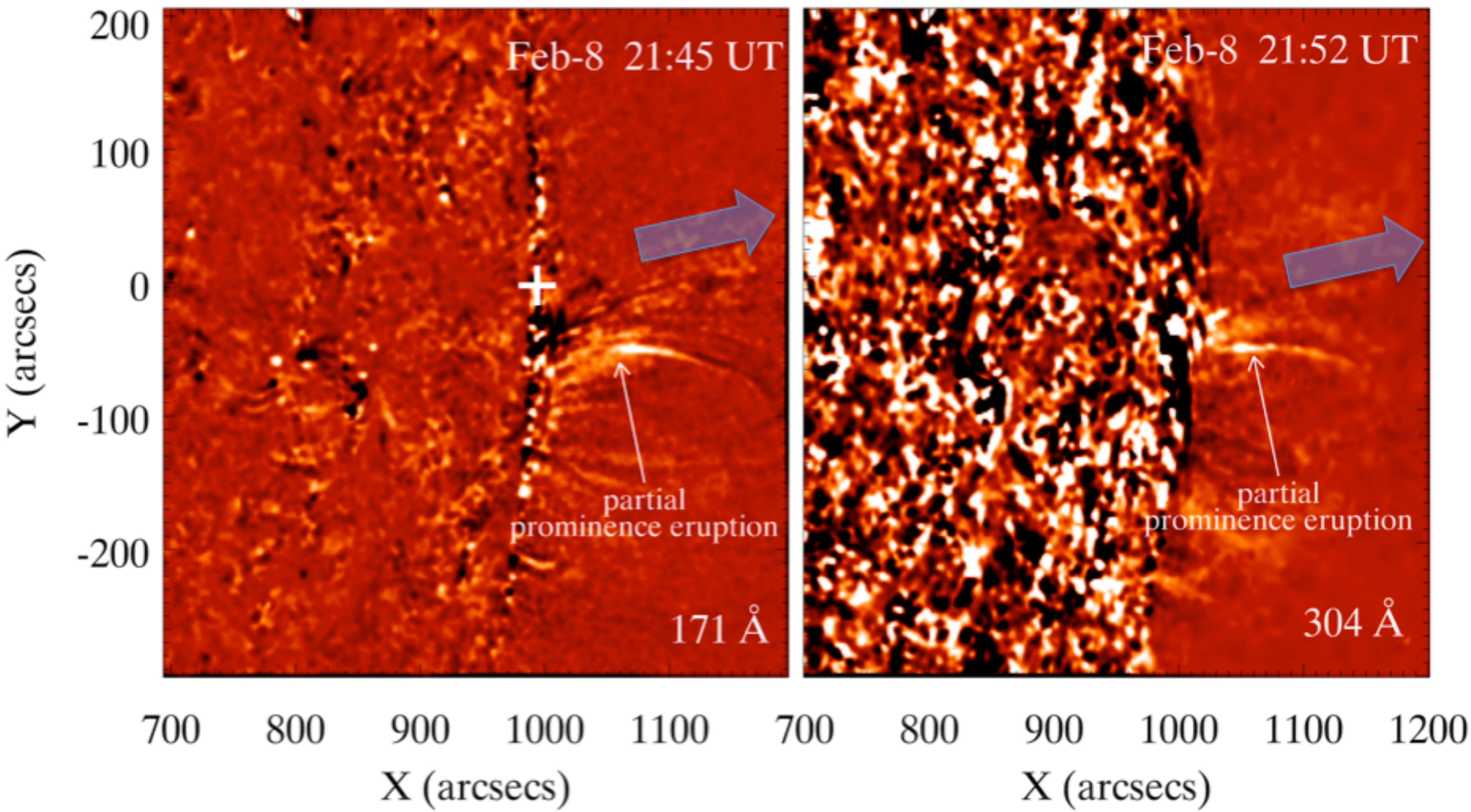

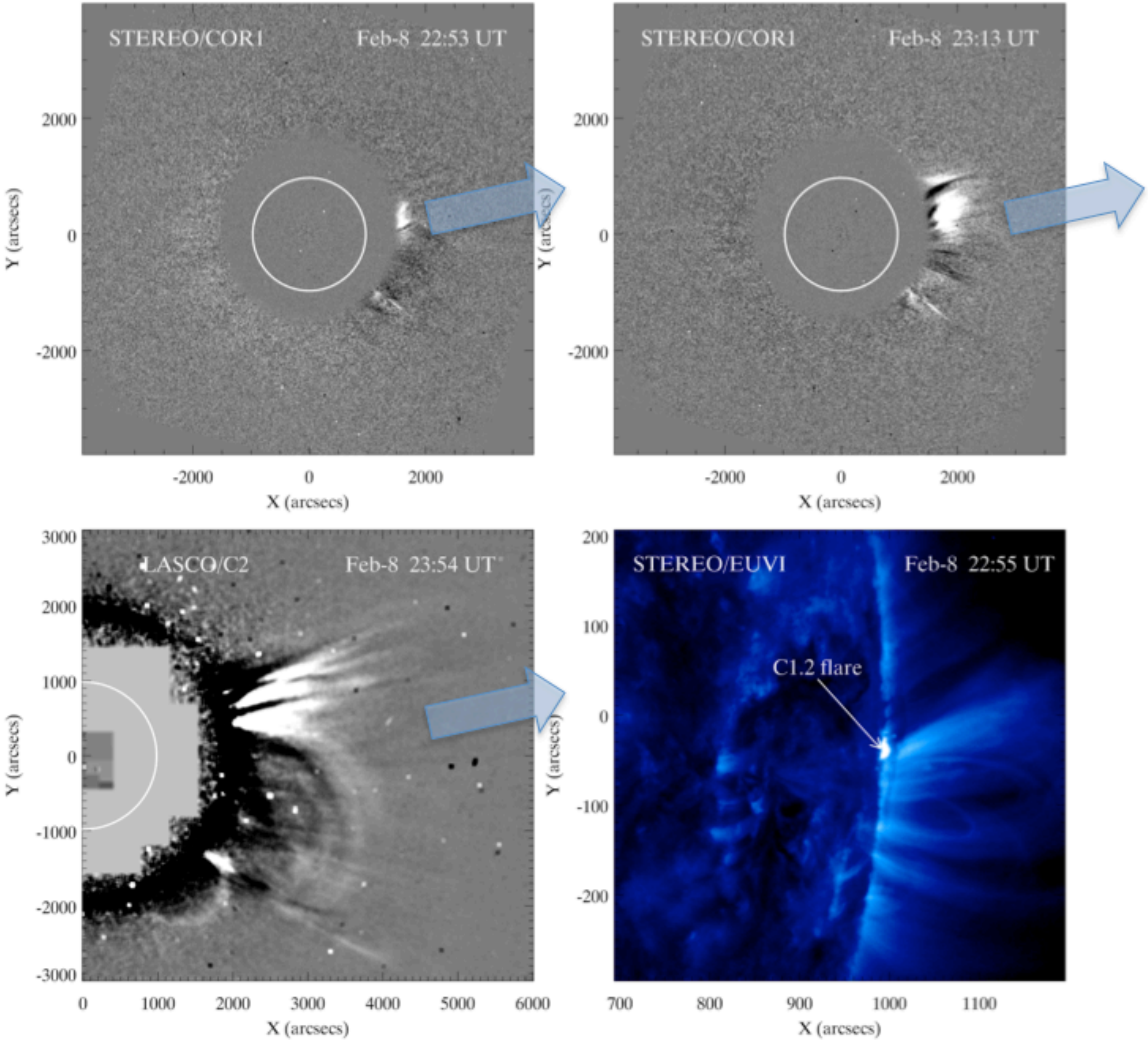

STEREO/COR1
Feb-8 22:53 UT
STEREO/COR1
Feb-8 23:13 UT
LASCO/C2
Feb-8 23:54 UT
STEREO/EUVI
Feb-8 22:55 UT
C1.2 flare
X (arcsecs)
Y (arcsecs)

Prominence oscillation: Possible precursor of CME/flare event

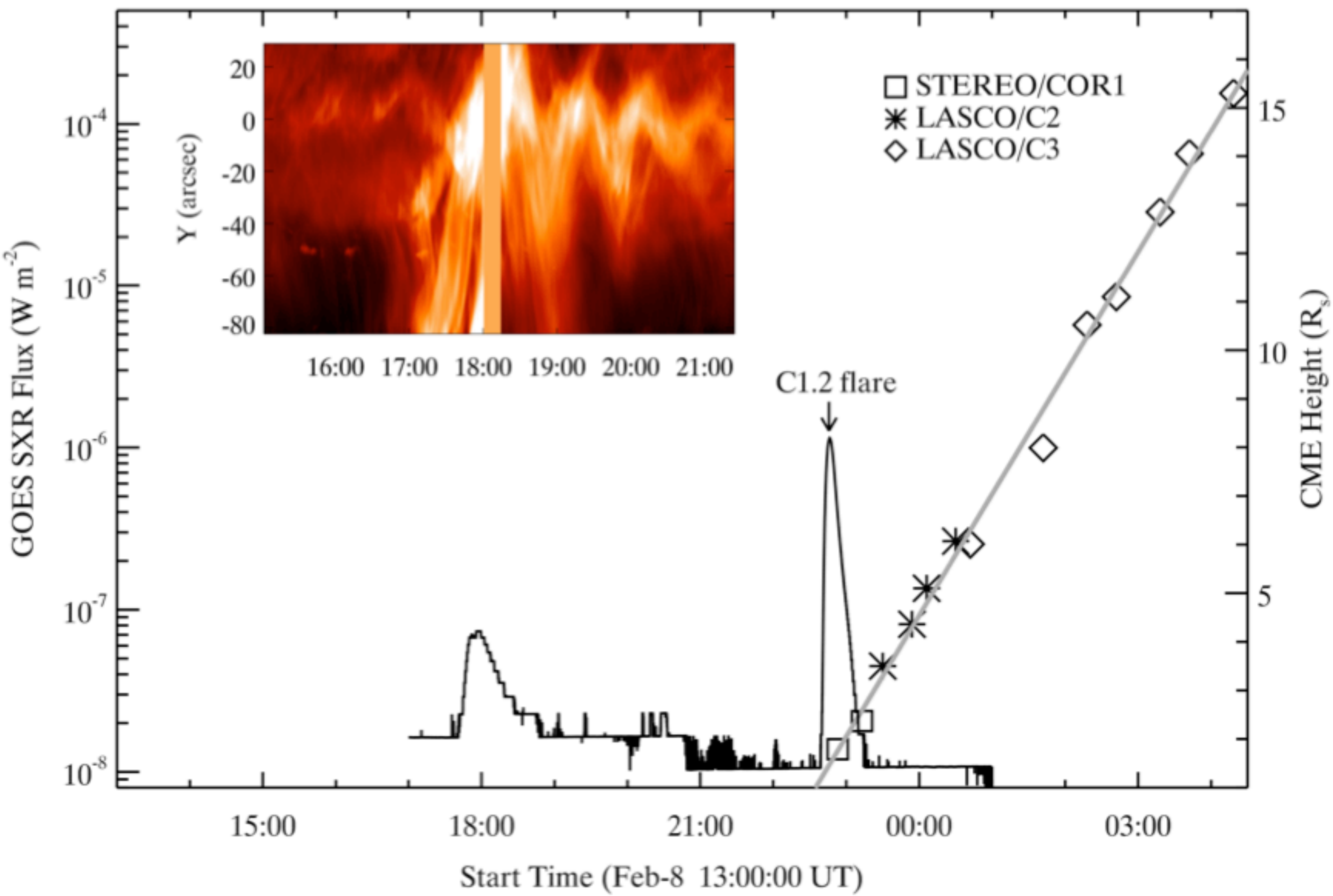

Part 2 **parameter survey of longitudinal prominence oscillation simulations**

1D HD Equations

MPI-AMRVAC in KU Leuven

$$\frac{\partial \rho}{\partial t} + \frac{\partial}{\partial s}(\rho v) = 0\,, \tag{1}$$

$$\frac{\partial}{\partial t}(\rho v) + \frac{\partial}{\partial s}(\rho v^2 + p) = \rho g_{\parallel}(s)\,, \tag{2}$$

$$\frac{\partial \varepsilon}{\partial t} + \frac{\partial}{\partial s}(\varepsilon v + p v) = \rho g_{\parallel} v + H - n_{\mathrm{H}} n_{\mathrm{e}} \Lambda(T) + \frac{\partial}{\partial s}\left(\kappa \frac{\partial T}{\partial s}\right), \tag{3}$$

$$g_{\parallel}(s) = \begin{cases} -g_{\odot}, & s \leqslant s_1; \\ -g_{\odot} \cos\left(\dfrac{\pi}{2}\dfrac{s - s_1}{s_2 - s_1}\right), & s_1 < s \leqslant s_2; \\ g_{\odot} \dfrac{\pi D}{2(L/2 - s_2)} \sin\left(\pi \dfrac{s - s_2}{L/2 - s_2}\right), & s_2 < s \leqslant L/2, \end{cases}$$

BK

$$H_0(s) = \begin{cases} E_0 \exp(-s/H_m), & s < L/2; \\ E_0 \exp[-(L - s)/H_m], & L/2 \leqslant s < L; \end{cases}$$

CH

$$H_1(s) = \begin{cases} E_1, & s \leqslant s_{\mathrm{tr}}; \\ E_1 \exp[-(s - s_{\mathrm{tr}})/\lambda], & s_{\mathrm{tr}} < s \leqslant L/2; \\ E_1 \exp[-(L - s_{\mathrm{tr}} - s)/\lambda], & L/2 < s \leqslant L - s_{\mathrm{tr}}; \\ E_1, & s > L - s_{\mathrm{tr}}; \end{cases}$$

10 Mm

$$s_1 = 5\ \mathrm{Mm} \quad s_2 = s_1 + \pi r/2\ \mathrm{Mm}$$

$$R = 2w^2/(D\pi^2)$$ curvature radius

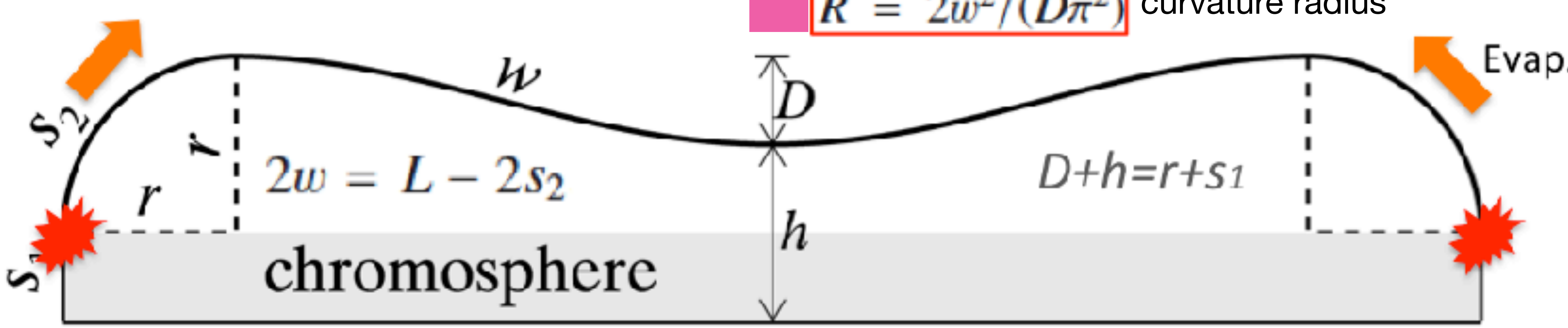

Four steps:

1. Formation
2. Growth (Xia et al. 2011)
3. Relaxation
4. **Oscillation**

from observation

$S1=$	5.0 Mm
$S2=$	20.7 Mm
$D=$	8.1 Mm
$2w=$	107.3 Mm
$L=$	148.7 Mm

v_0=40 km/s

$$A = 18.6 \text{ Mm}$$

$$P = 56 \text{ min}$$

$$\tau = 202 \text{ min}$$

In this event, radiative loss is insufficient to account for the observed damping! Other mechanisms may at work. (e.g., mass accretion)

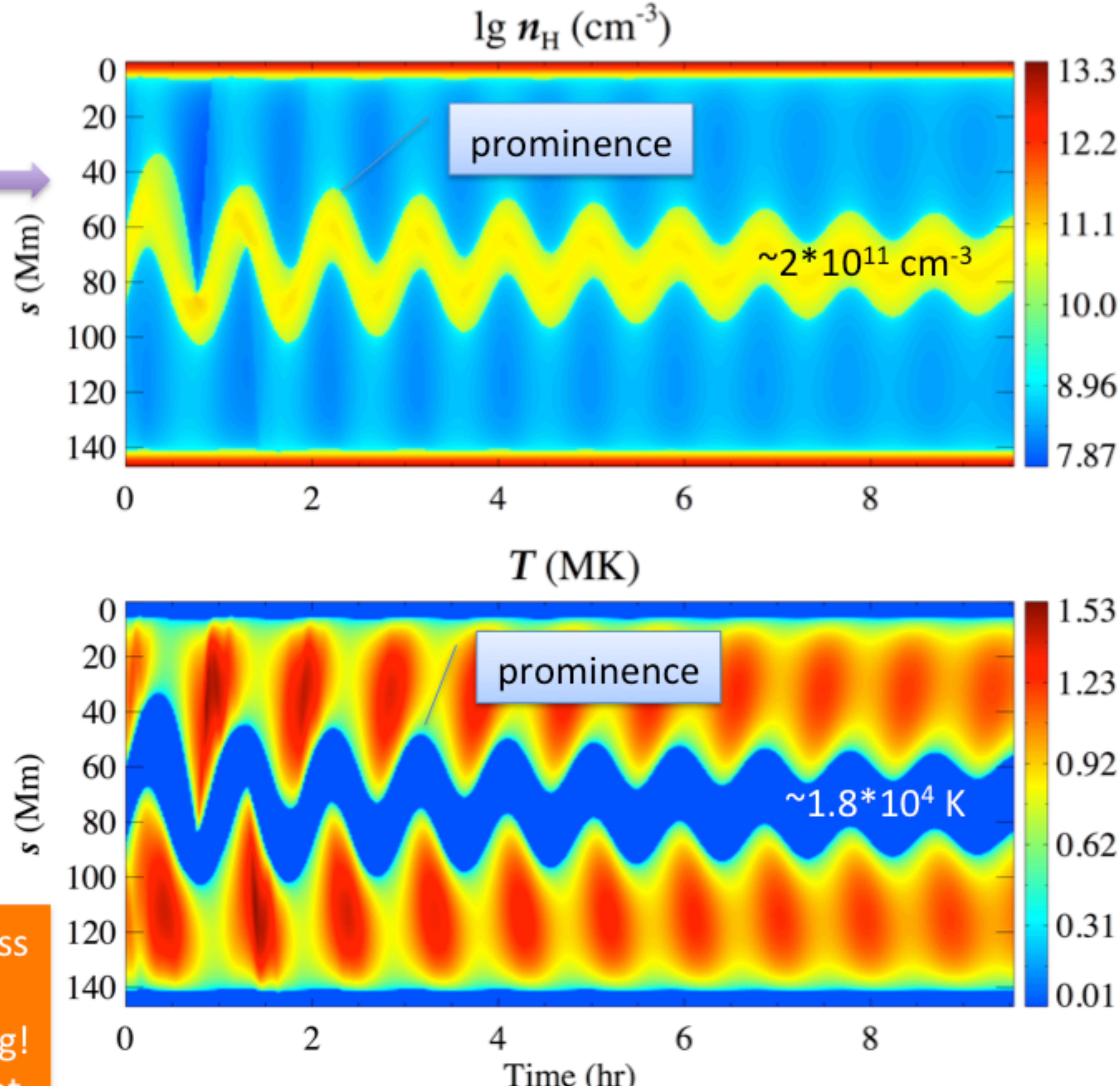

$r = 20$ Mm $D = 10$ Mm $L = 260$ Mm

$A_0 = 34.9$ Mm $P = 84.3$ min $\tau = 272$ min

Triggering mechanism

Velocity perturbation | transient heating (microflare)

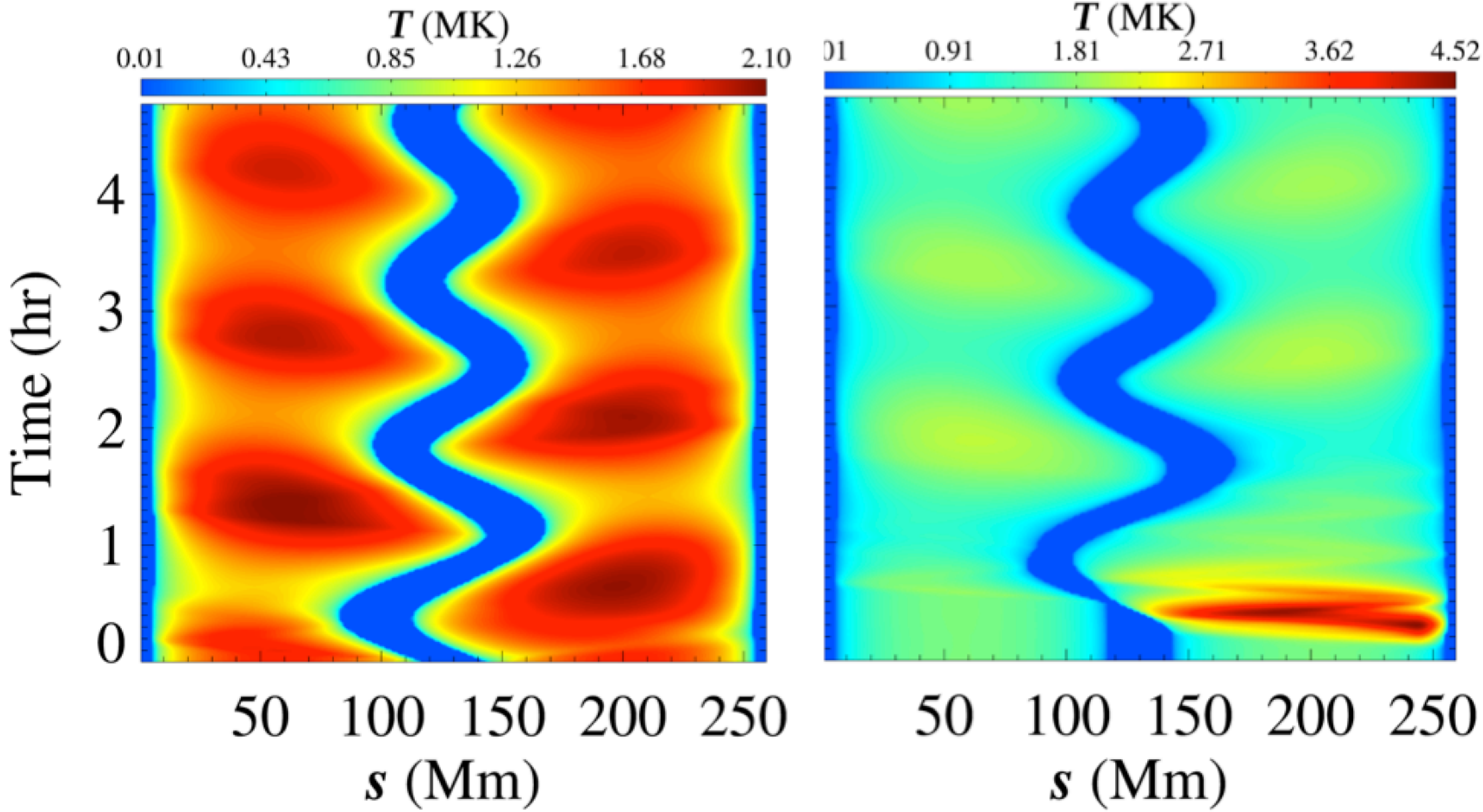

2013 A&A 554, A124

Parameter survey:

Prominence length and mass before oscillating

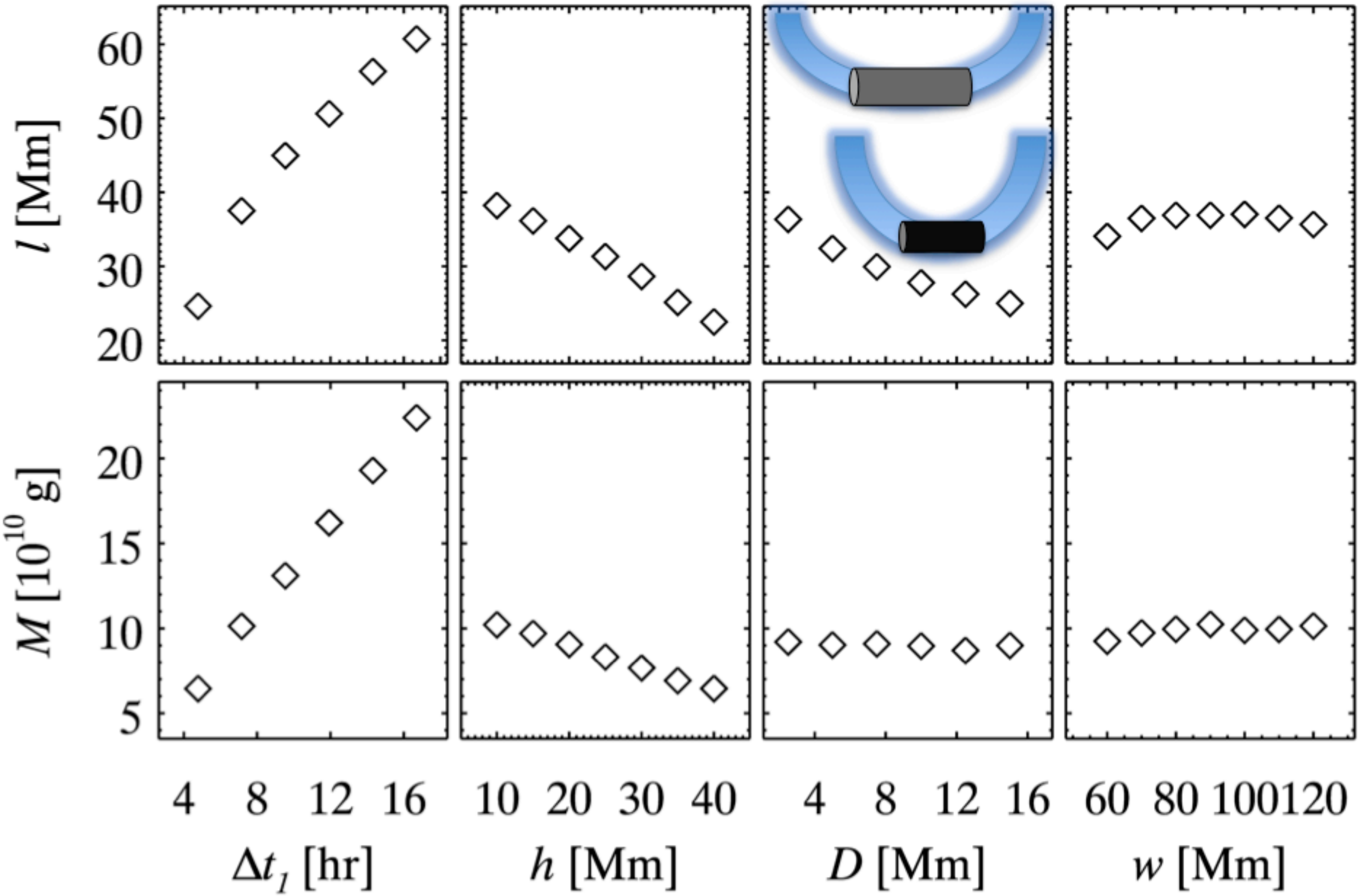

CH heating time

Parameter survey: Period and decay time of prominence oscillations

$$P \sim l^{0.16} h^{-0.05} D^{-0.54} w^{0.91} v_0^{0.05} \qquad \tau \sim l^{1.63} h^{-0.18} D^{0.66} w^{-1.21} v_0^{-0.30}$$

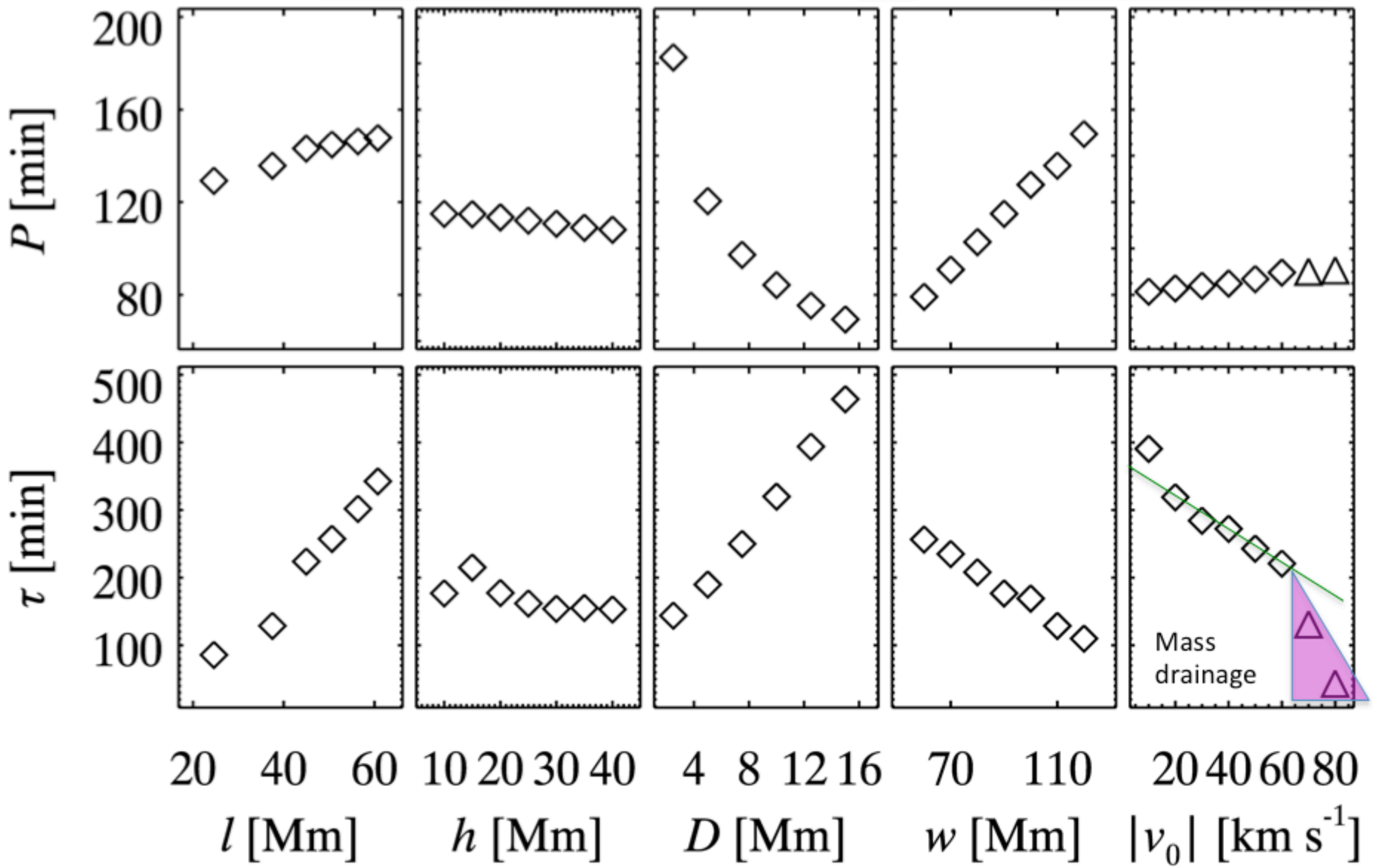

Dominant restoring force: gravity along the dip

$$\frac{\partial}{\partial t}(\rho v) + \frac{\partial}{\partial s}(\rho v^2 + p) = \rho g_{\parallel}(s)$$

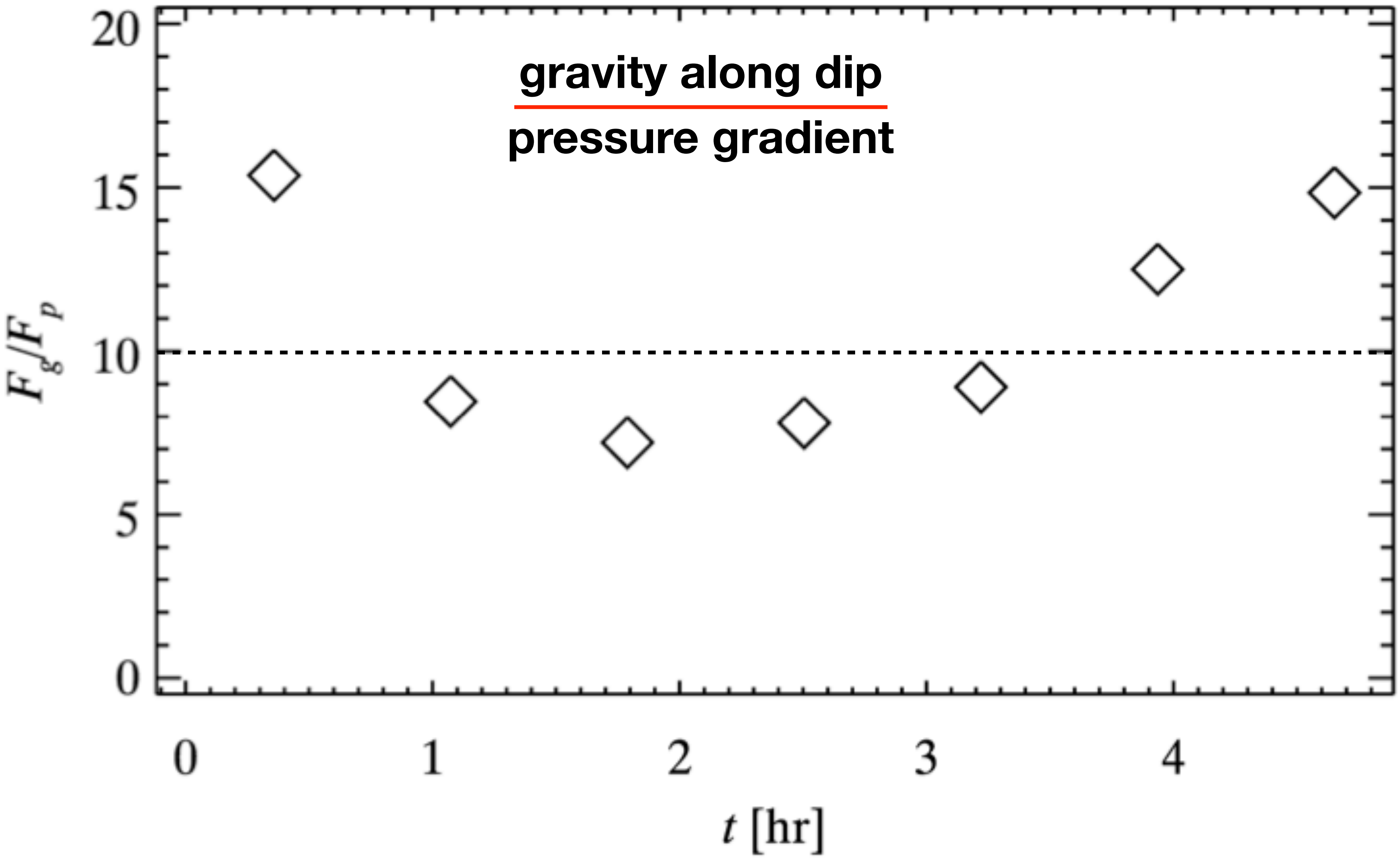

Comparison of period between analytical solution and simulation

key factor

Curvature radius of dip: $R = 2w^2/(D\pi^2)$

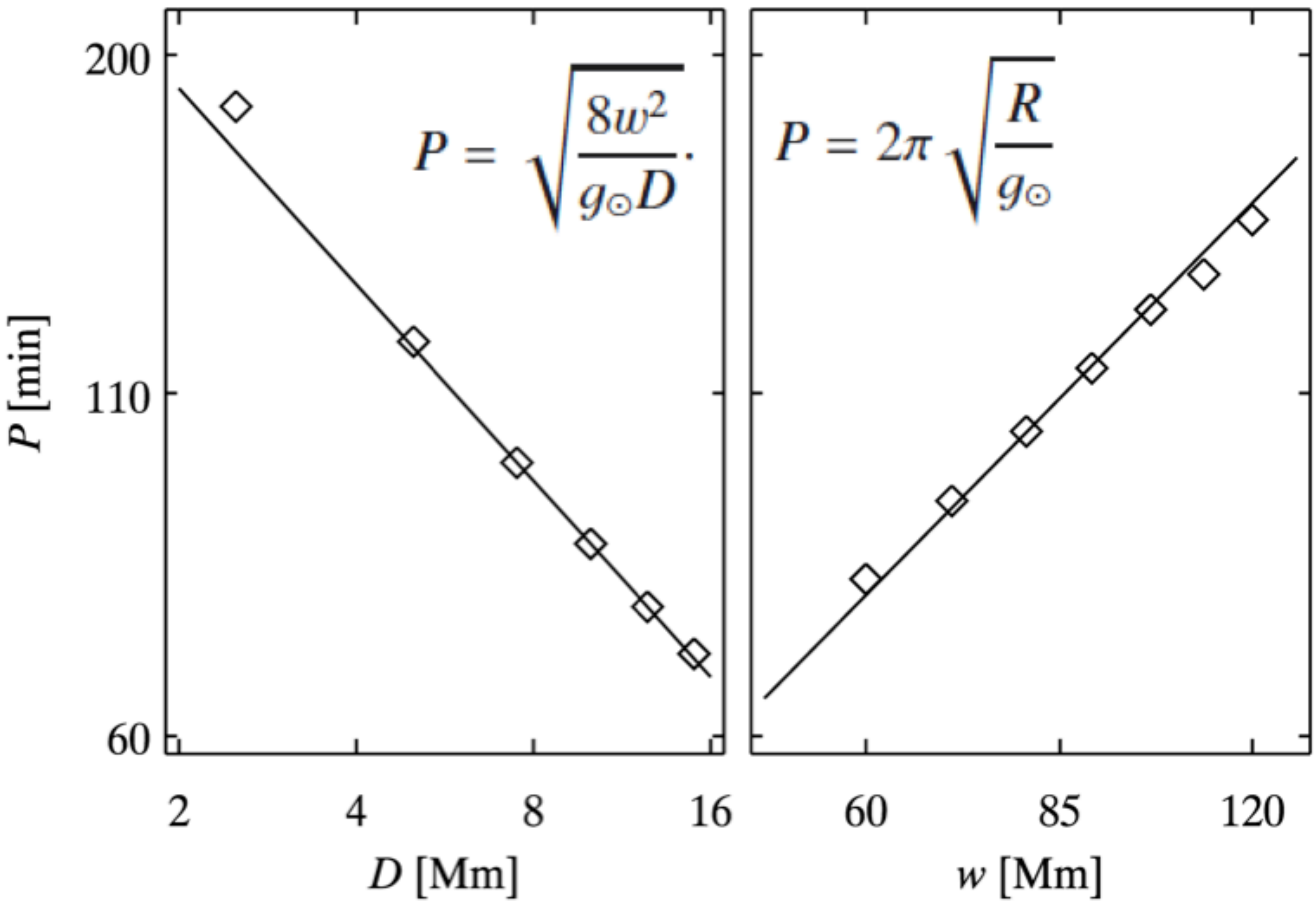

Dominant damping mechanism: radiative loss

$$\frac{\partial \varepsilon}{\partial t} + \frac{\partial}{\partial s}(\varepsilon v + p v) = \rho g_{\parallel} v + H - n_{\mathrm{H}} n_{\mathrm{e}} \Lambda(T) + \frac{\partial}{\partial s}\left(\kappa \frac{\partial T}{\partial s}\right)$$

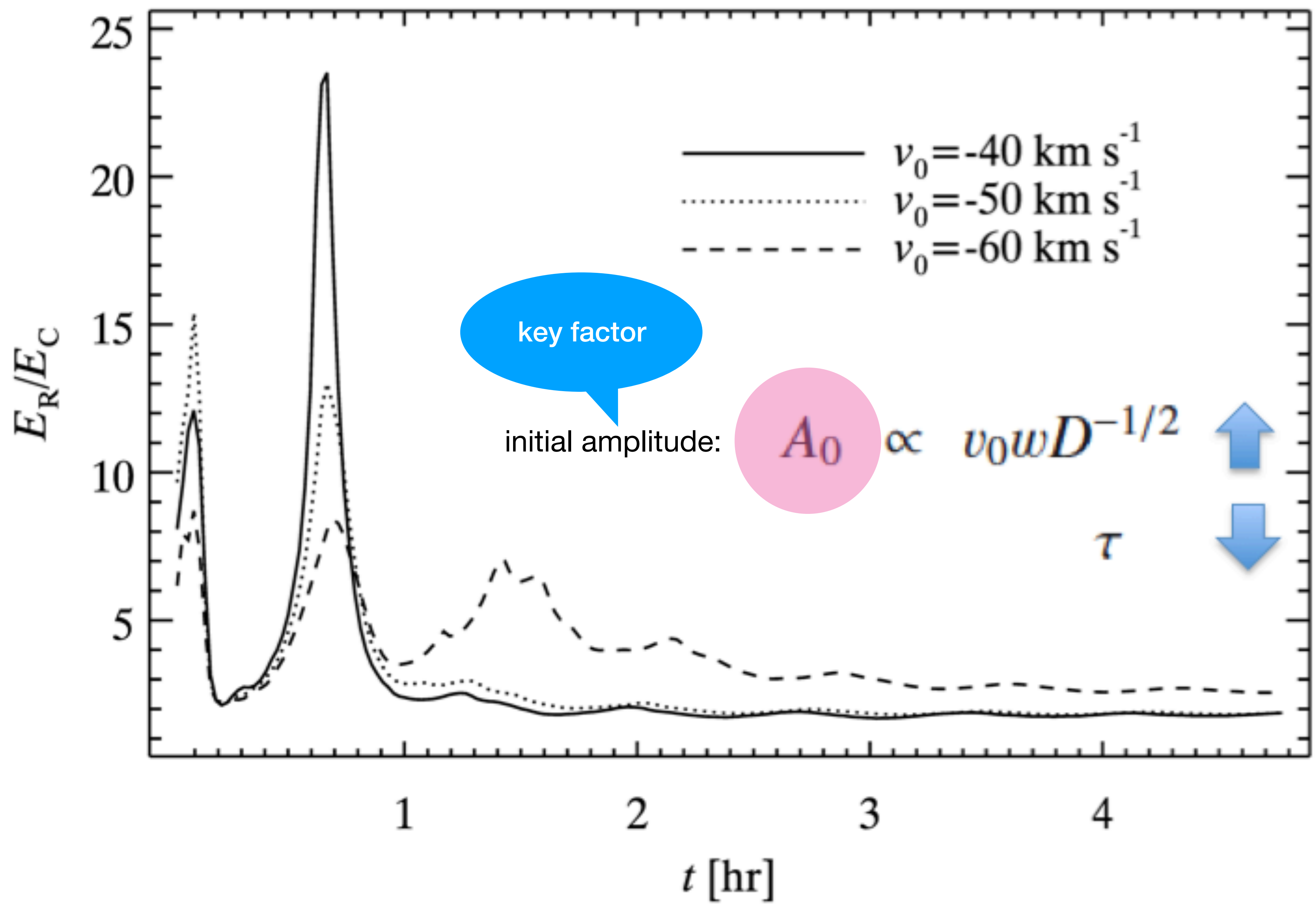

Total radiative loss

$$x^{-2} + (1-x)^{-2}$$

$x = 0.5$

Bottom of dip

The effect of mass drainage in the case of huge perturbation

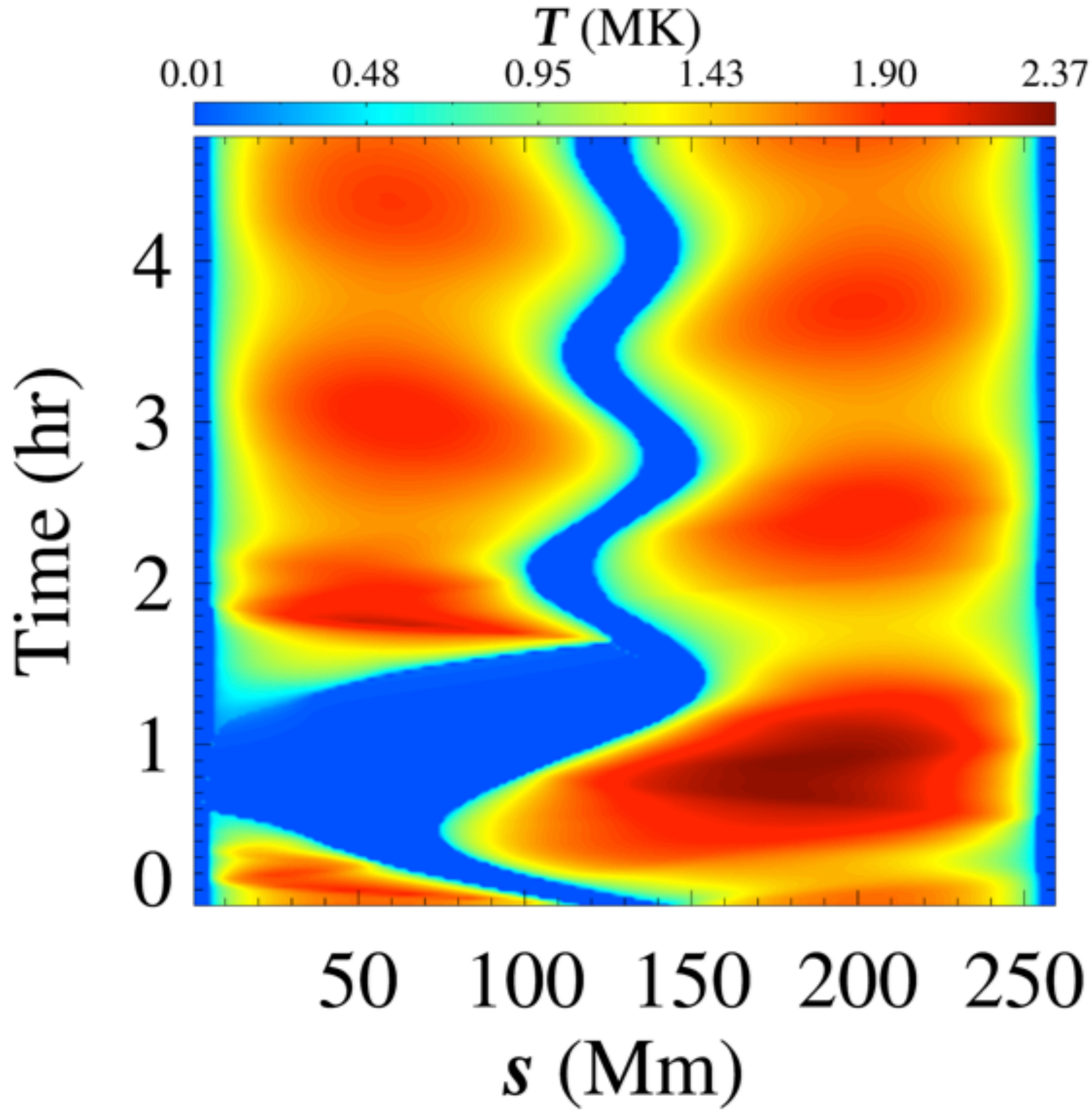

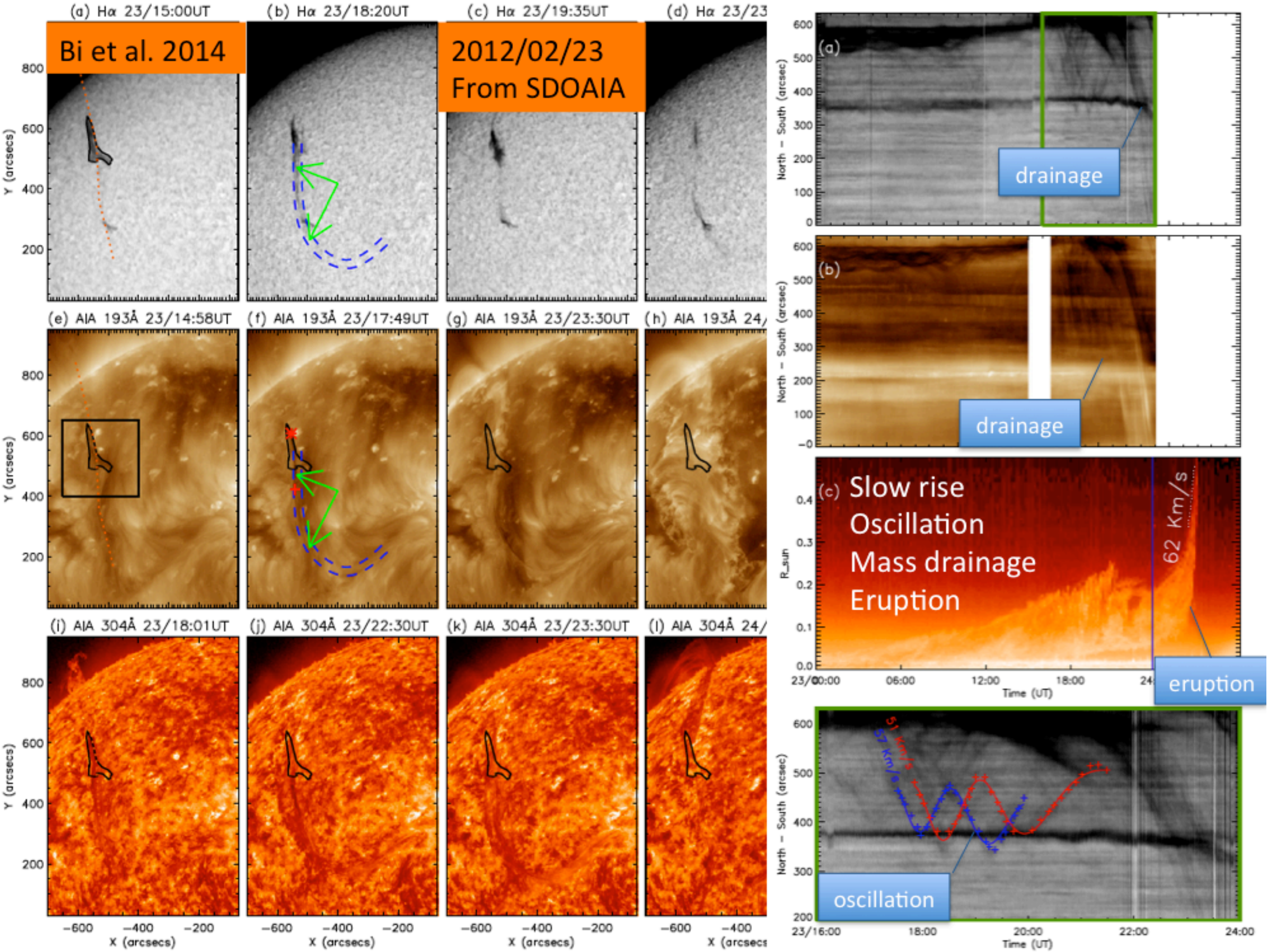

Bi et al. 2014
2012/02/23
From SDOAIA
drainage
drainage
Slow rise
Oscillation
Mass drainage
Eruption
62 Km/s
eruption
51 Km/s
57 Km/s
oscillation

summary

For large-amplitude longitudinal prominence oscillations:

1. Triggering mechanism: impulsive velocity perturbation, microflare
2. Restoring force: gravity > gas pressure when *R* is not so large
3. Damping mechanism: radiative loss > thermal conduction
   Mass drainage plays a role in the case of huge perturbation

Q

Observationally:

- **Are there continuous oscillation after mass drainage?**
- **What is the difference before & after drainage?**

Part 3 longitudinal oscillations in a solar filament with mass drainage

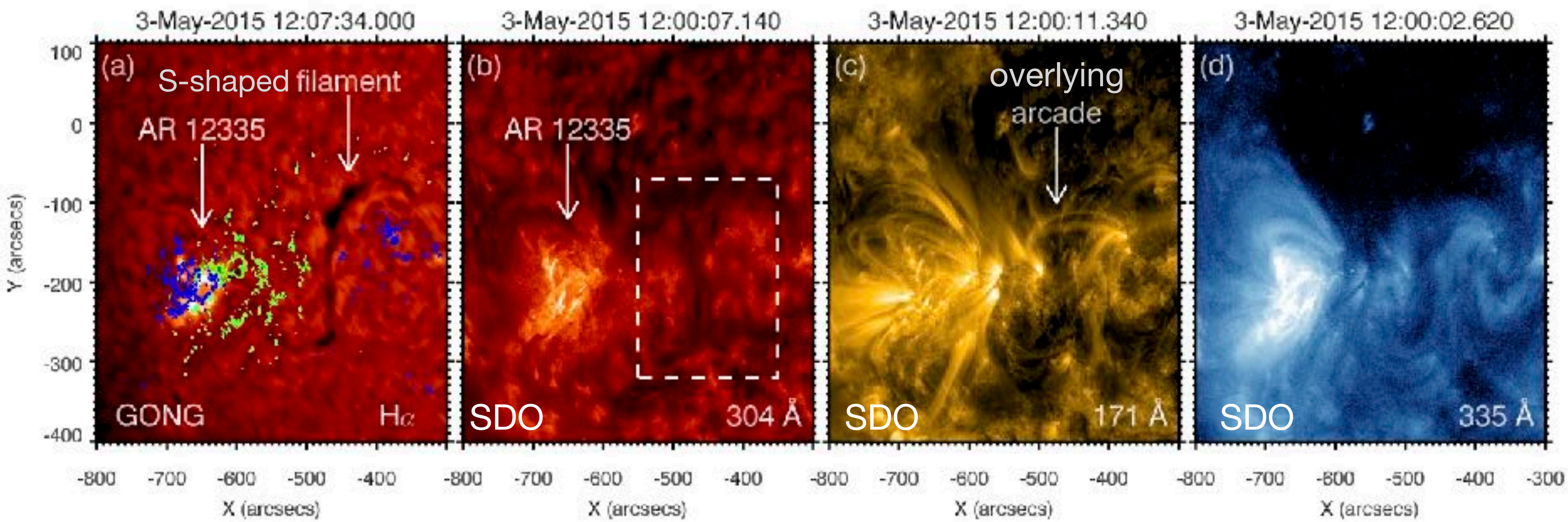

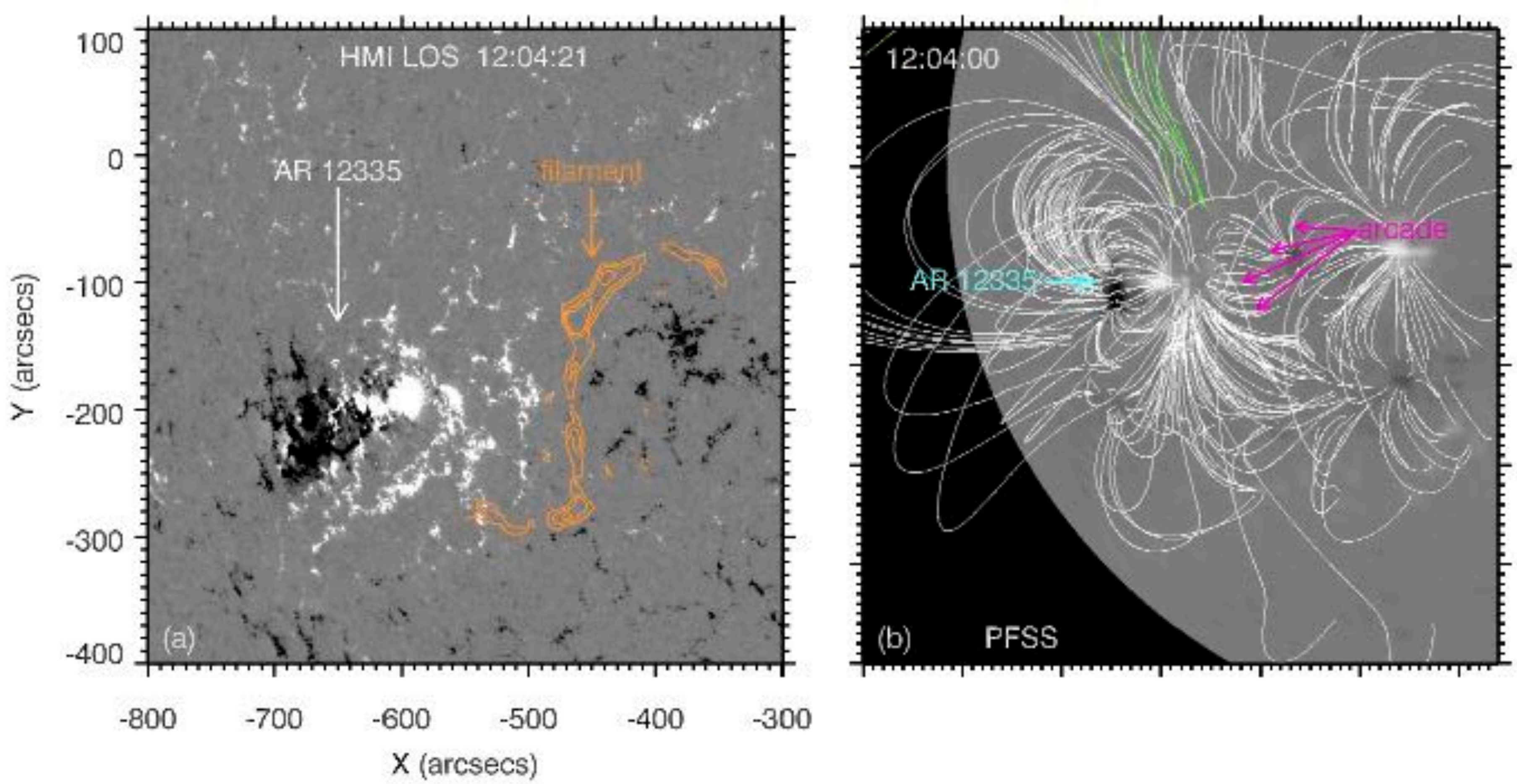

Trigger of oscillations — evidence of MR (I): bidirectional flows in the filament channel

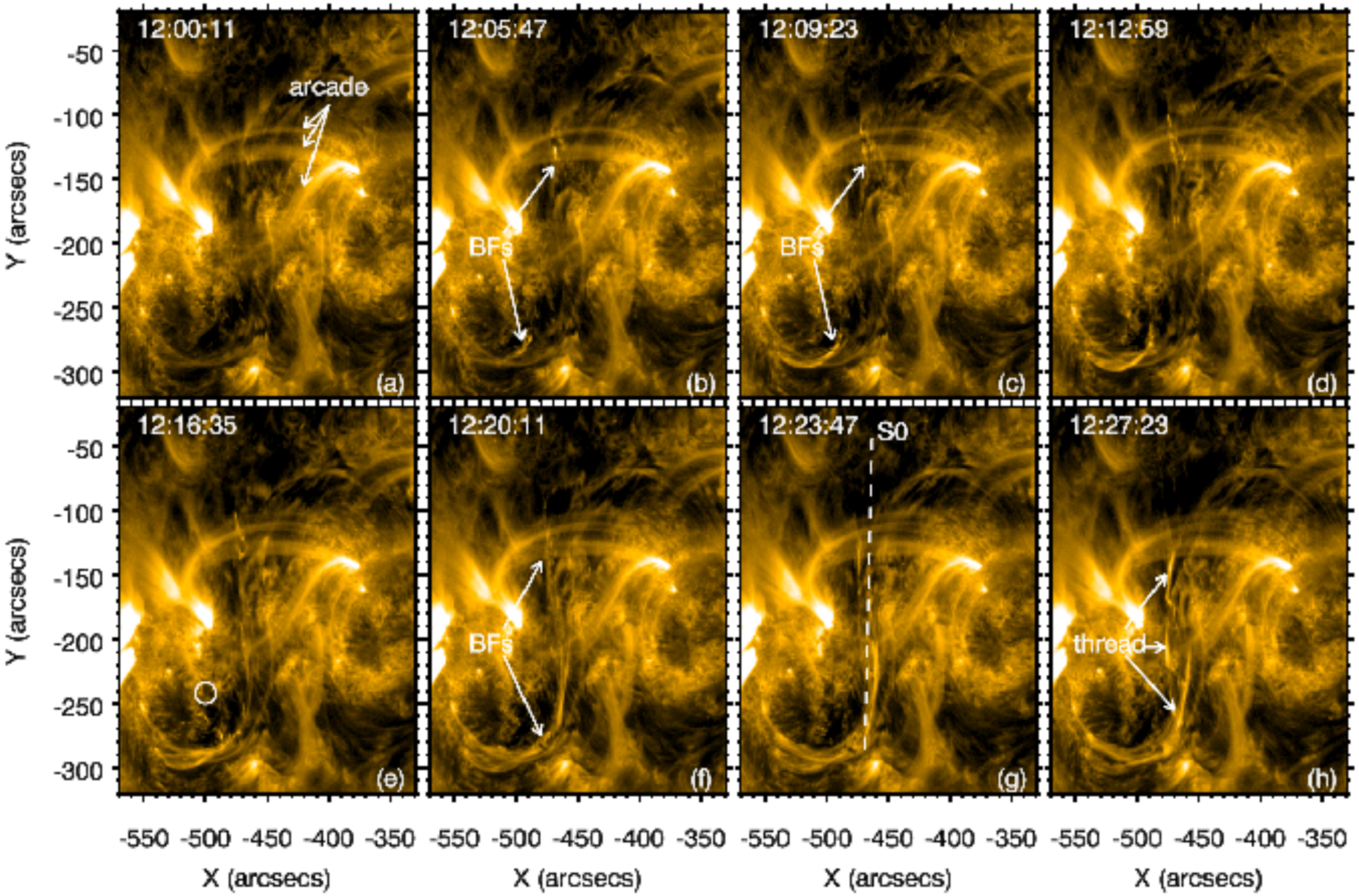

time-slice diagram of S0

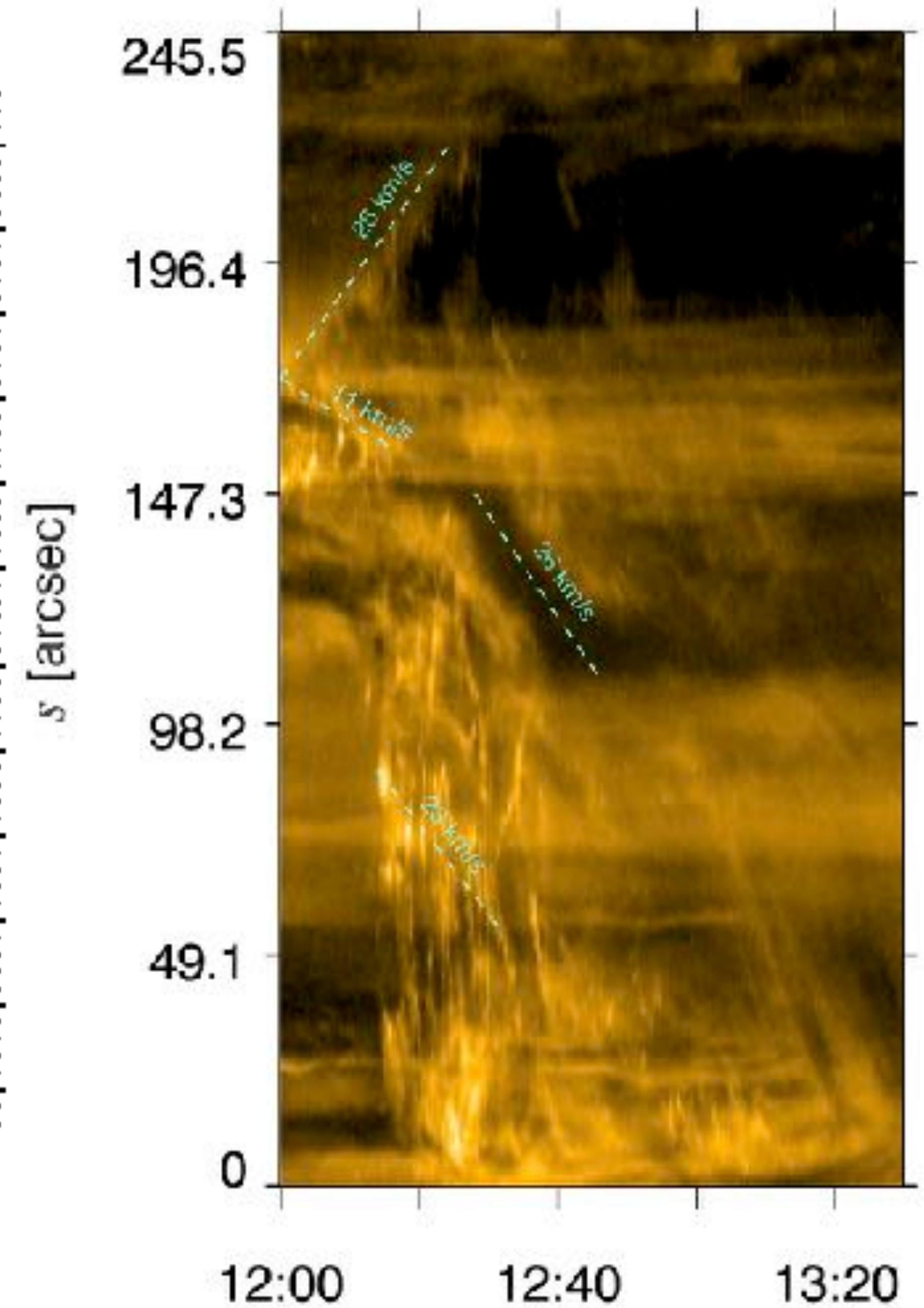

Trigger of oscillations — evidence of MR (II): brightenings of the fine threads in EUV & SXR

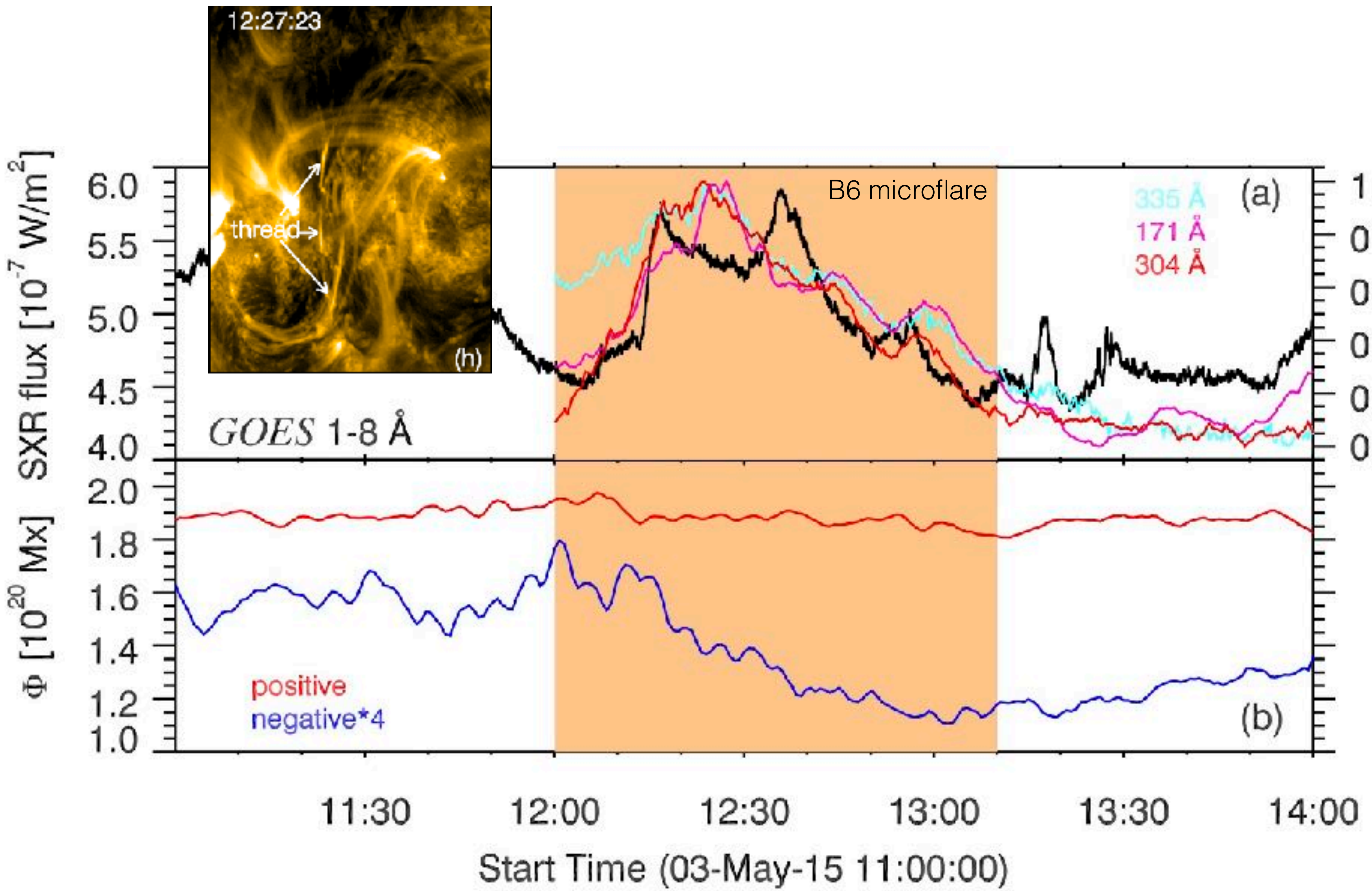

Trigger of oscillations — evidence of MR (III): magnetic cancellation in the photosphere

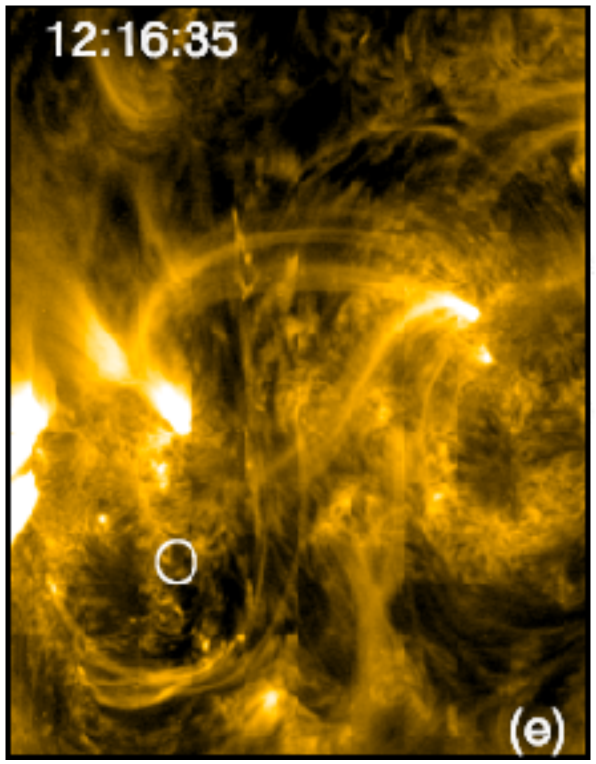

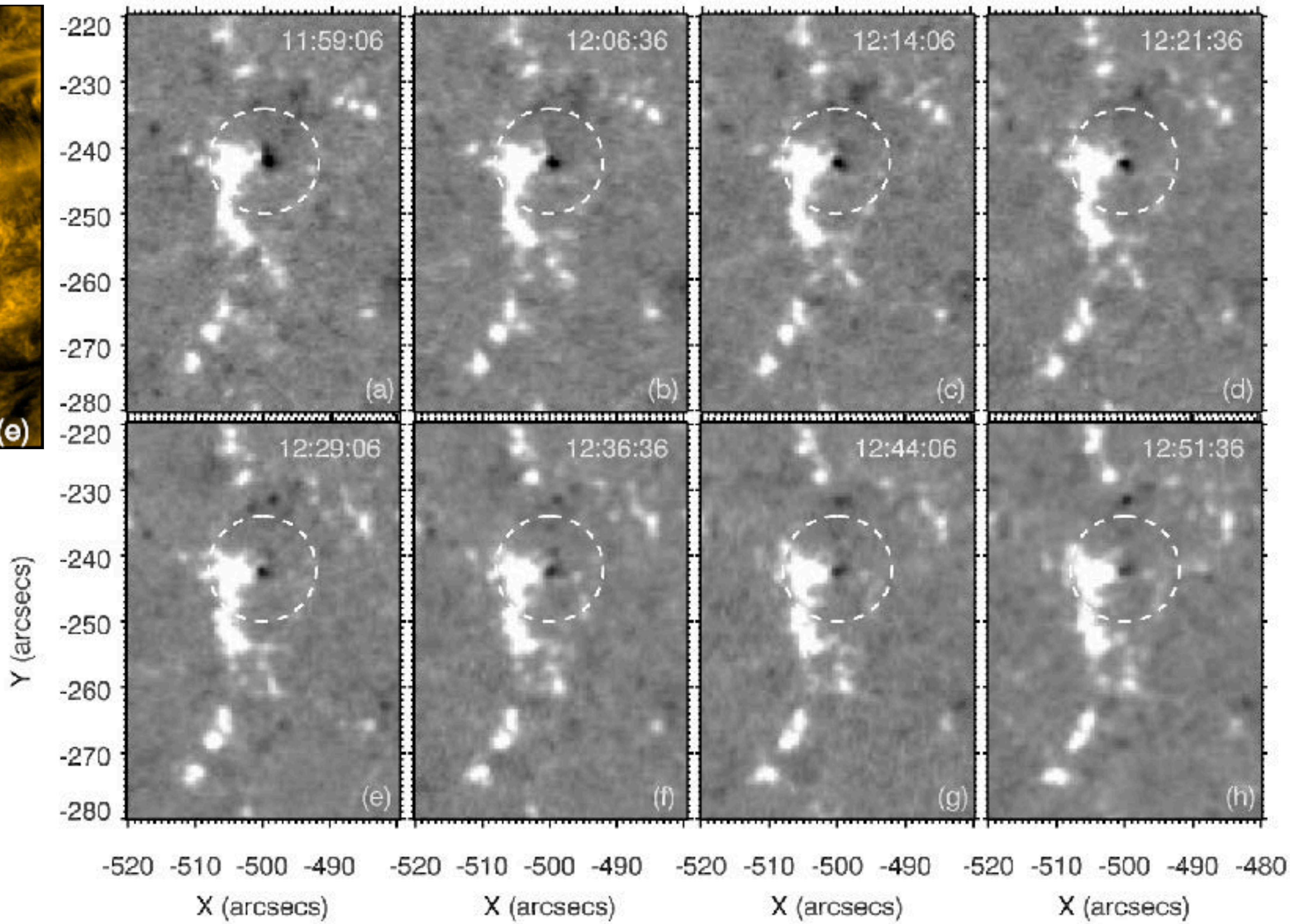

filament oscillation

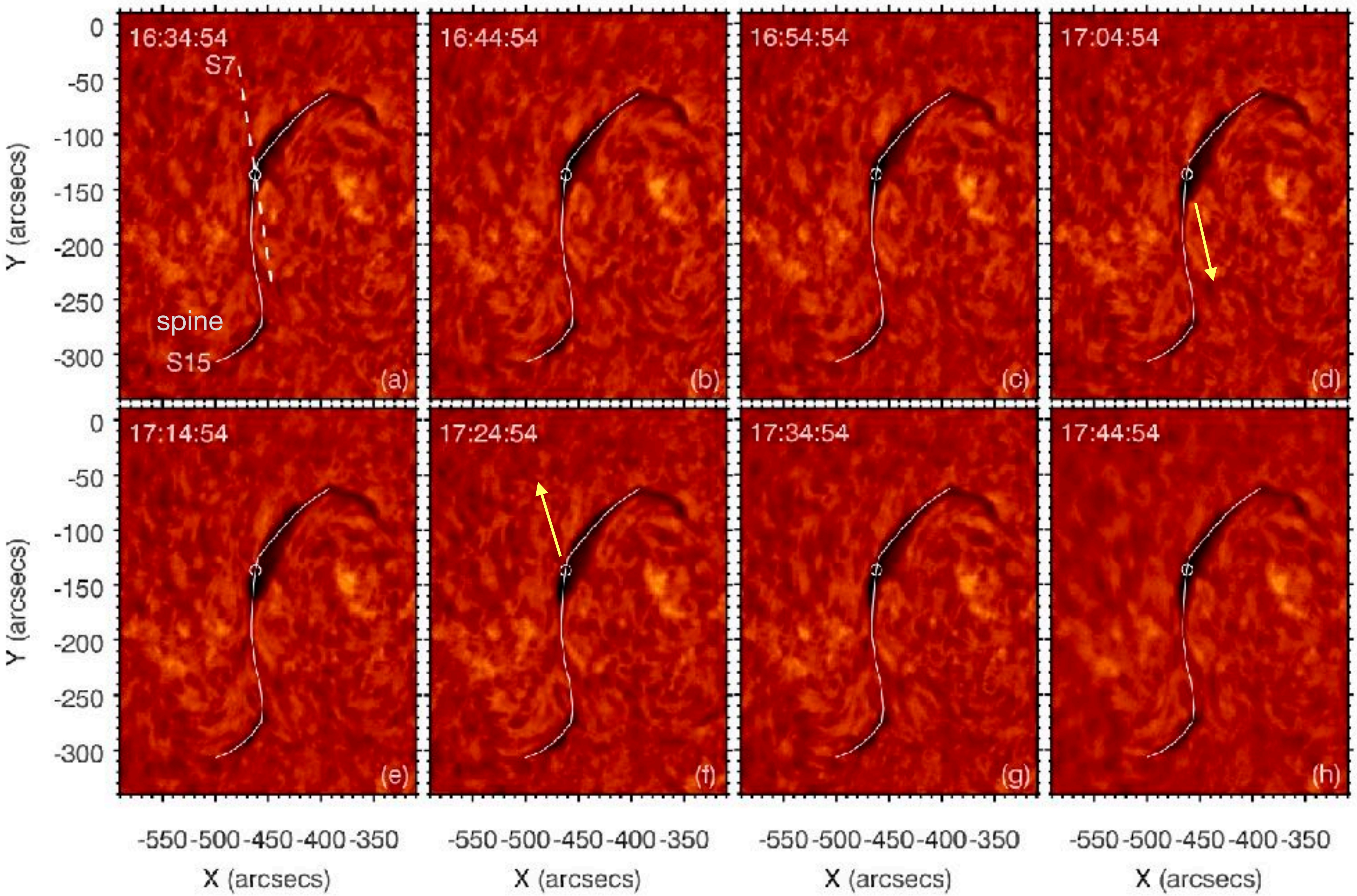

mass drainage

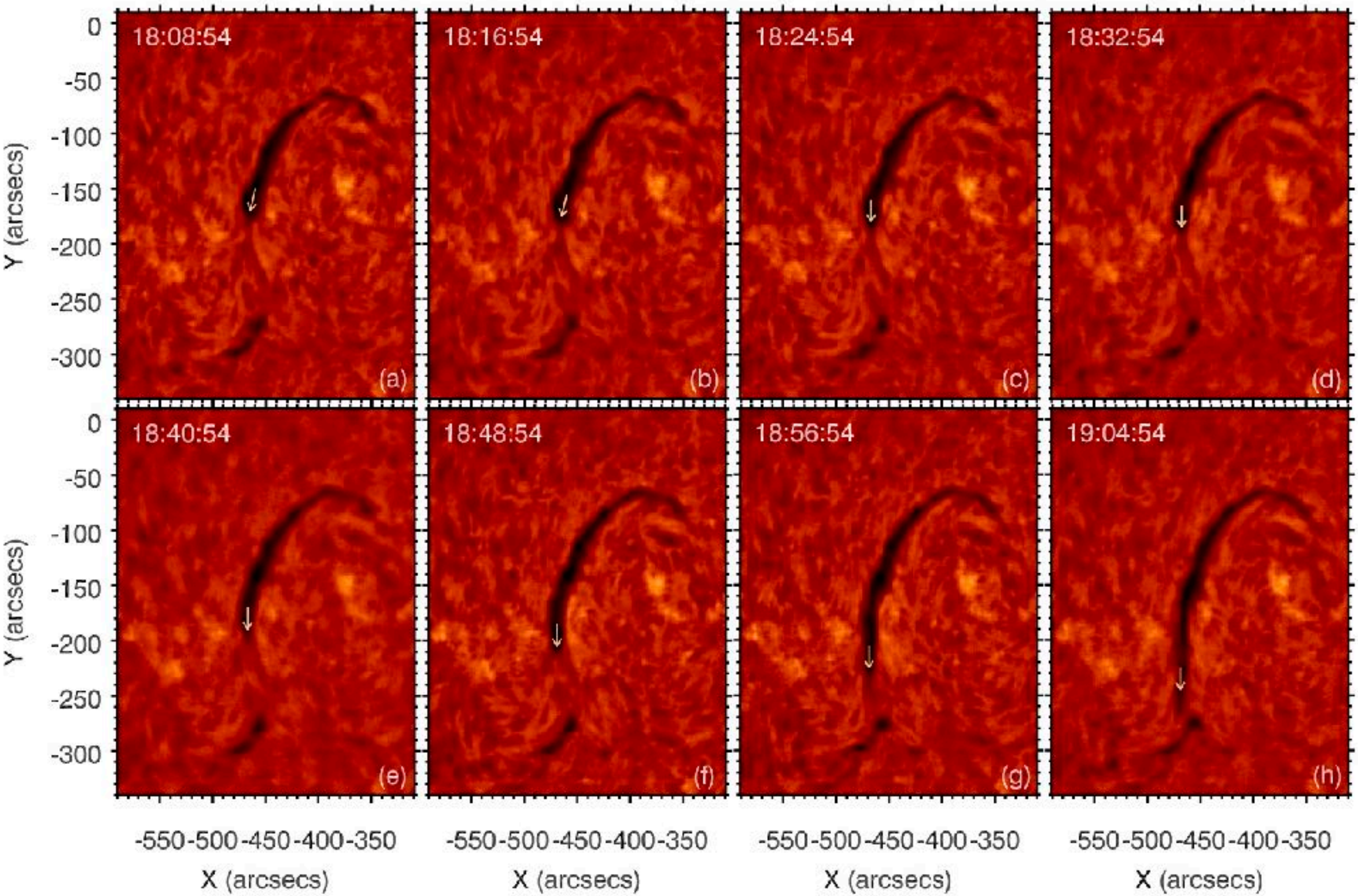

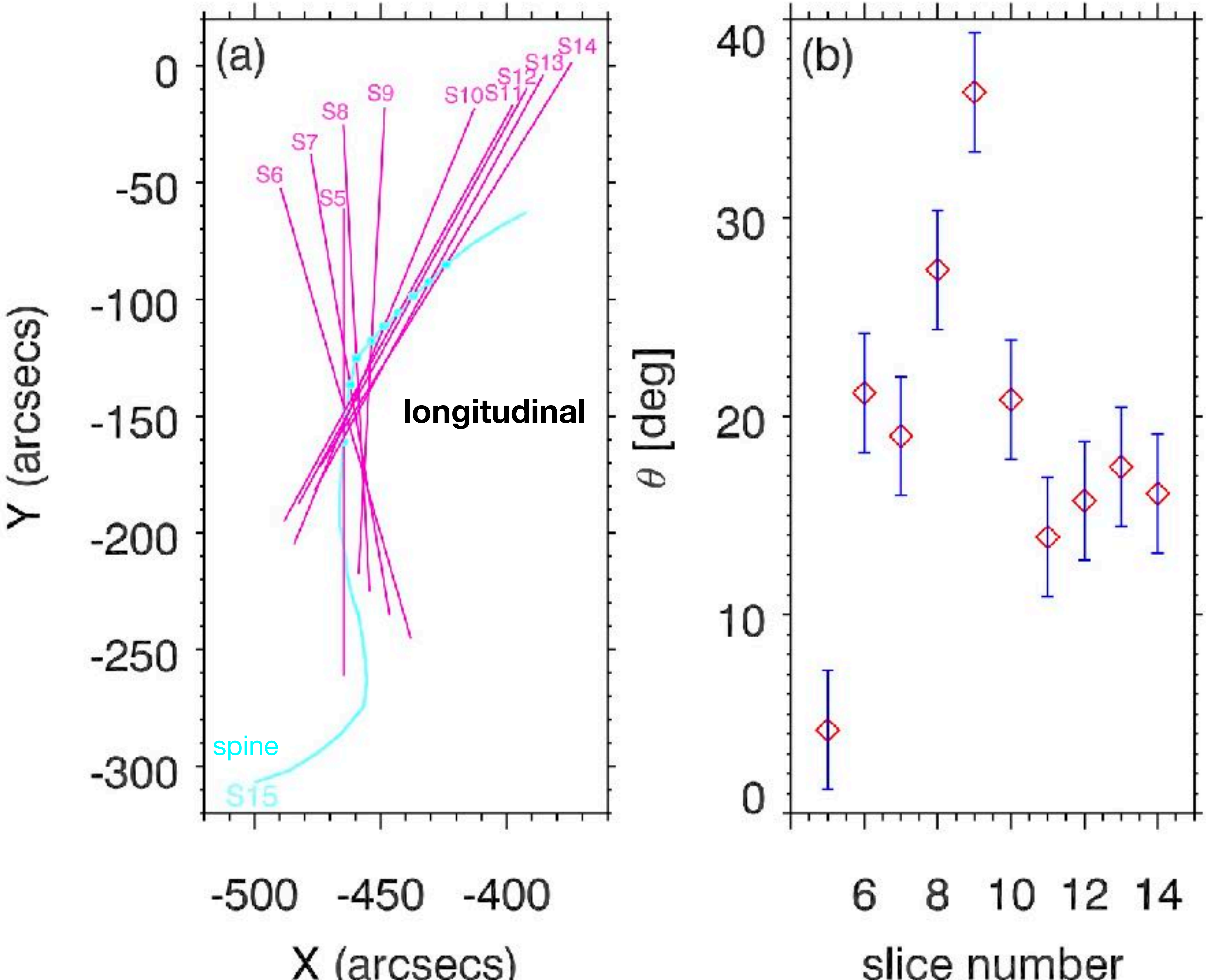

(a)
S5
S6
S7
S8
S9
S10
S11
S12
S13
S14
S15
spine
longitudinal
Y (arcsecs)
X (arcsecs)
0
-50
-100
-150
-200
-250
-300
-500
-450
-400
(b)
θ [deg]
slice number
0
10
20
30
40
6
8
10
12
14

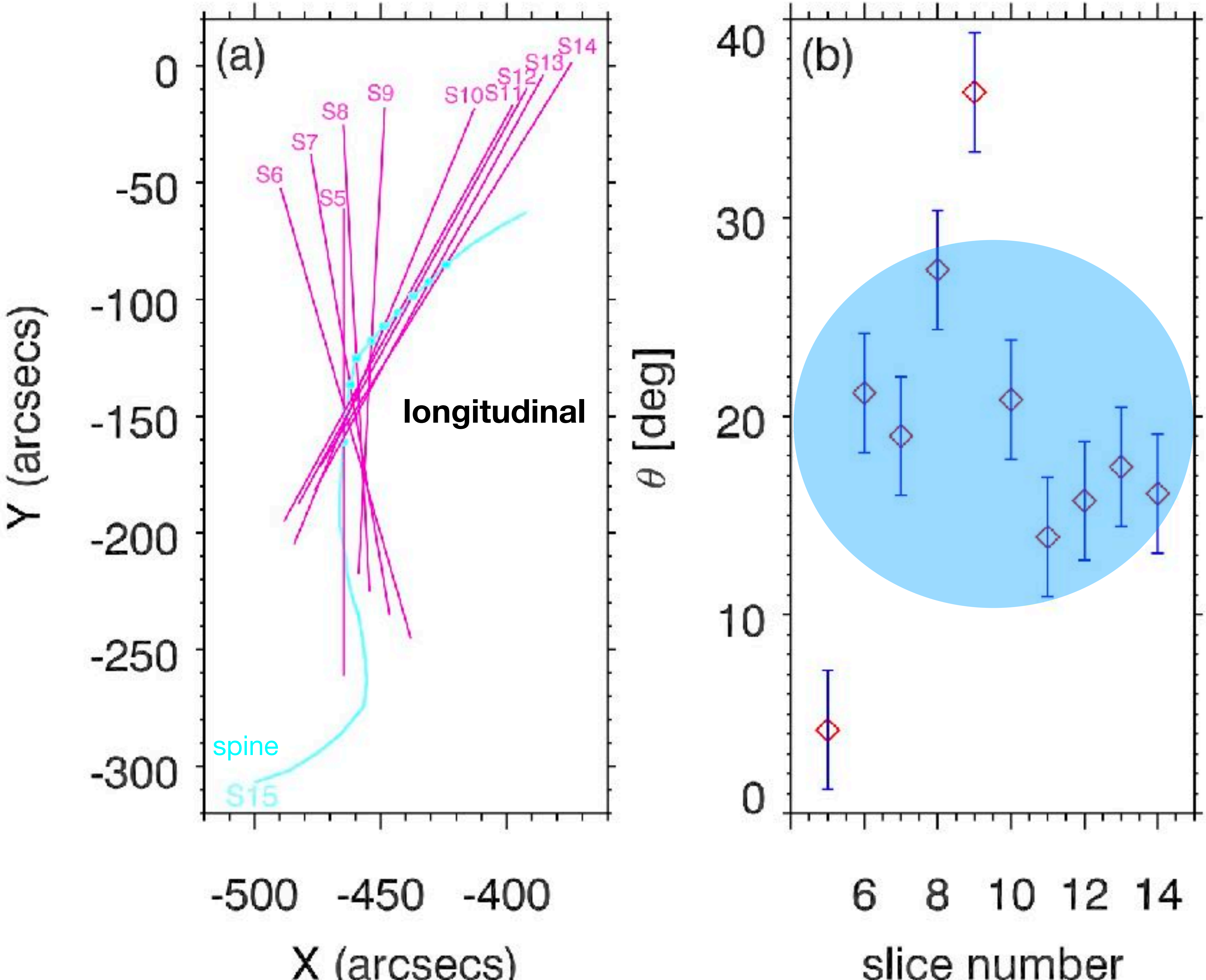

(a)
S14
S13
S12
S11
S10
S9
S8
S7
S6
S5
longitudinal
spine
S15
Y (arcsecs)
0
-50
-100
-150
-200
-250
-300
-500
-450
-400
X (arcsecs)
(b)
θ [deg]
40
30
20
10
0
6
8
10
12
14
slice number

evolution: MR -> oscillations -> mass drainage -> continuous oscillations

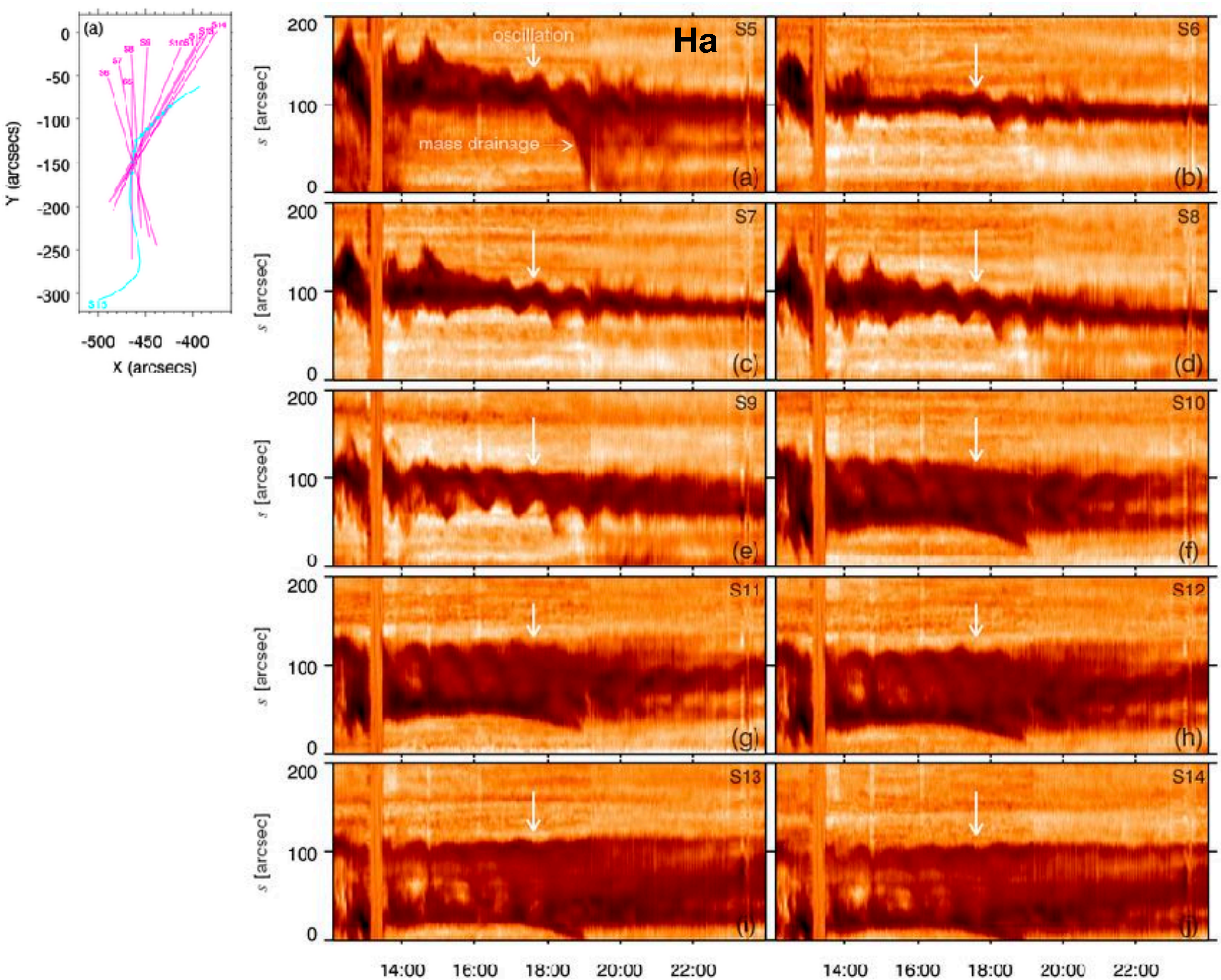

evolution: MR -> oscillations -> mass drainage -> continuous oscillations

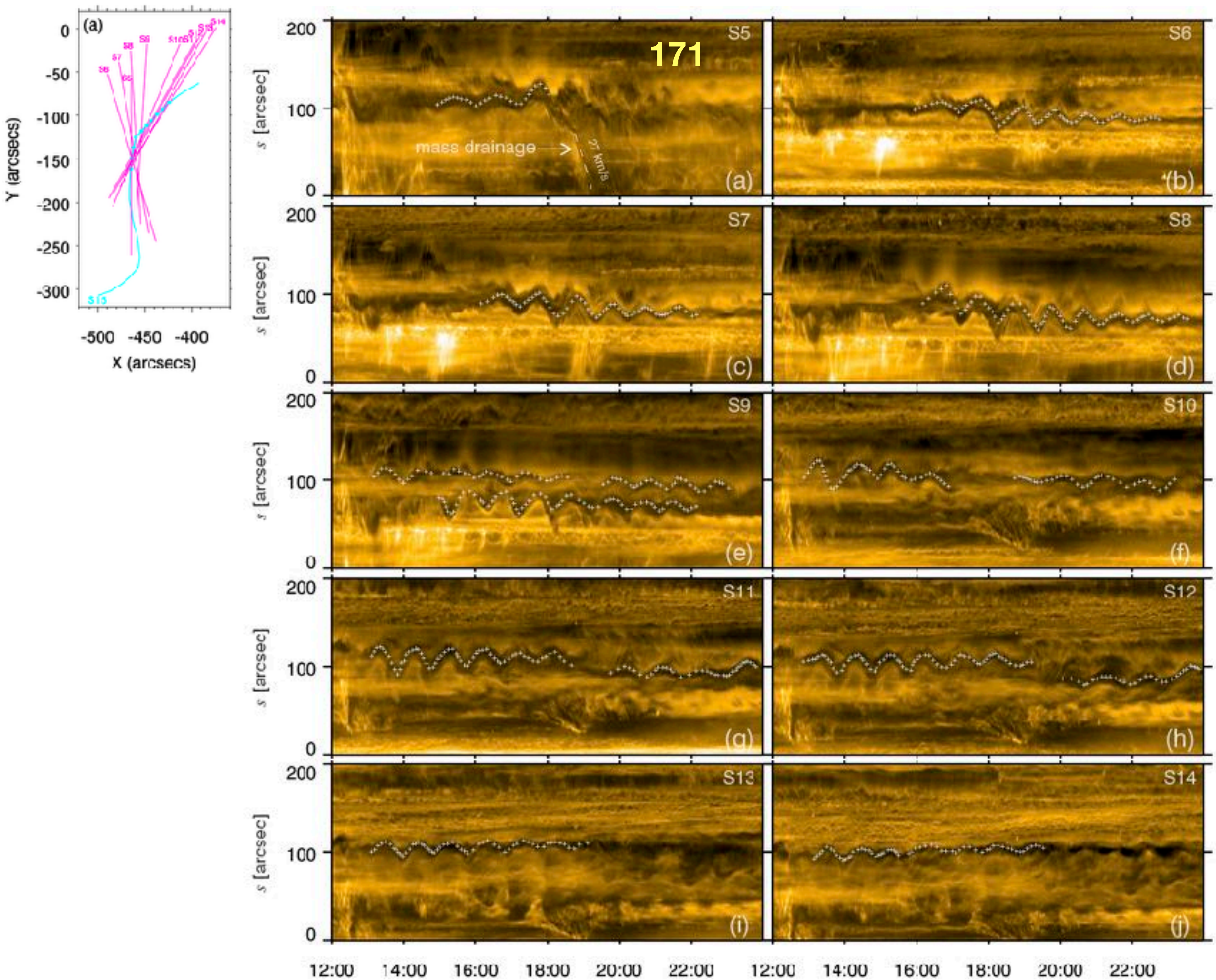

displacement: $$y = y_0 + bt + A\sin(\frac{2\pi}{P}t + \phi)e^{-t/\tau}$$ (mpfit.pro)

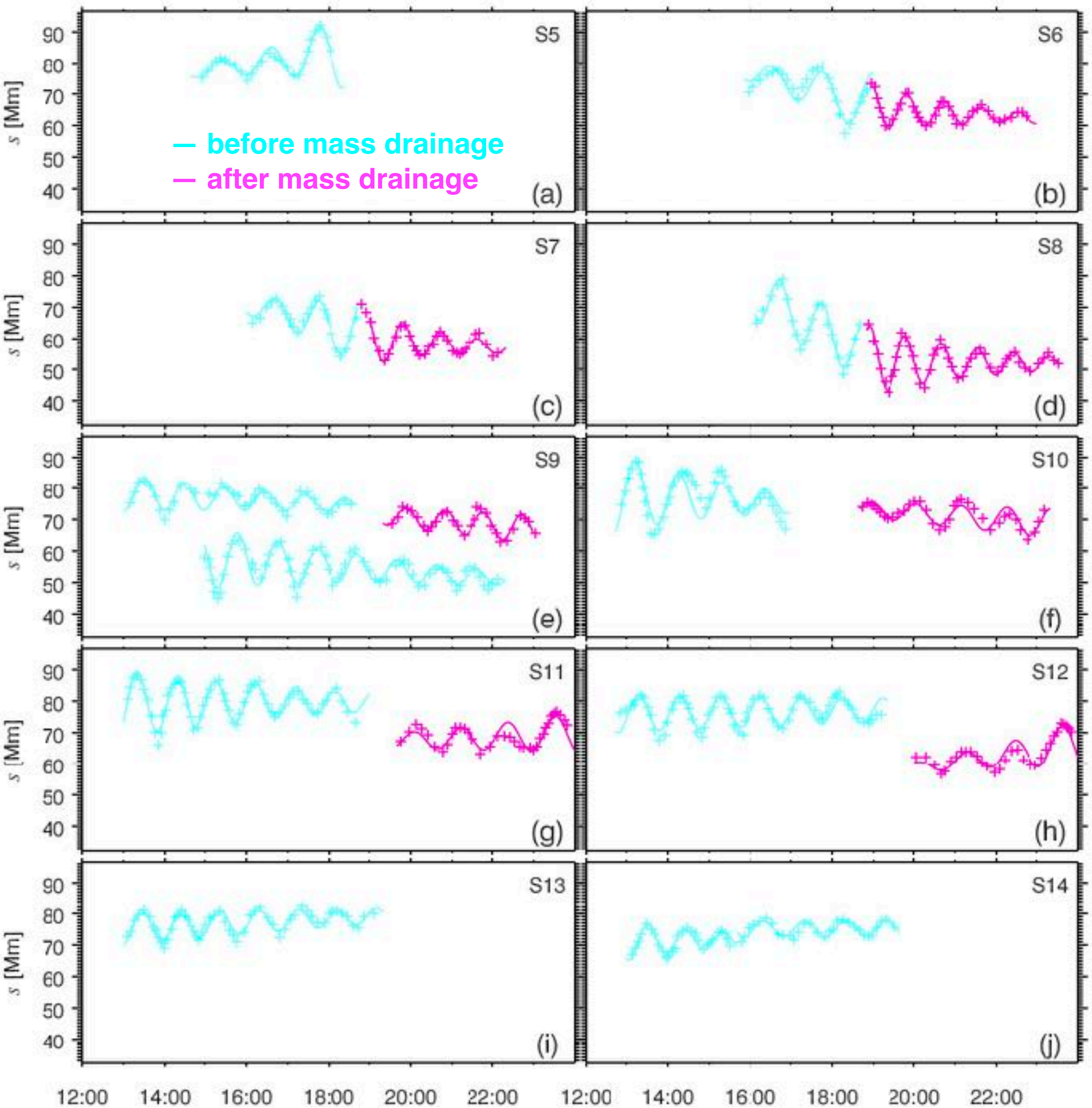

velocity: *v=dy/dt* ~30 km/s, large-amplitude

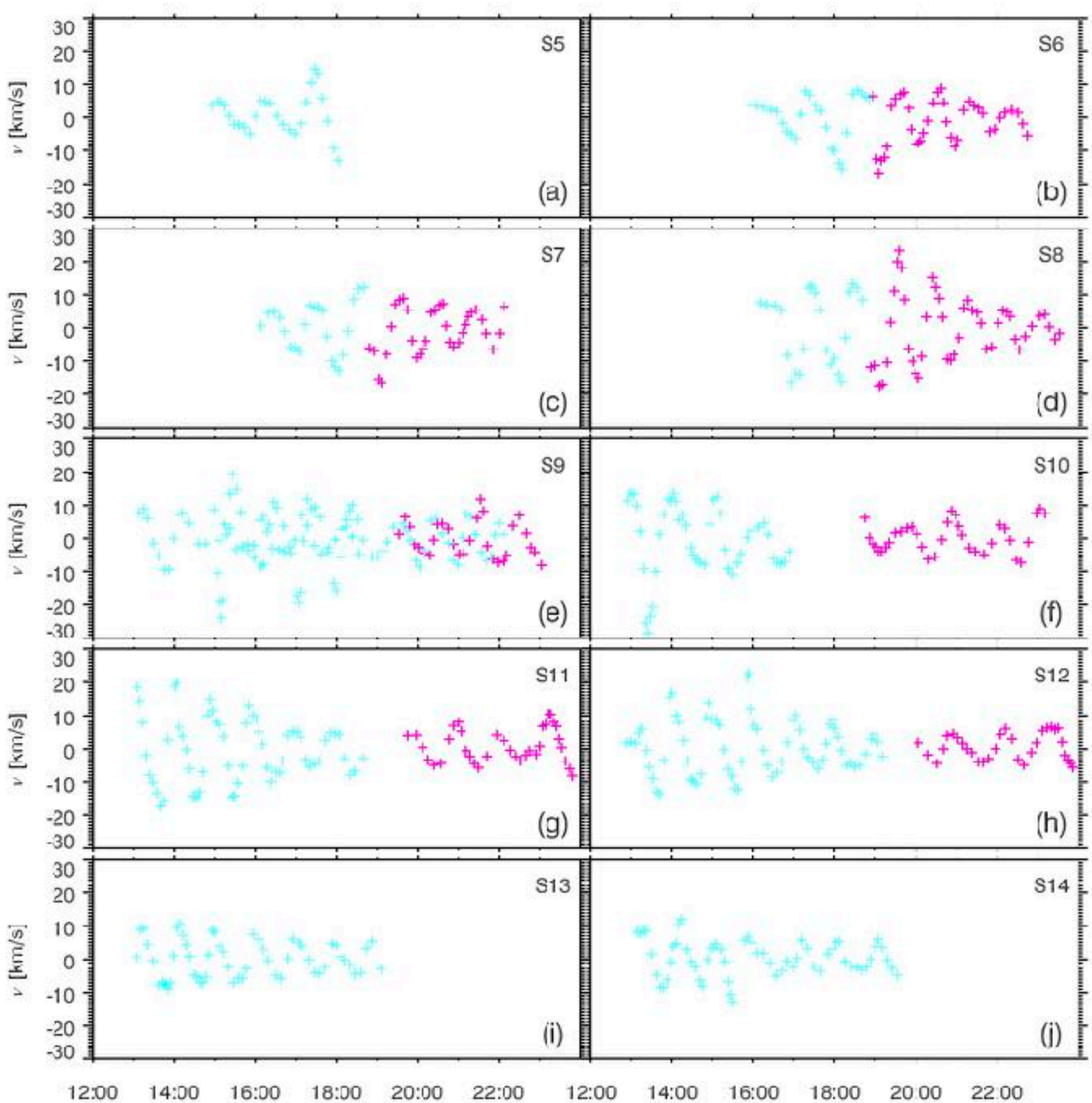

results of fitting

Slice	ϕ (rad)	P (s)	τ (s)	τ/P
S5	−0.96	4221.50	−6643.58	−1.57
S6	0.22	4392.44	−9488.63	−2.16
S6	0.17	3234.76	8968.83	2.77
S7	2.69	3892.72	−8192.06	−2.10
S7	1.42	3299.90	7555.92	2.29
S8	0.47	3647.18	−88302.90	−24.21
S8	−0.73	3162.51	10477.20	3.31
S9	1.37	3534.62	19656.30	5.56
S9	2.24	3386.17	−30292.90	−8.95
S9	−0.97	3495.27	16461.10	4.71
S10	3.77	3809.15	11387.30	2.99
S10	2.94	3978.81	−25054.50	−6.30
S11	2.30	3468.91	18338.90	5.29
S11	4.54	4135.59	−16907.70	−4.09
S12	2.75	3559.89	48121.20	13.52
S12	−1.09	4211.97	−9133.60	−2.17
S13	1.42	3429.04	27612.80	8.05
S14	0.35	3245.81	8304.86	2.56
S14	−0.81	3573.13	373353.00	104.49

Out of phase oscillations

not a rigid body

— **before mass drainage**

— **after mass drainage**

Damp

Grow

COMPLEX OSCILLATIONS

results of fitting

Slice	ϕ (rad)	P (s)
S5	−0.96	4221.50
S6	0.22	4392.44
S6	0.17	3234.76
S7	2.69	3892.72
S7	1.42	3299.90
S8	0.47	3647.18
S8	−0.73	3162.51
S9	1.37	3534.62
S9	2.24	3386.17
S9	−0.97	3495.27
S10	3.77	3809.15
S10	2.94	3978.81
S11	2.30	3468.91
S11	4.54	4135.59
S12	2.75	3559.89
S12	−1.09	4211.97
S13	1.42	3429.04
S14	0.35	3245.81
S14	−0.81	3573.13

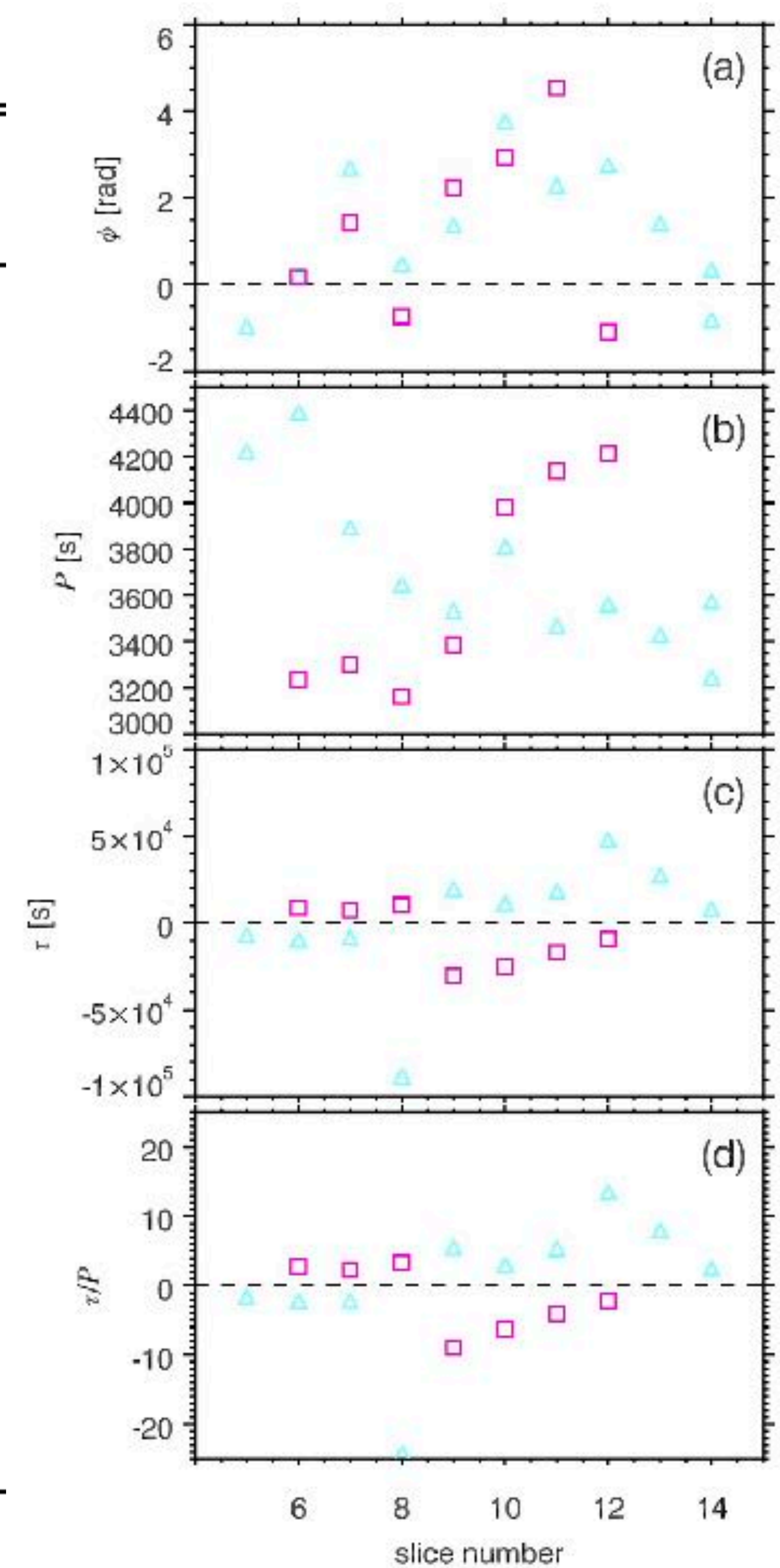

Out of phase oscillations

not a rigid body

— before mass drainage
— after mass drainage

Damp

Grow

COMPLEX OSCILLATIONS

restoring force of longitudinal oscillation:

1. **gravity of the filament** (Luna & Karpen 2012; Luna et al. 2012; Zhang et al. 2012, 2013; Luna et al. 2016a,b)
2. **gravity+magnetic tension** (Li & Zhang 2012)
3. **gravity+magnetic pressure** (Shen et al. 2014)
4. **magnetic pressure gradient** (Vrsnak et al. 2007)

$$P = 2\pi\sqrt{\frac{R}{g_\odot}}, \quad R = 2w^2/(D\pi^2)$$

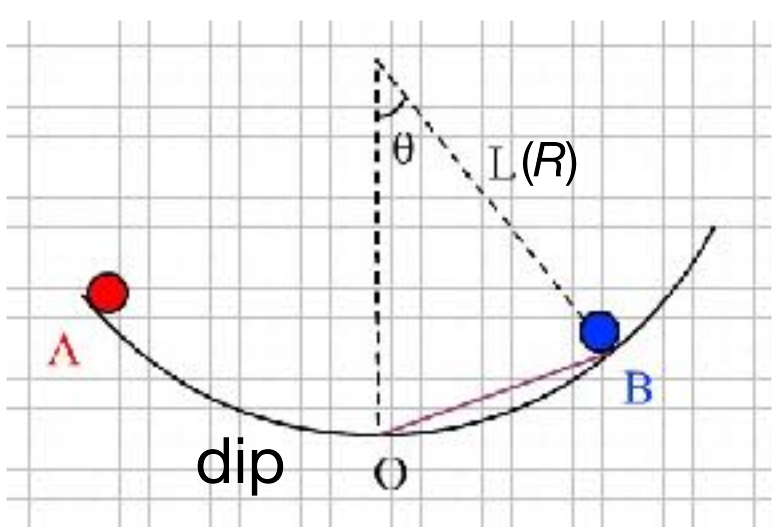

pendulum

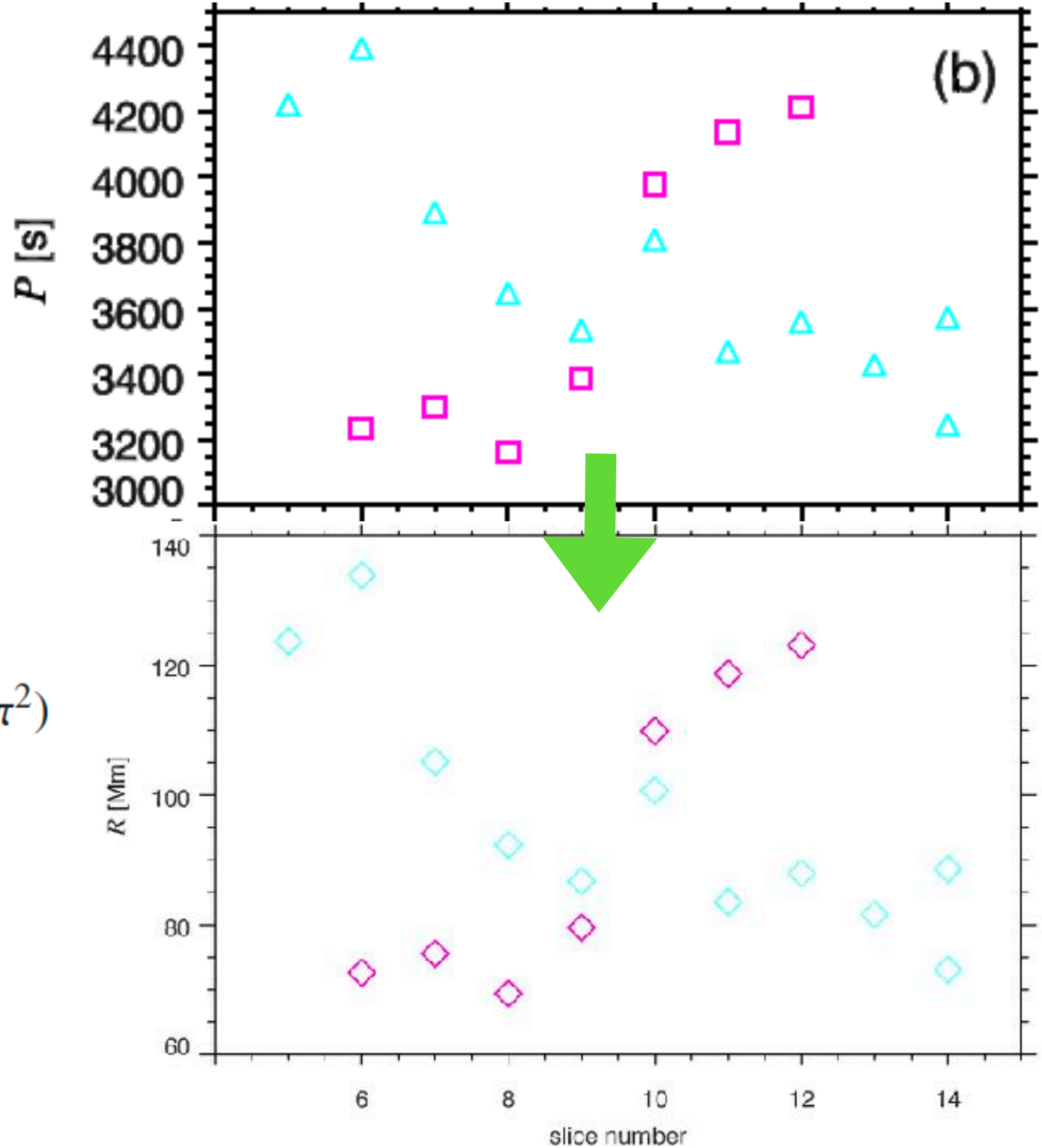

How to interpret the oscillations? thread-thread interactions

Zhou et al. 2017

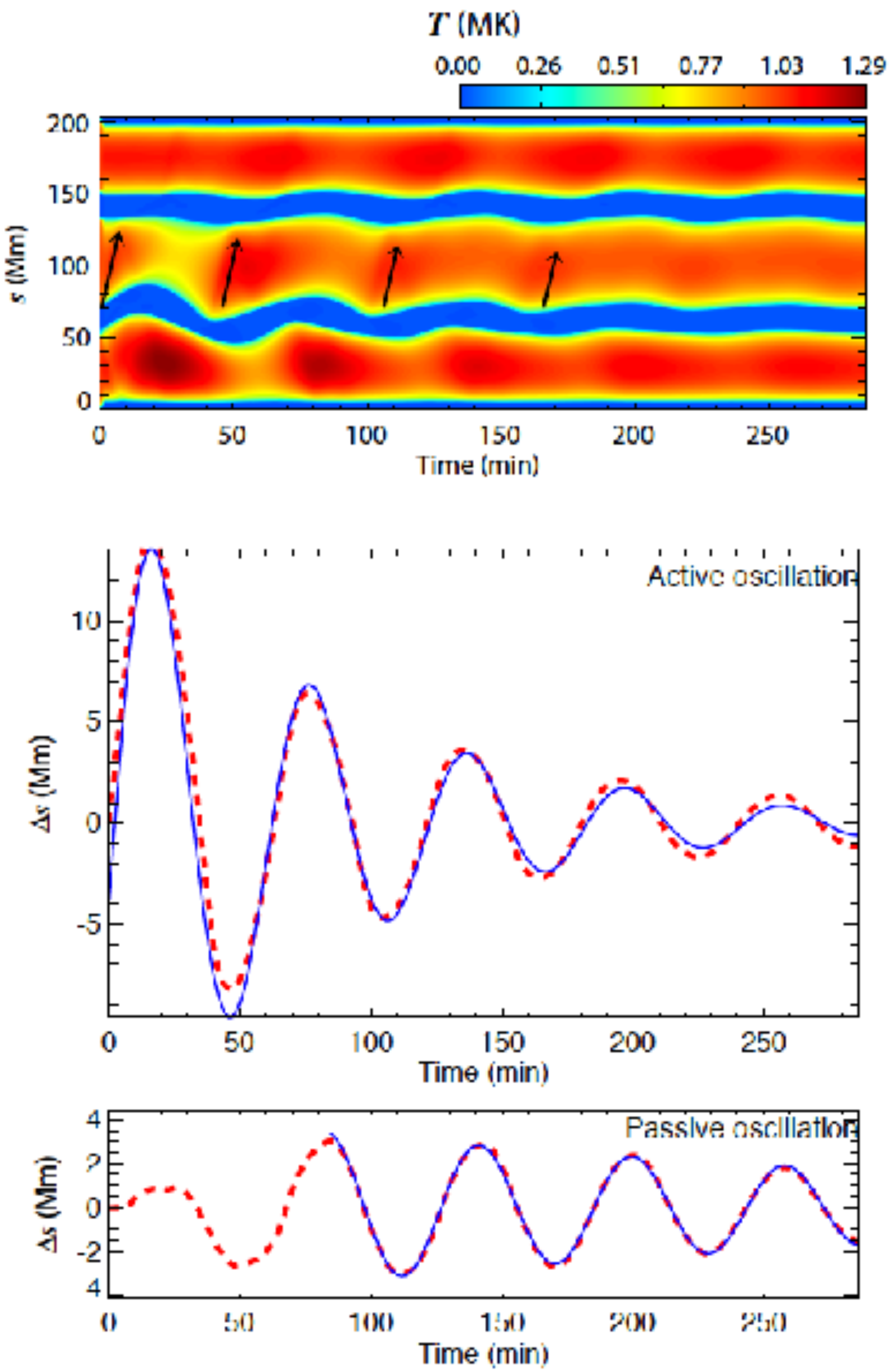

schematic cartoon

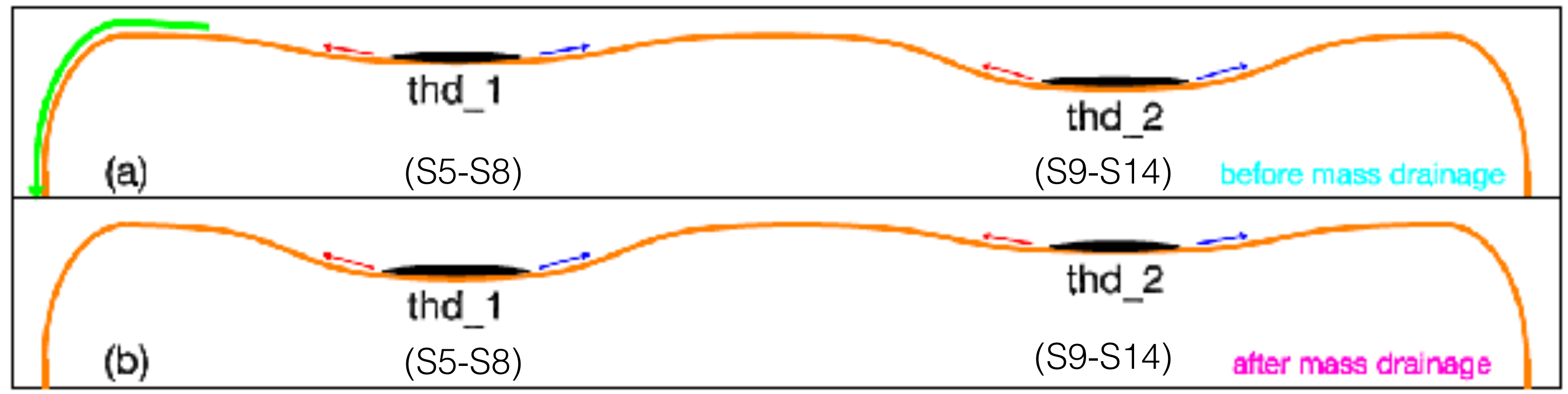

	thd_1	thd_2
before mass drainage	passive oscillation growing longer period	active oscillation damping shorter period
after mass drainage	active oscillation damping shorter period	passive oscillation growing longer period

mass drainage may play an important role
in altering the magnetic configuration

Part 4 Simultaneous Transverse and Longitudinal Oscillations in a Quiescent Prominence Triggered by a Coronal Jet

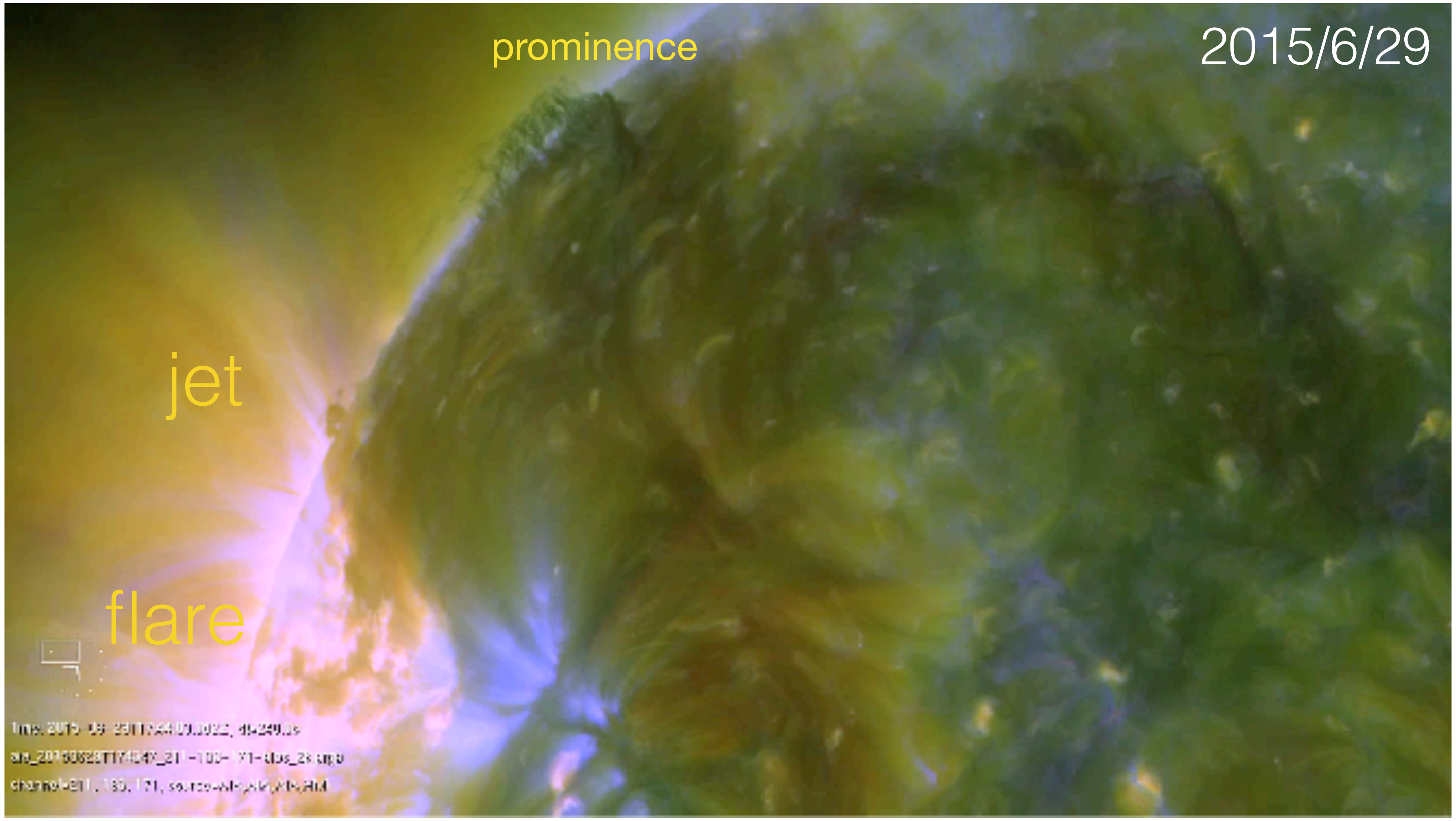

Part 4 Simultaneous Transverse and Longitudinal Oscillations in a Quiescent Prominence Triggered by a Coronal Jet

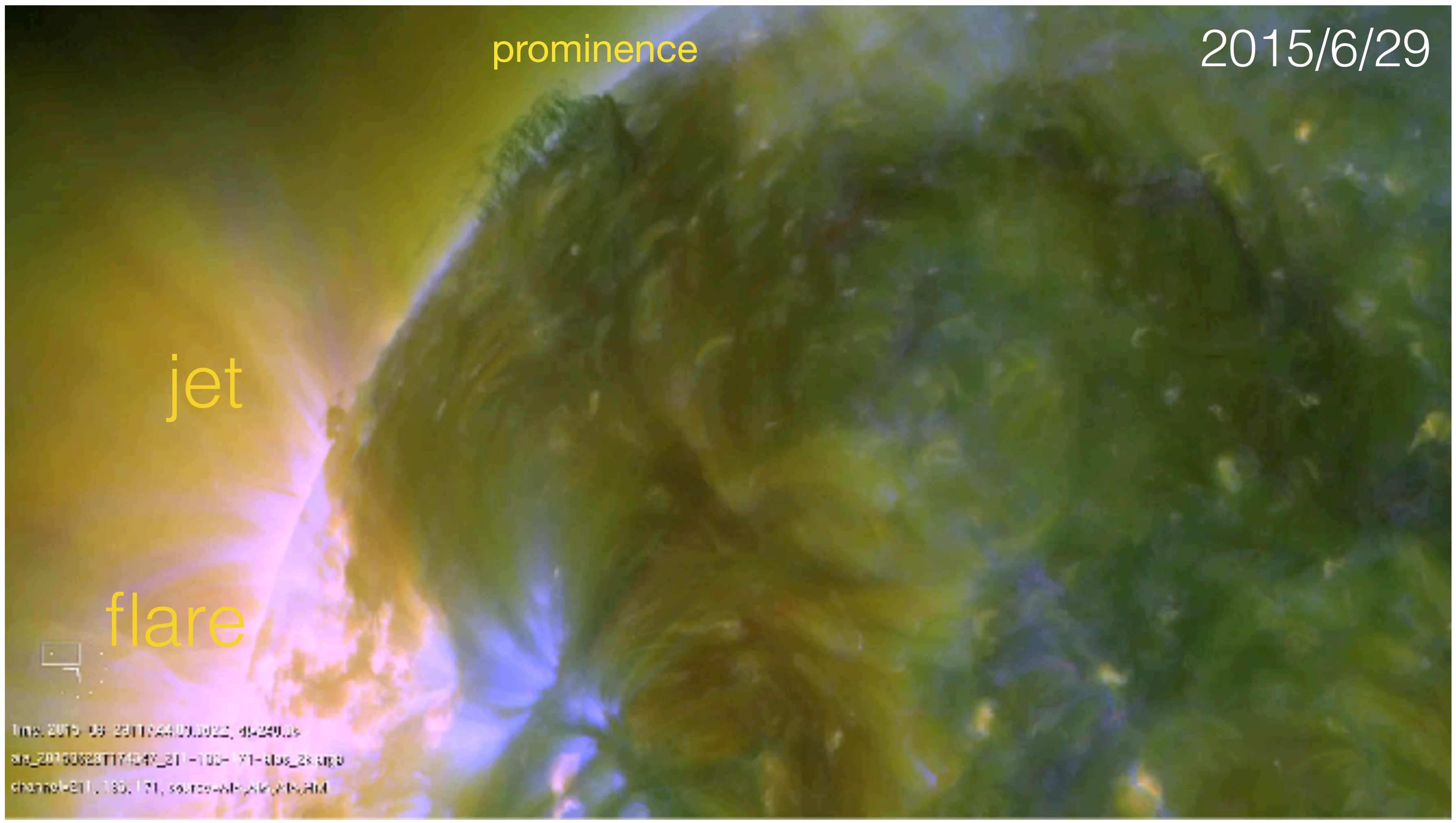

The prominence and AR 12373 in Ha and EUV wavelengths

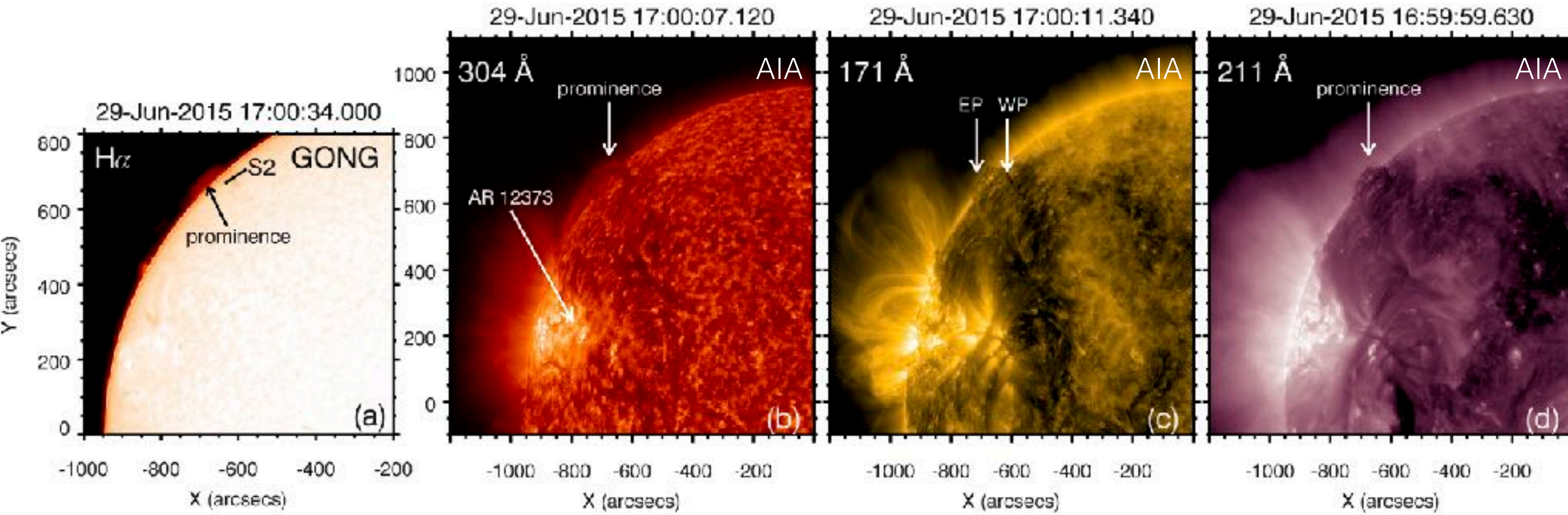

EP: eastern part of prominence
WP: western part of prominence

HMI LOS magnetogram & PFSS magnetic field lines

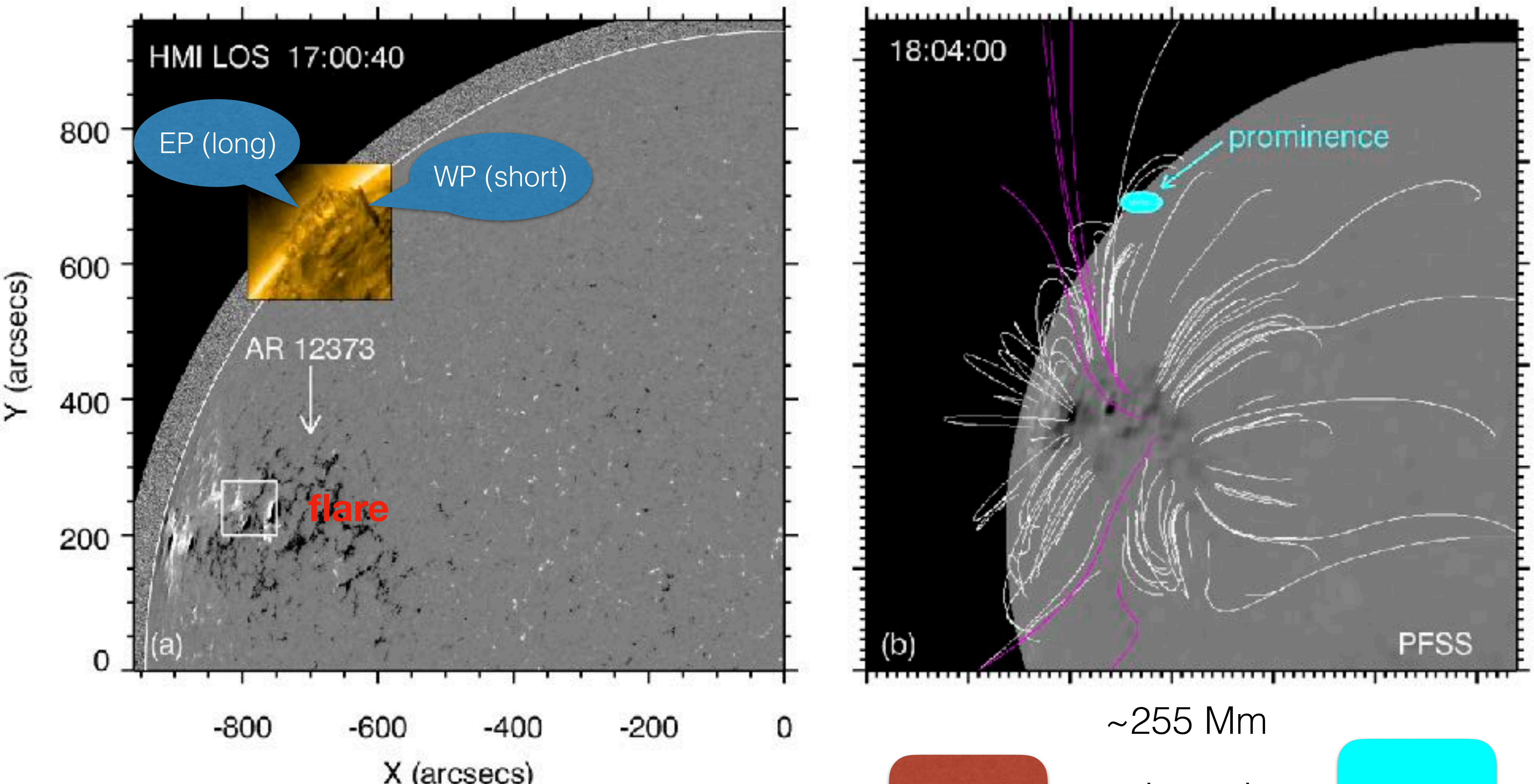

~255 Mm

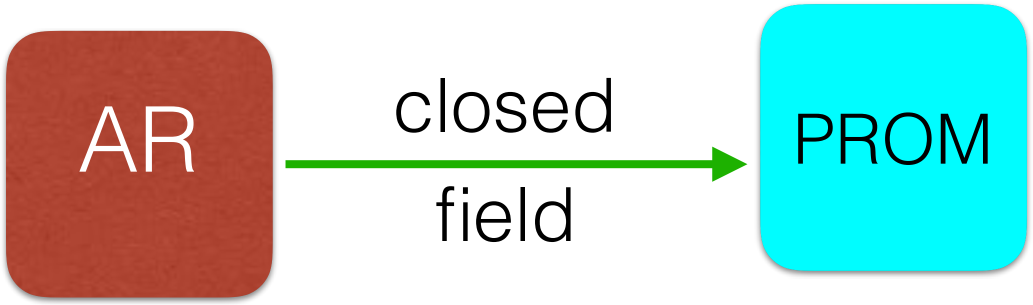

AIA base-difference images in 171 A

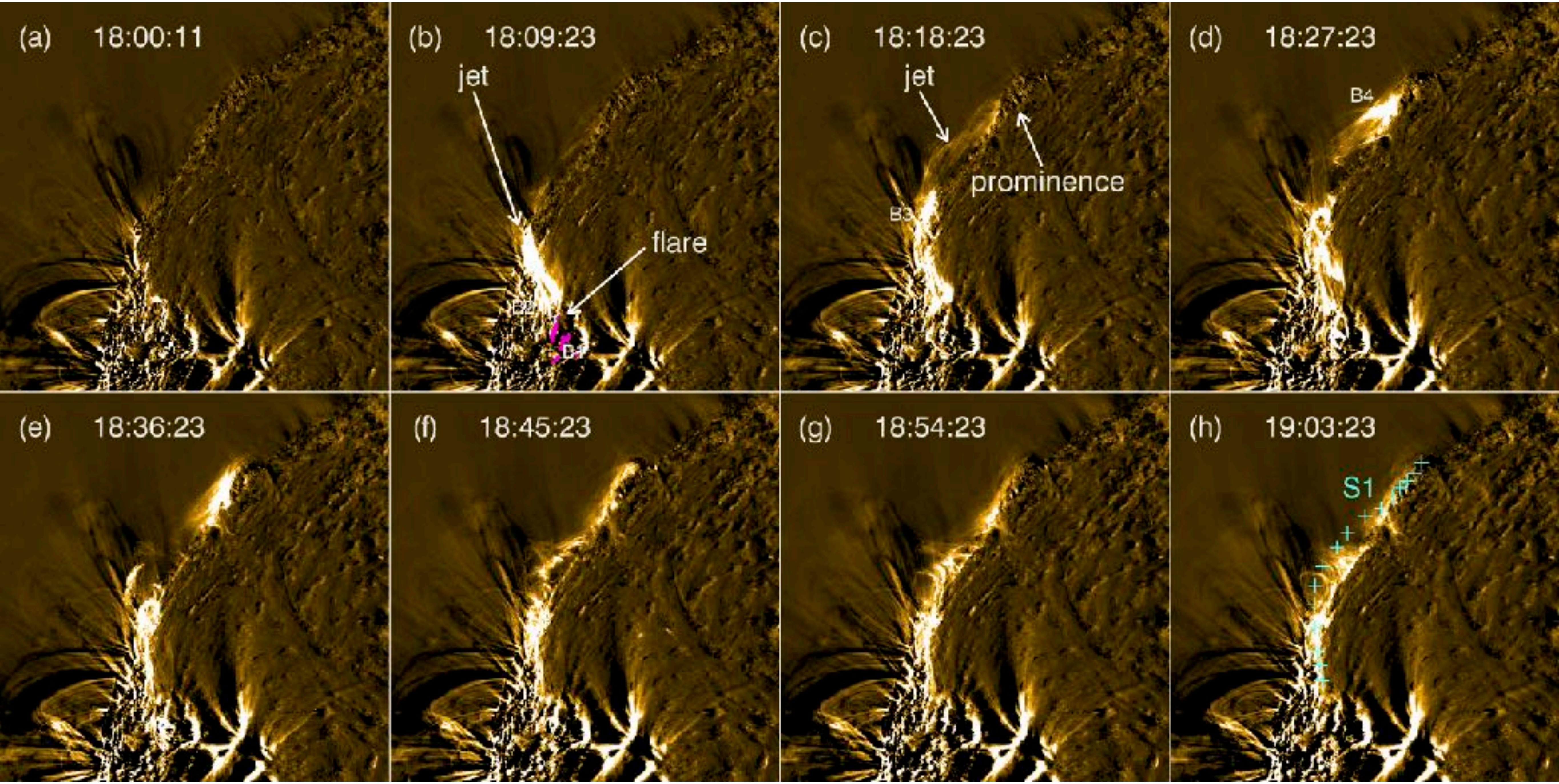

base-difference images

original image

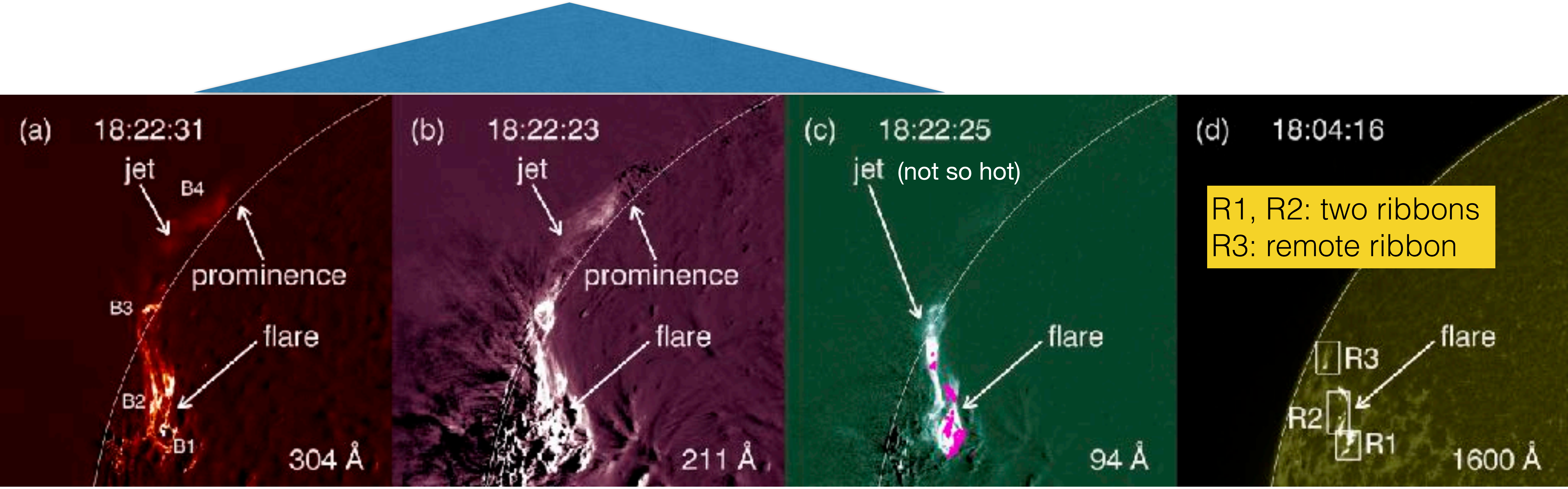

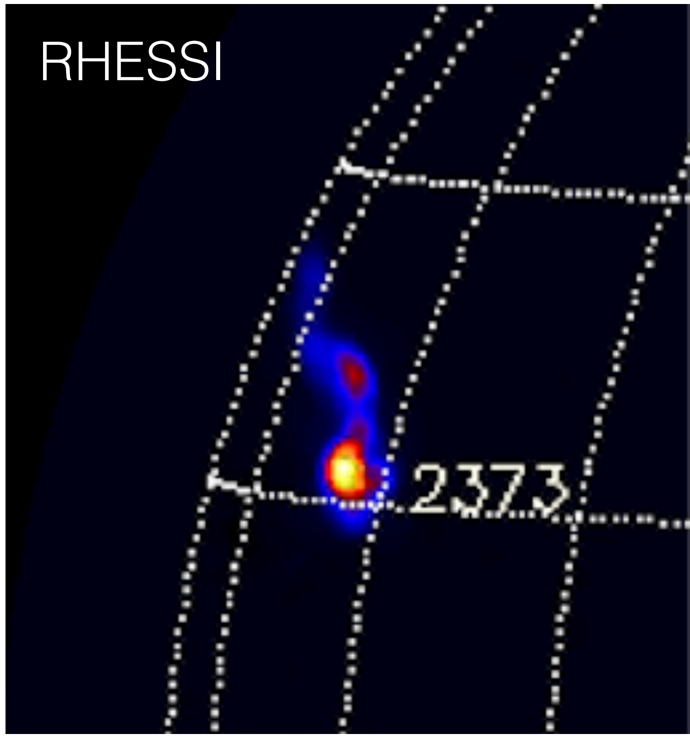

light curves of the flare

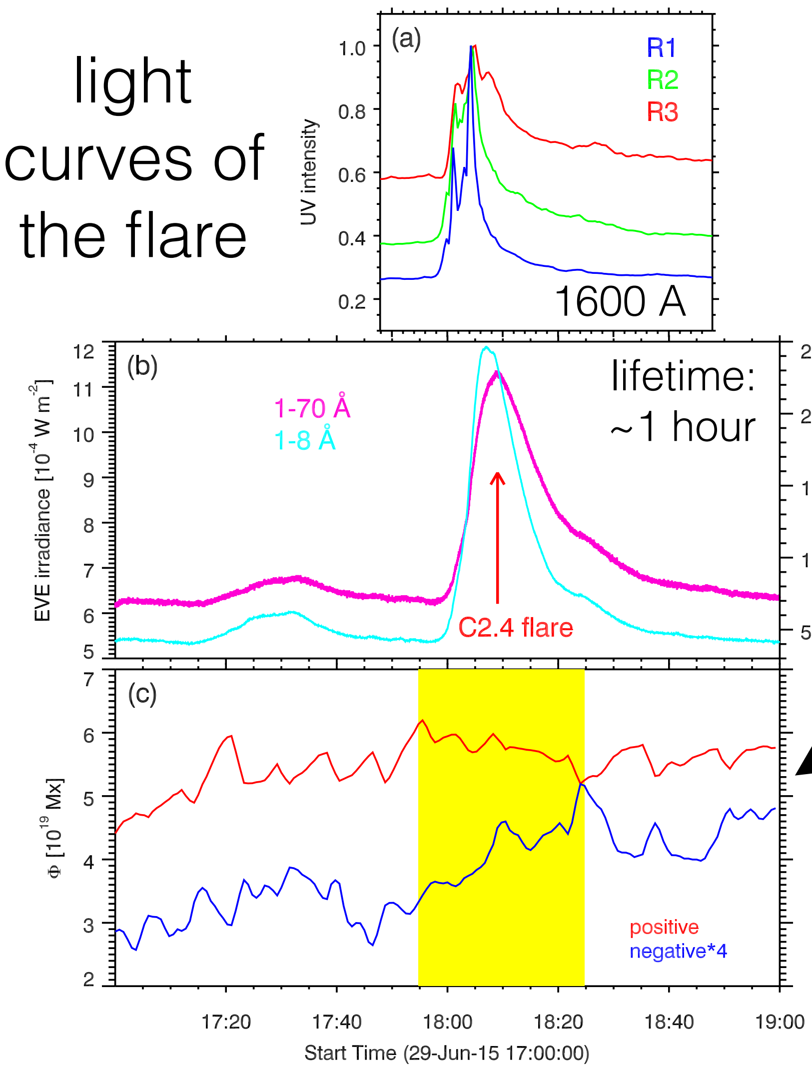

HMI LOS magnetograms

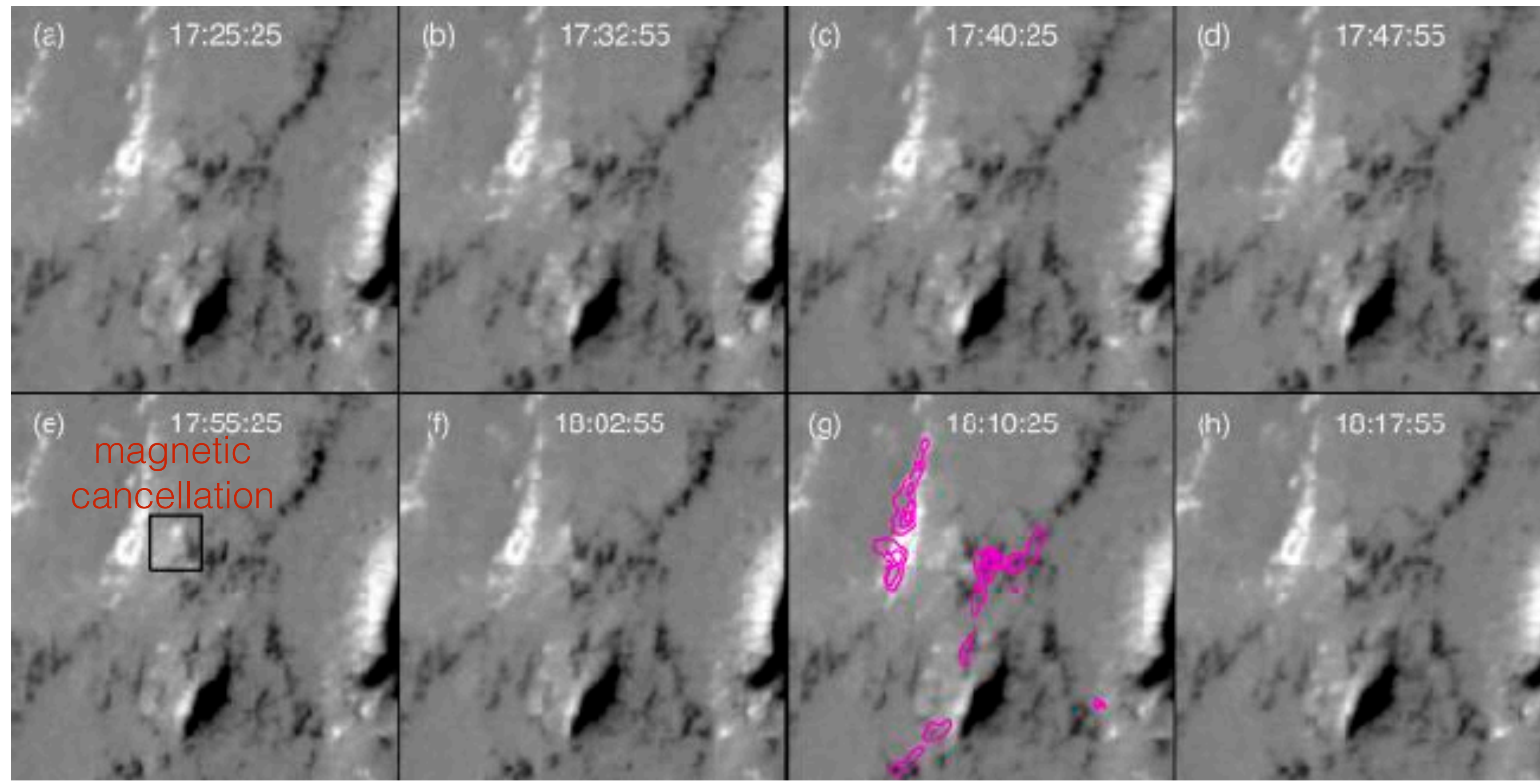

flare & jet were possibly triggered by magnetic cancellation time-slice diagrams along S1

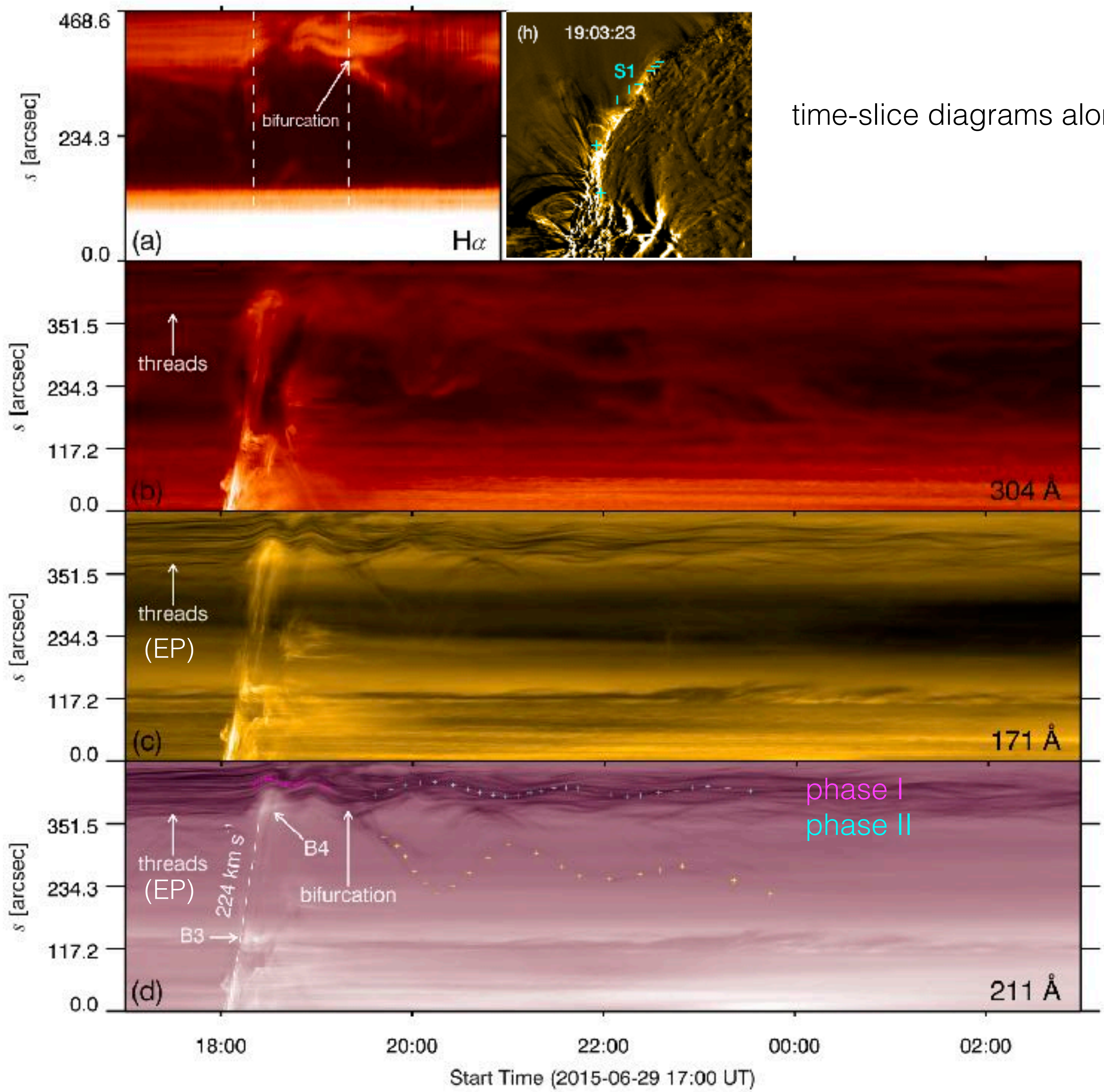

transverse oscillation of EP

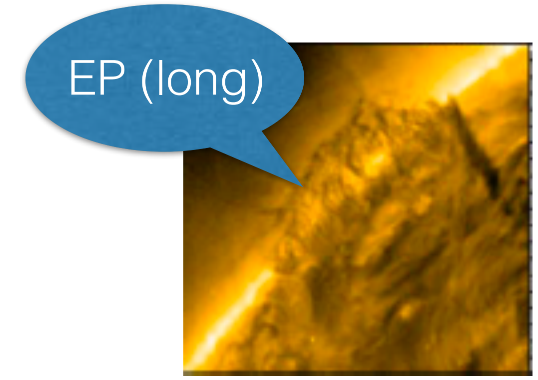

curve-fitting: $$y = y_0 + bt + A_0 \sin(\frac{2\pi}{P}t + \phi_0)e^{-t/\tau}$$

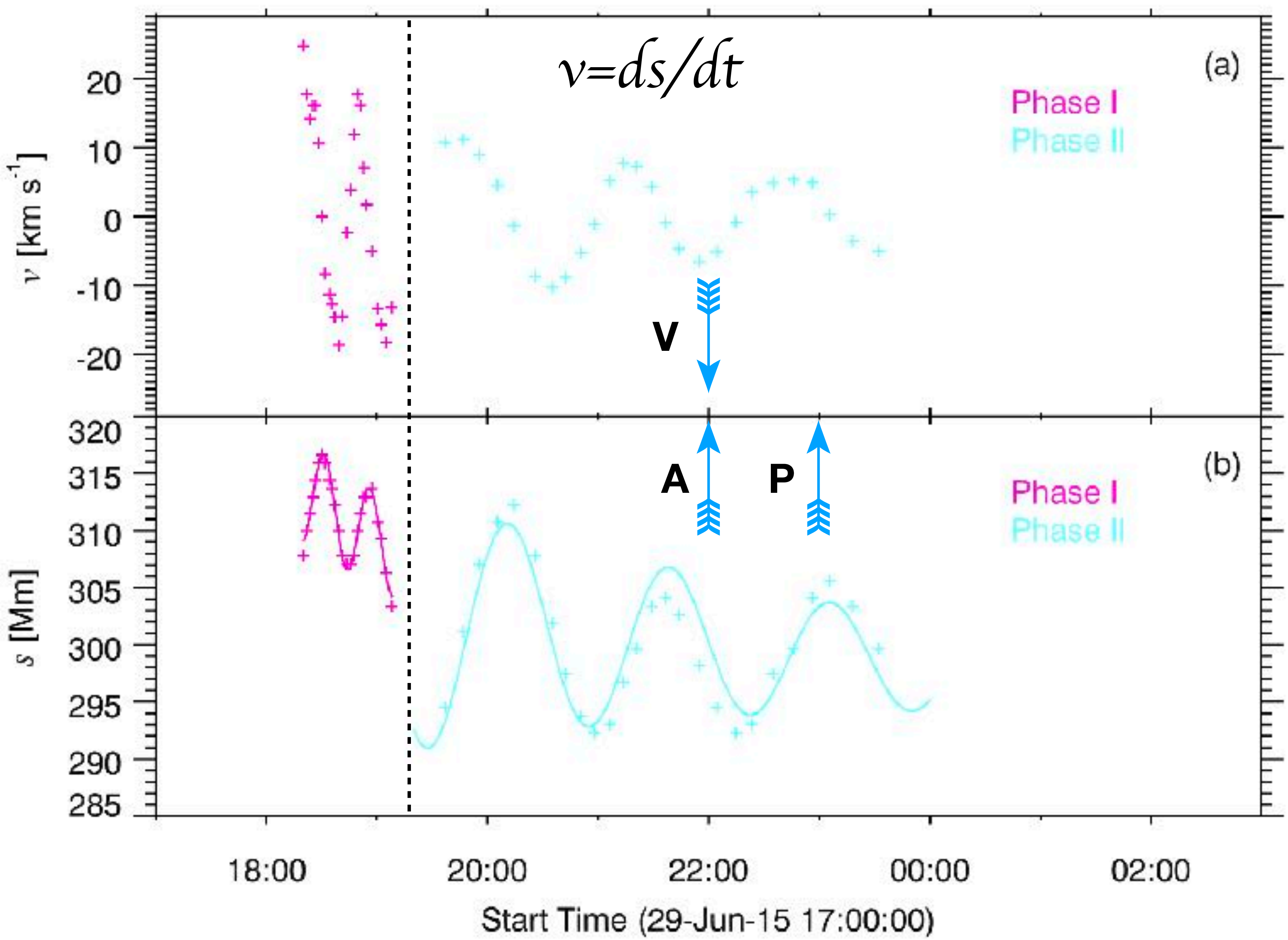

transverse oscillation of WP

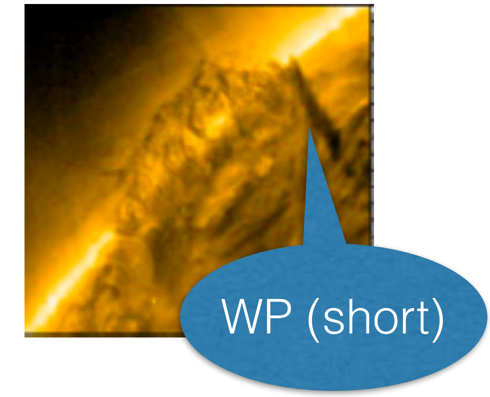

time-slice diagram along S2

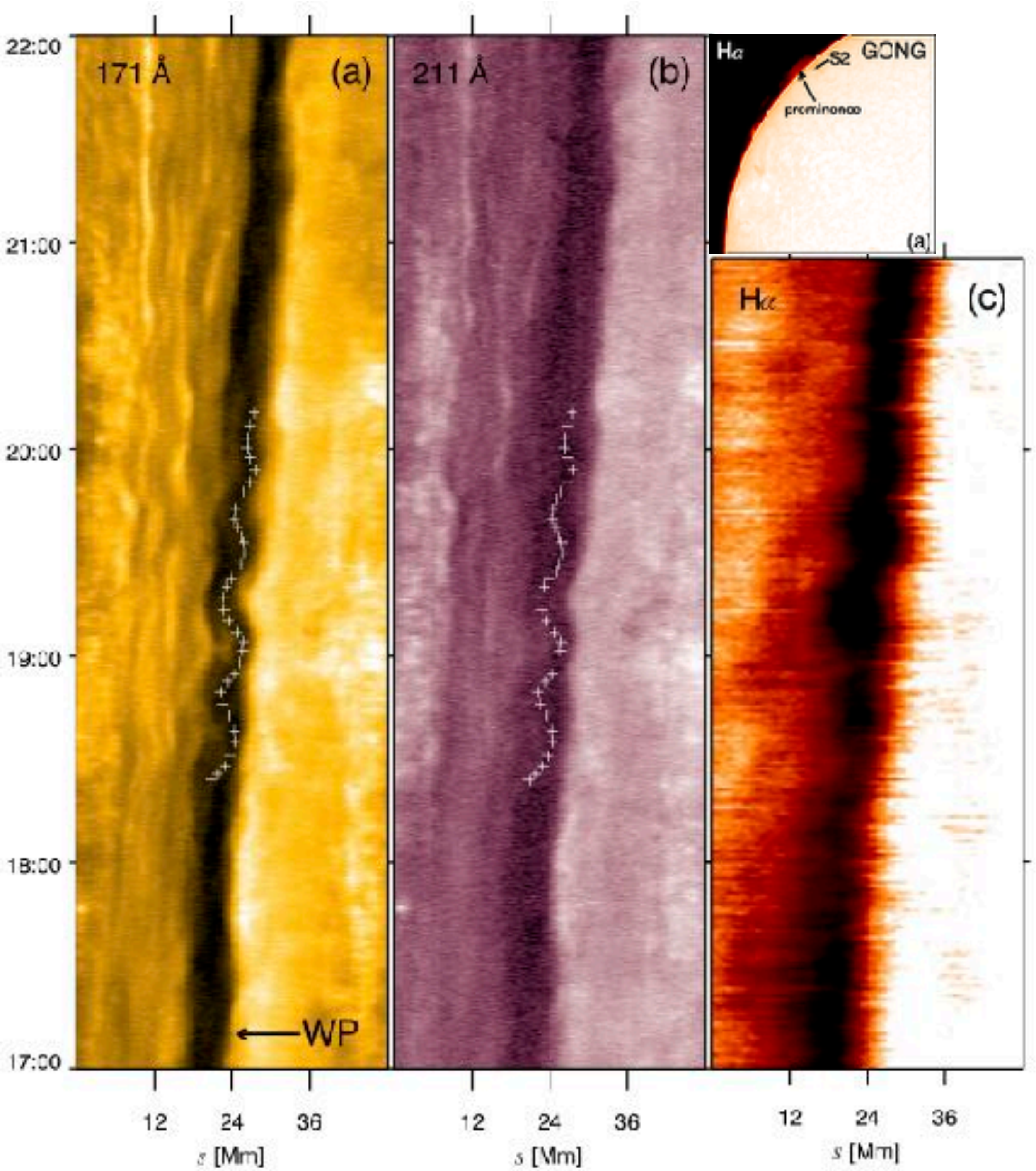

curve-fitting:

$$y = y_0 + bt + A_0 \sin(\frac{2\pi}{P}t + \phi_0)e^{-t/\tau}$$

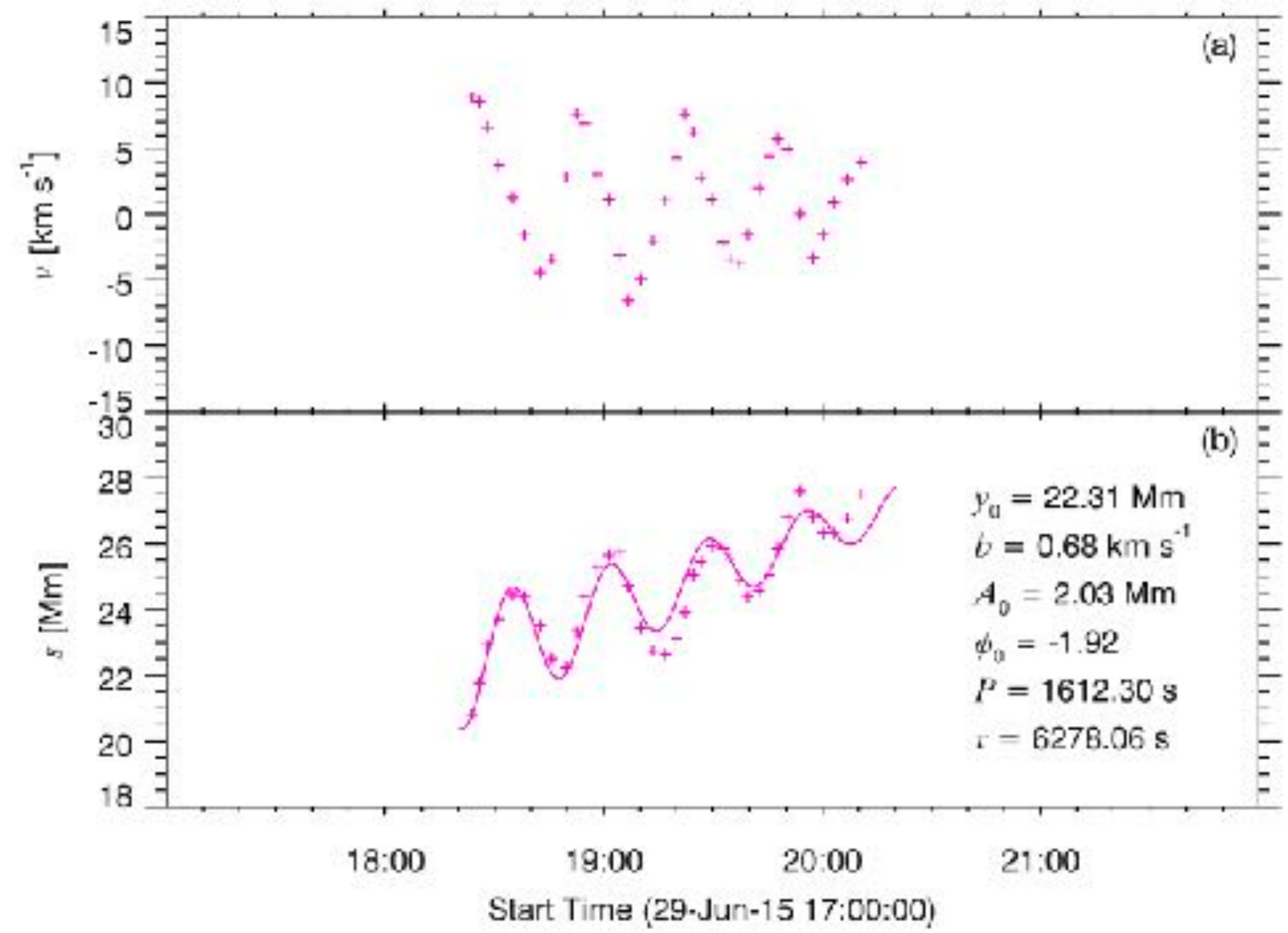

longitudinal oscillation of horizontal threads

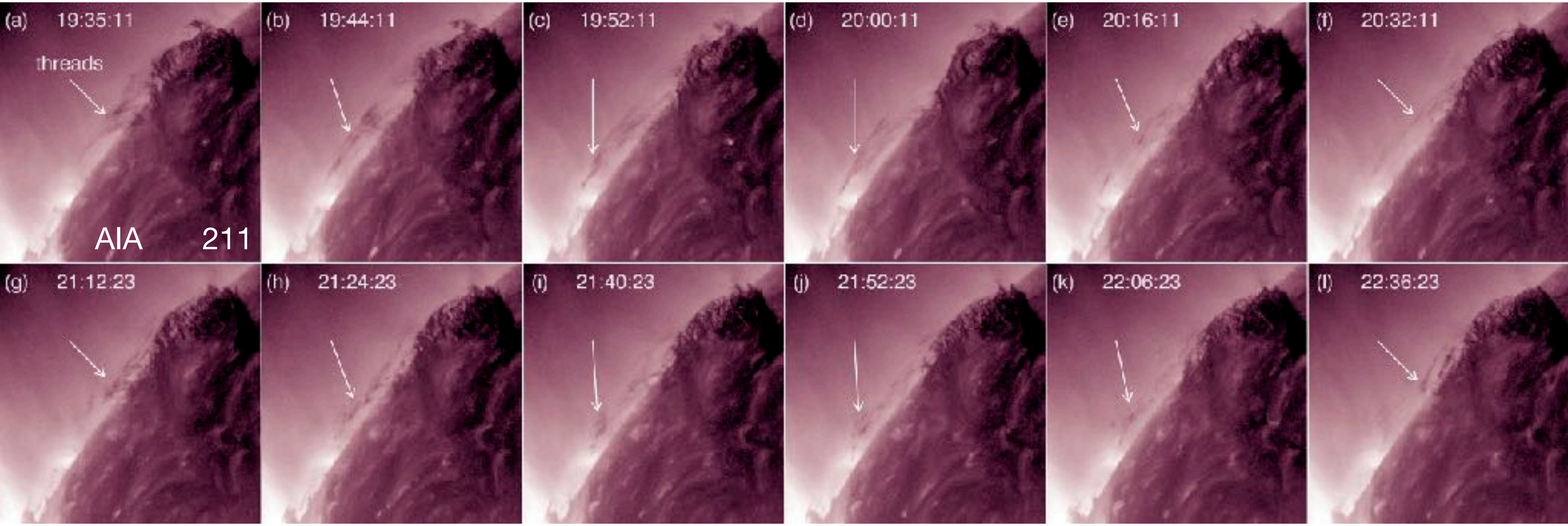

longitudinal oscillation of horizontal threads

curve fitting: $$y = y_0 + bt + A_0 \sin(\frac{2\pi}{P} t + \phi_0) e^{-t/\tau}$$

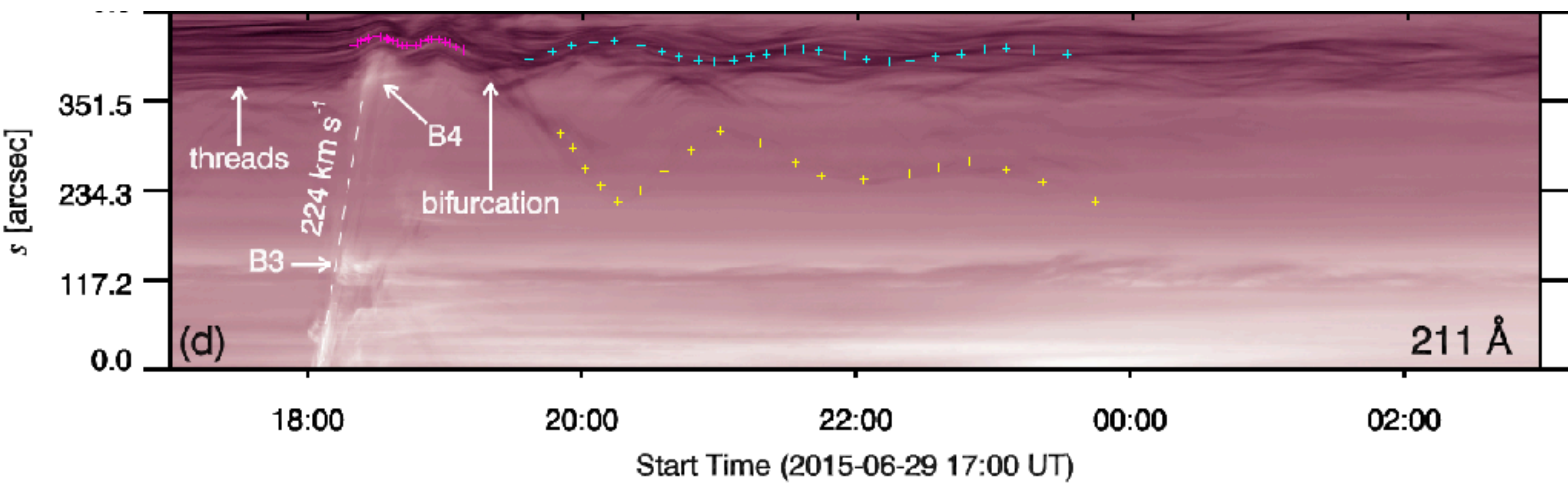

longitudinal oscillation of horizontal threads

curve fitting: $$y = y_0 + bt + A_0 \sin(\frac{2\pi}{P}t + \phi_0)e^{-t/\tau}$$

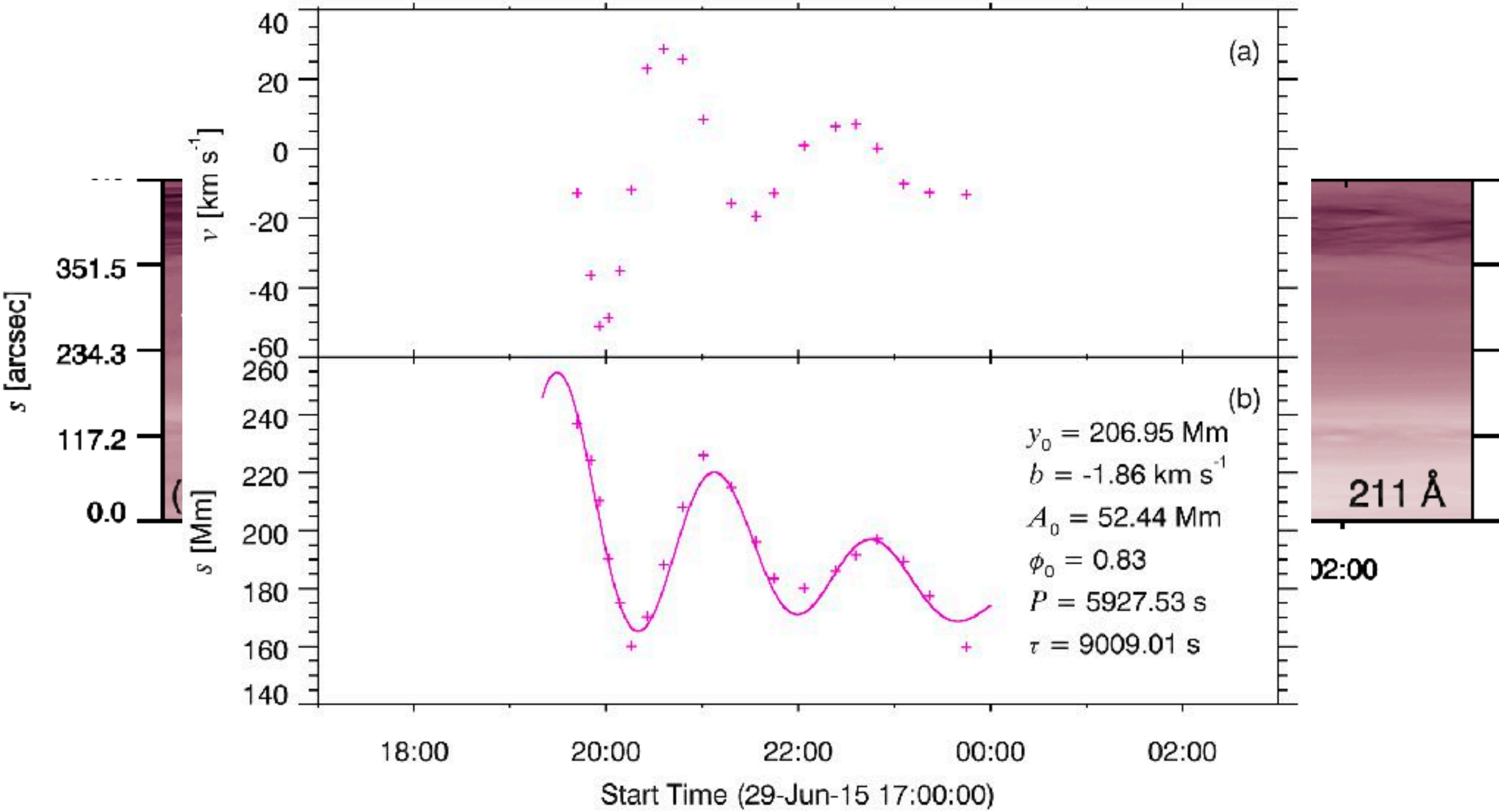

Table 2. Fitted parameters of the prominence oscillations

	Time (UT)	b (km s^{-1})	A_0 (Mm)	ϕ_0 (rad)	P (min)	τ (hr)	τ/P	type
EP	18:20–19:20[a]	-1.80	4.49	-1.30	24.85	7.53	18.18	transverse
	19:20–23:59[b]	-0.23	11.27	-2.15	87.41	4.42	3.03	transverse
WP	18:20–20:20[c]	0.68	2.03	-1.92	26.87	1.74	3.89	transverse
	19:20–23:59[d]	-1.86	52.44	0.83	98.72	2.50	1.52	longitudinal

[a]Phase I of the prominence oscillation of EP
[b]Phase II of the prominence oscillation of EP
[c]Time of the prominence oscillation of WP
[d]Time of the horizontal threads oscillation

time-line of all activities

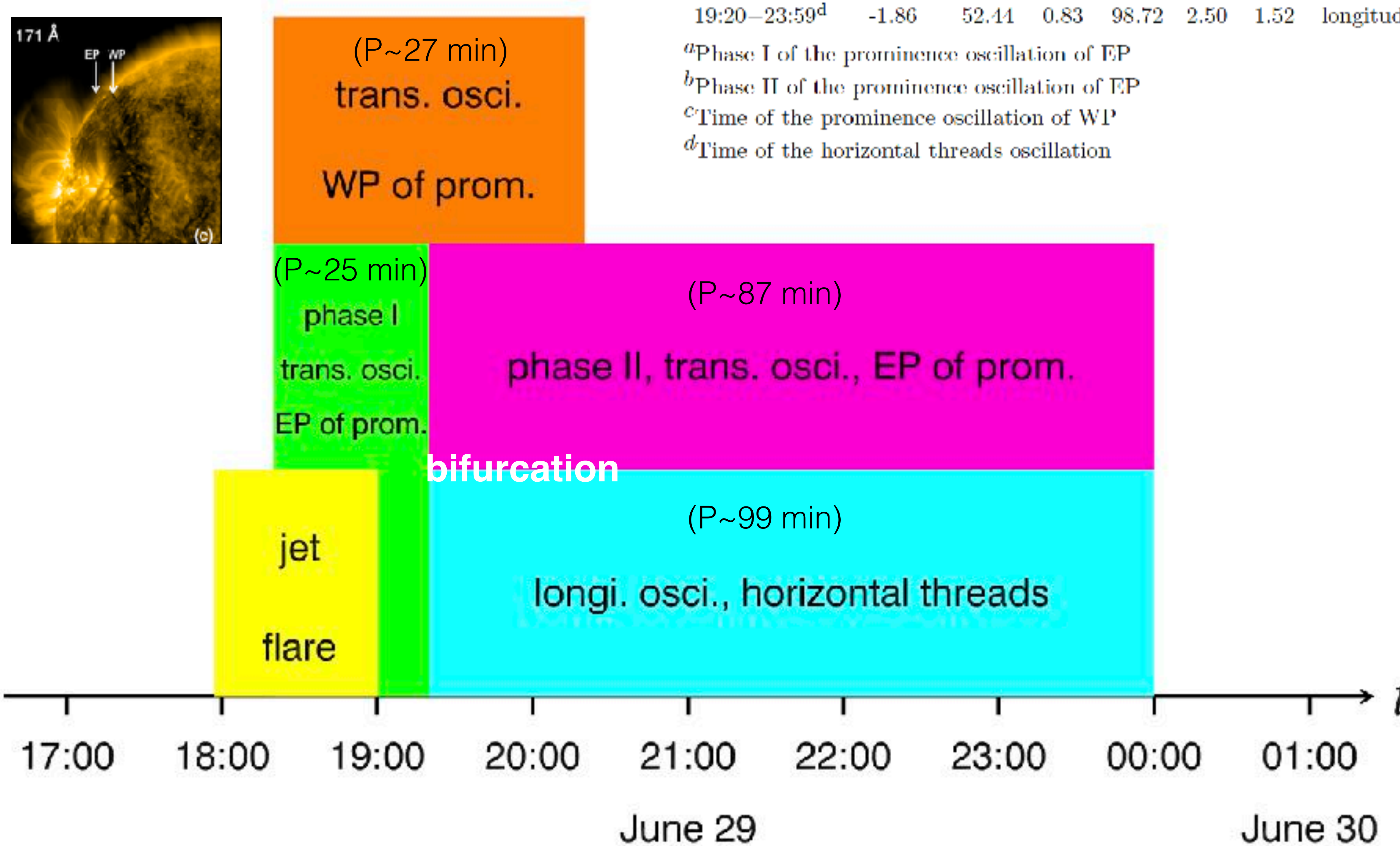

How are the prominence oscillations triggered?

1. **sub-flare, microflare near filament** (Jing et al. 2003; Vrsnak et al. 2007; Li & Zhang 2012; Zhang et al. 2012; Zhang et al. 2017)
2. **episodic jets** (Luna et al. 2014)
3. **shock** (Shen et al. 2014; Pant et al. 2016)
4. **EUV wave, Moreton wave**

coronal jet from remote flare site

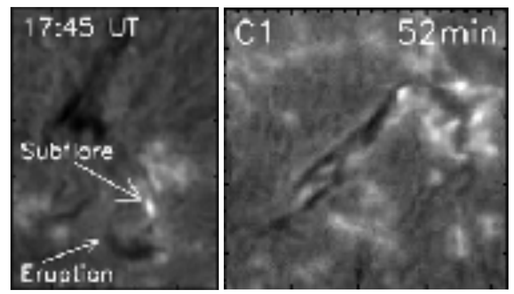

A. right direction
B. connection
C. enough power

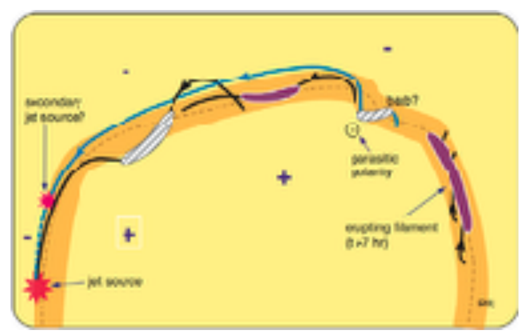

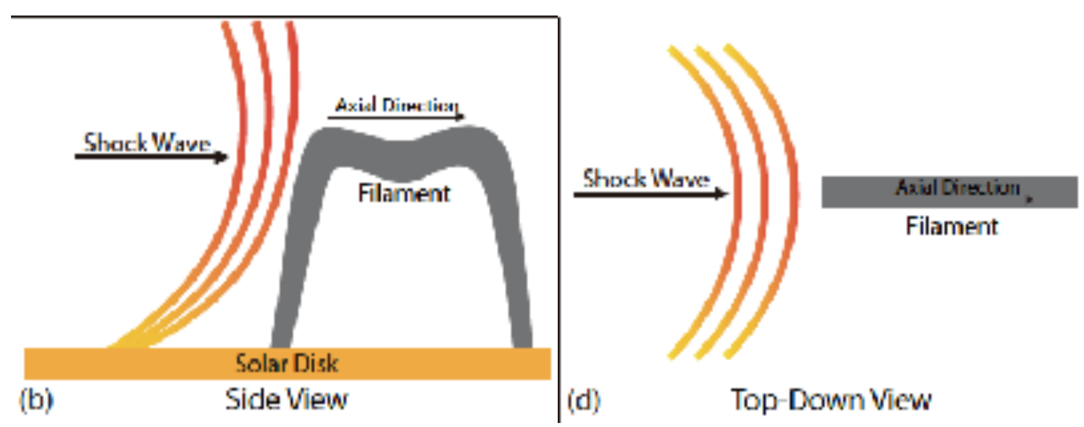

What is the role of bifurcation?

1. transfer of mass from EP to horizontal threads
2. start of longitudinal oscillation
3. change of magnetic configuration
4. change of period

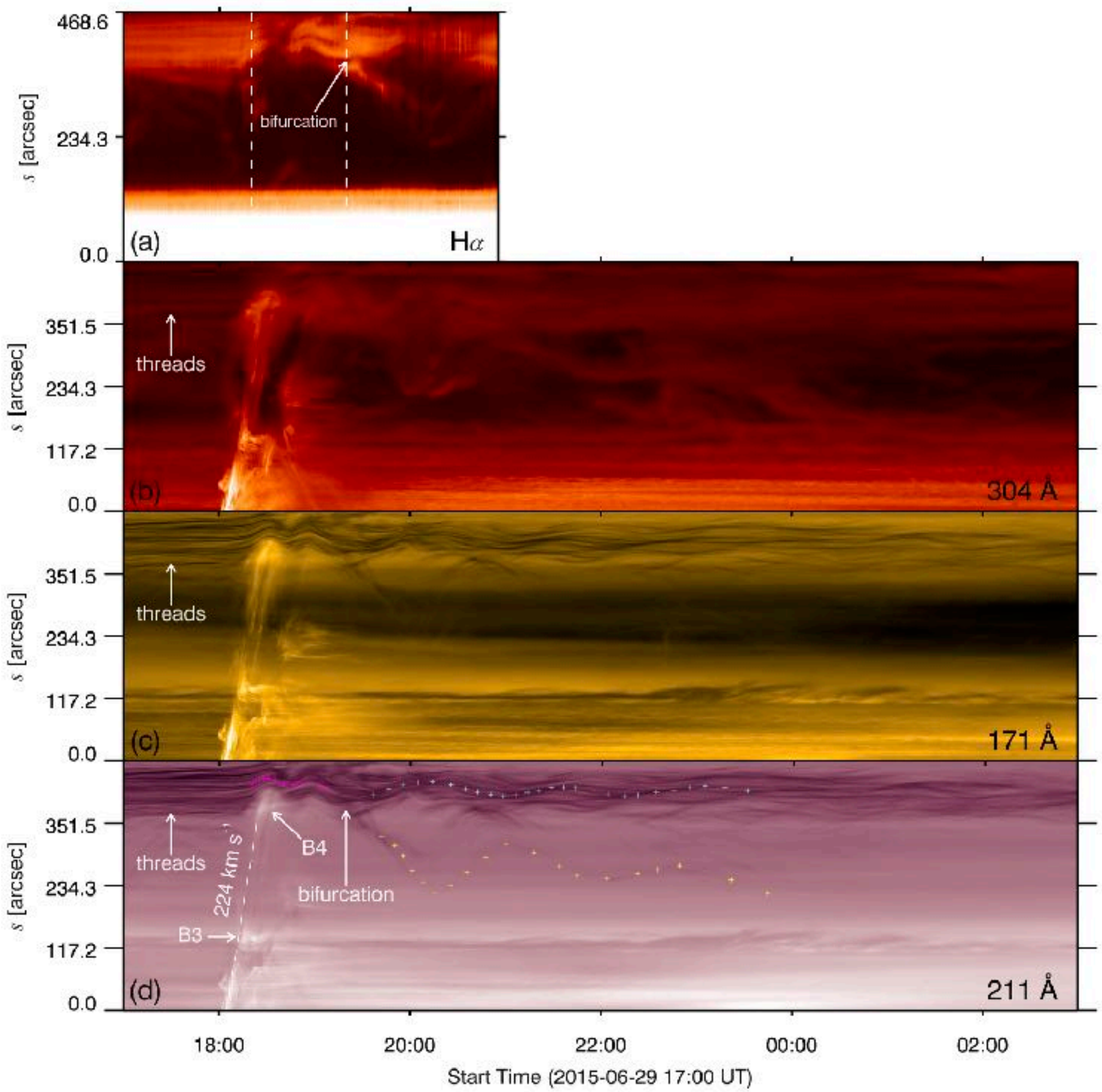

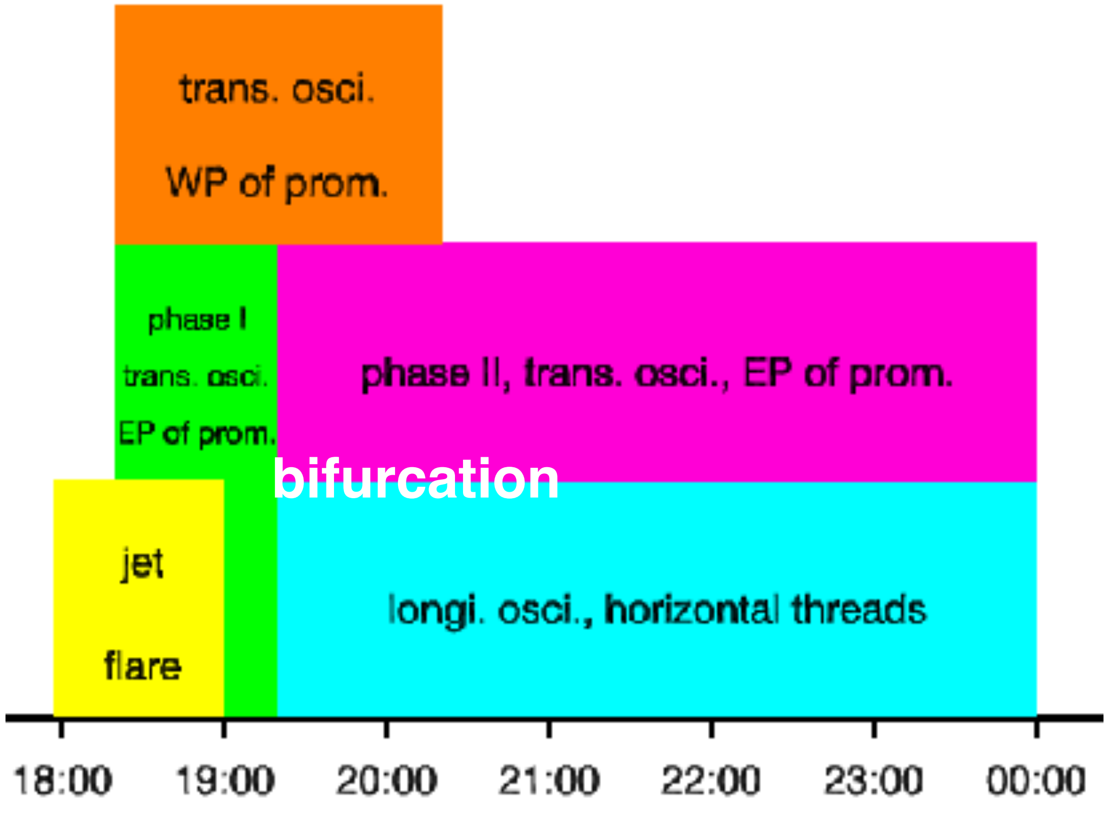

prominence seismology: diagnostic of R, B_{tr}

longitudinal oscillation: $P = 2\pi\sqrt{R/g_\odot}$

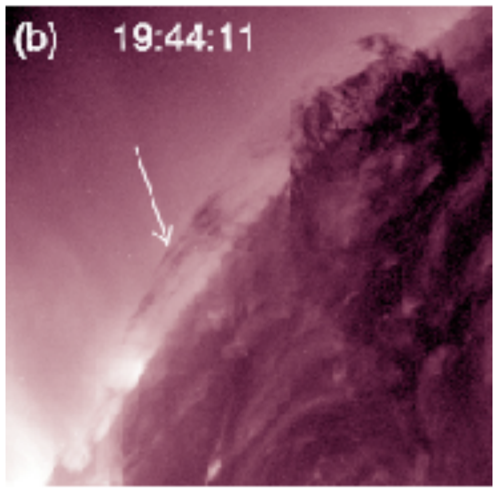

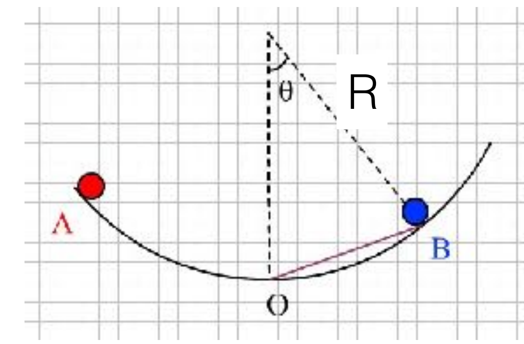

~99 min
(~1.65 hr)

~244 Mm
~R_s/4

$B_{tr}[\mathrm{G}] \geq 17 P[\mathrm{hr}]$

$B_{tr} \geq 28\ \mathrm{G}$

Part 5

Vertical Oscillation of a Coronal Cavity Triggered by an EUV Wave

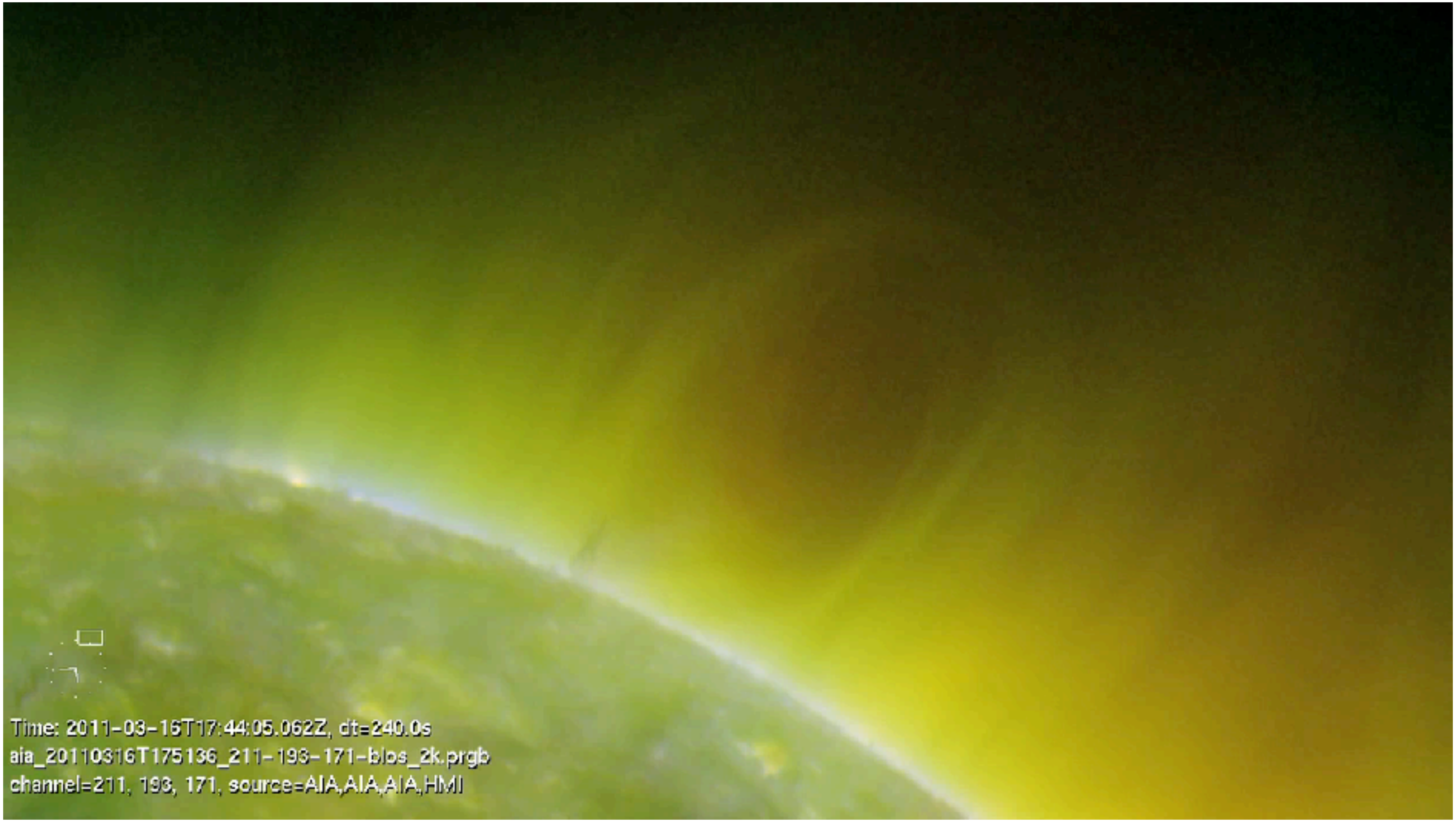

Part 5

Vertical Oscillation of a Coronal Cavity Triggered by an EUV Wave

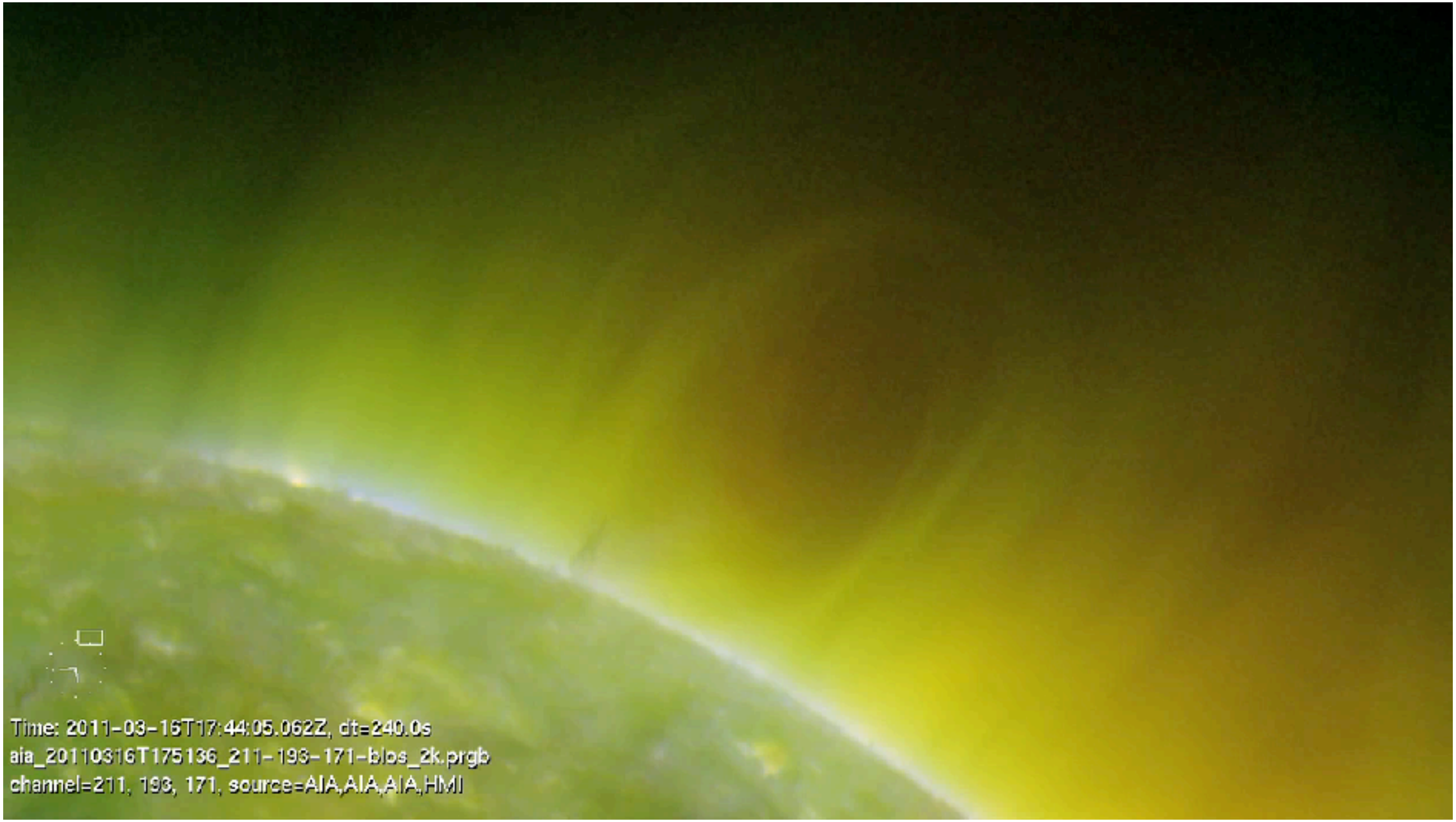

Part 5

Vertical Oscillation of a Coronal Cavity Triggered by an EUV Wave

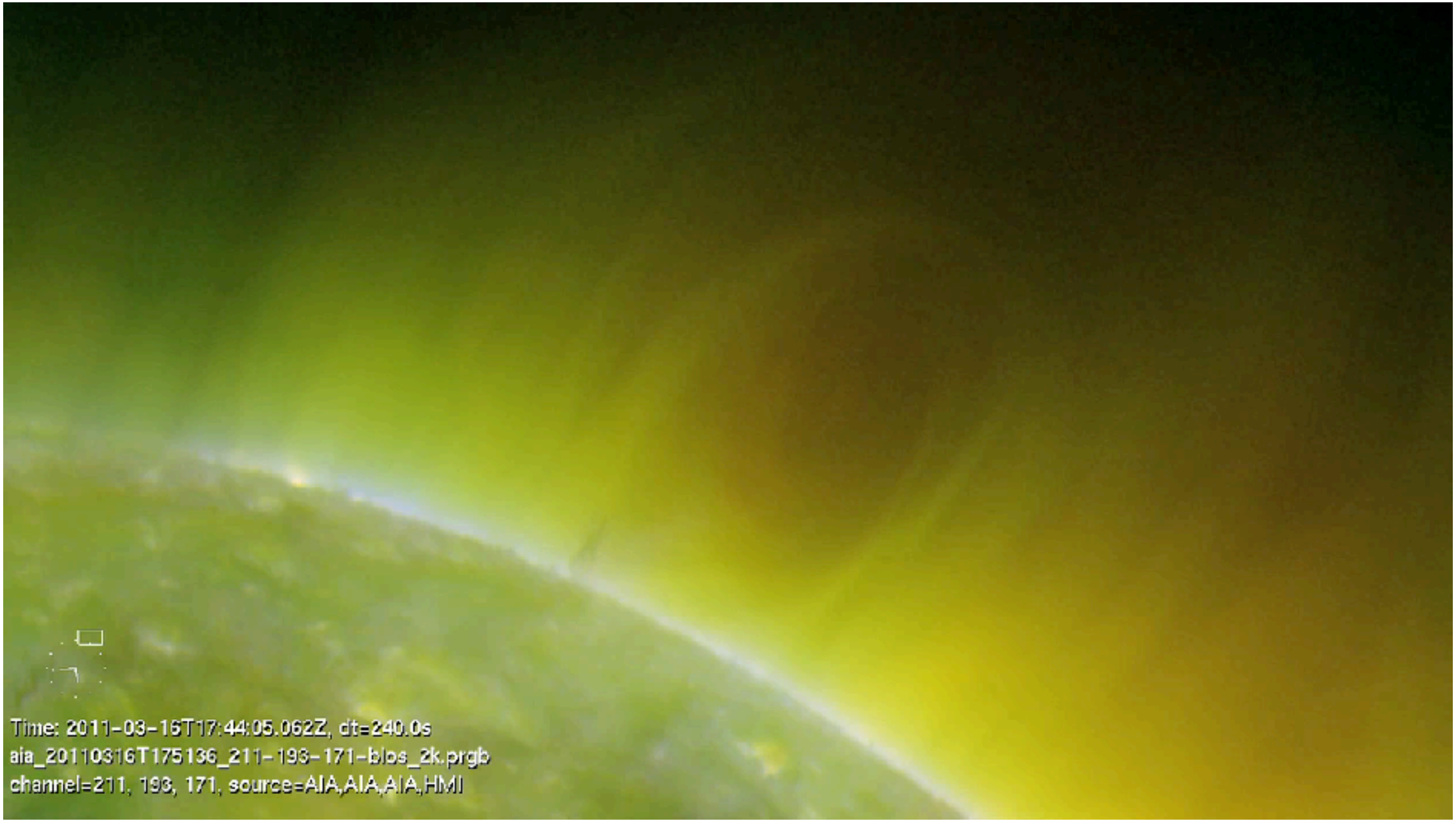

What happens when an EUV wave encounters a cavity?

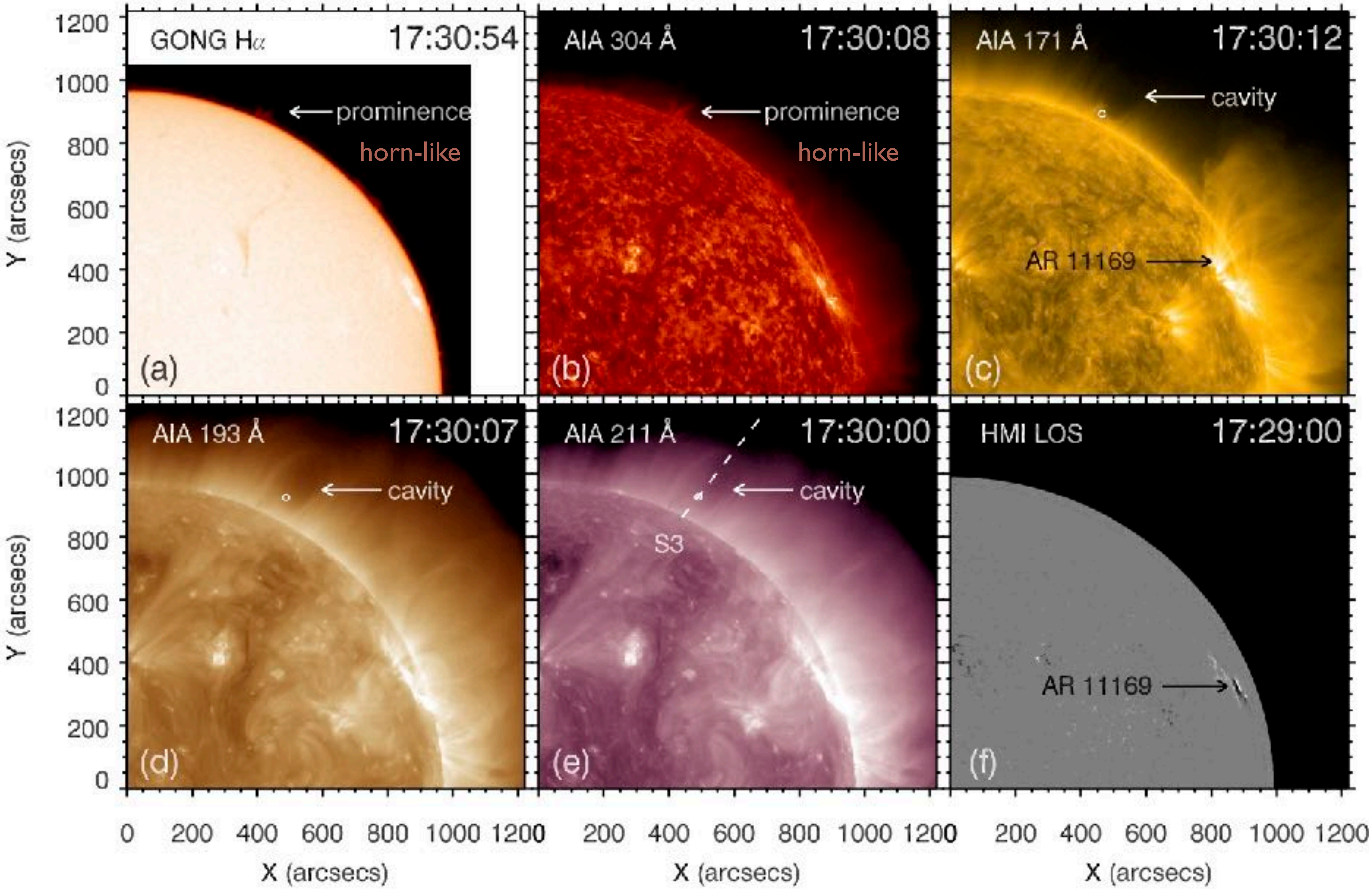
GONG Hα
17:30:54
prominence
horn-like
(a)
AIA 304 Å
17:30:08
prominence
horn-like
(b)
AIA 171 Å
17:30:12
cavity
AR 11169
(c)
AIA 193 Å
17:30:07
cavity
(d)
AIA 211 Å
17:30:00
cavity
S3
(e)
HMI LOS
17:29:00
AR 11169
(f)
Y (arcsecs)
X (arcsecs)
0
200
400
600
800
1000
1200

Height-time plot of CME and light curves of the flare in AR 11169

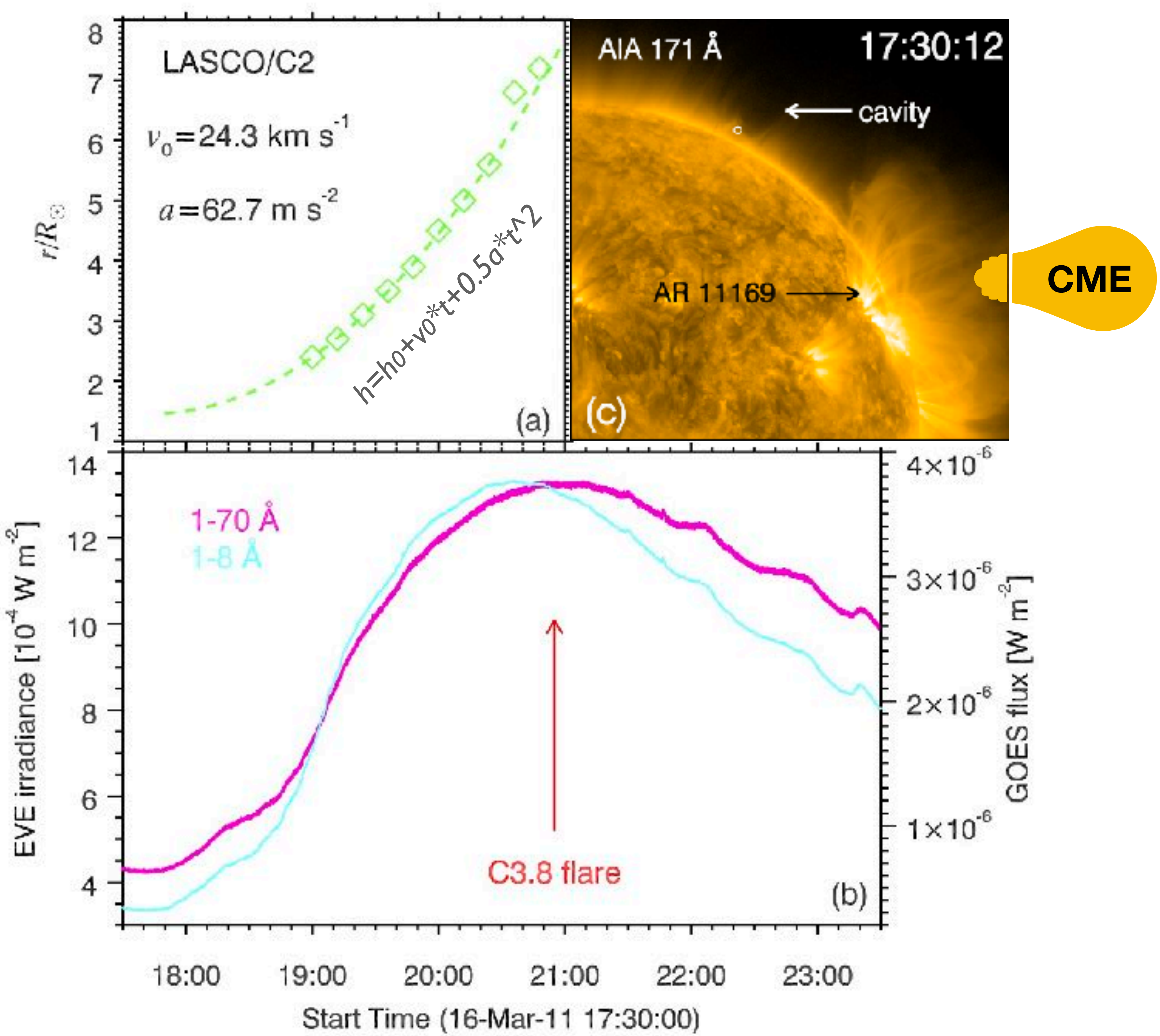

Ha and EUV images near flare peak time (~21:00 UT)

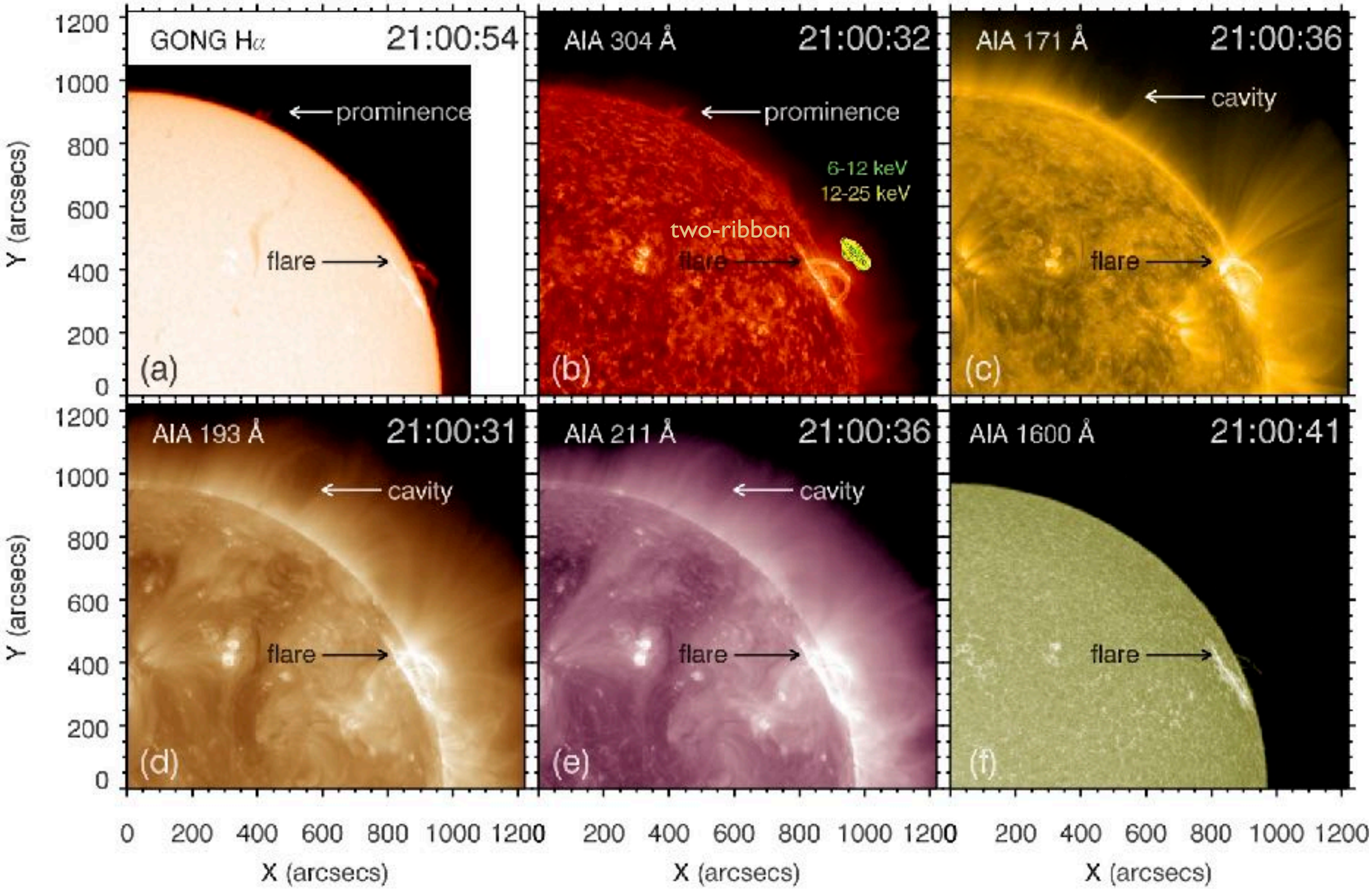

partial halo CME observed by LASCO/C2 and STA/COR1

velocity: 682 km/s
central position angle: 268\deg
angular width: 184\deg

three-part structure

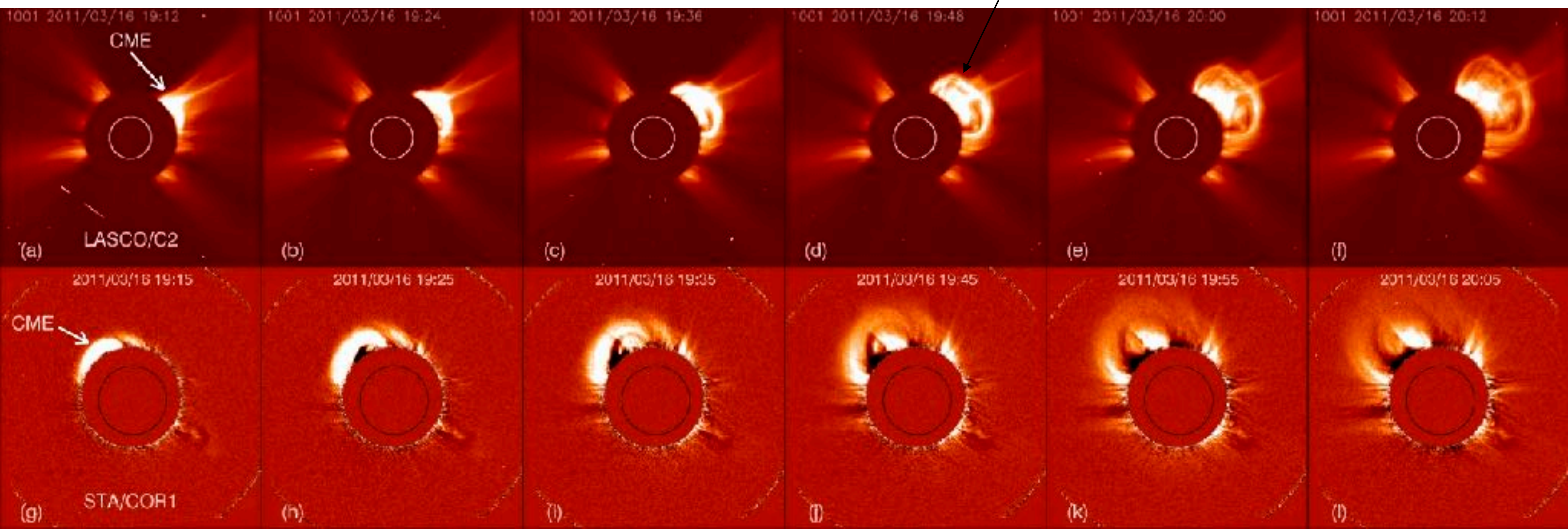

Base-differences images in AIA 171 A

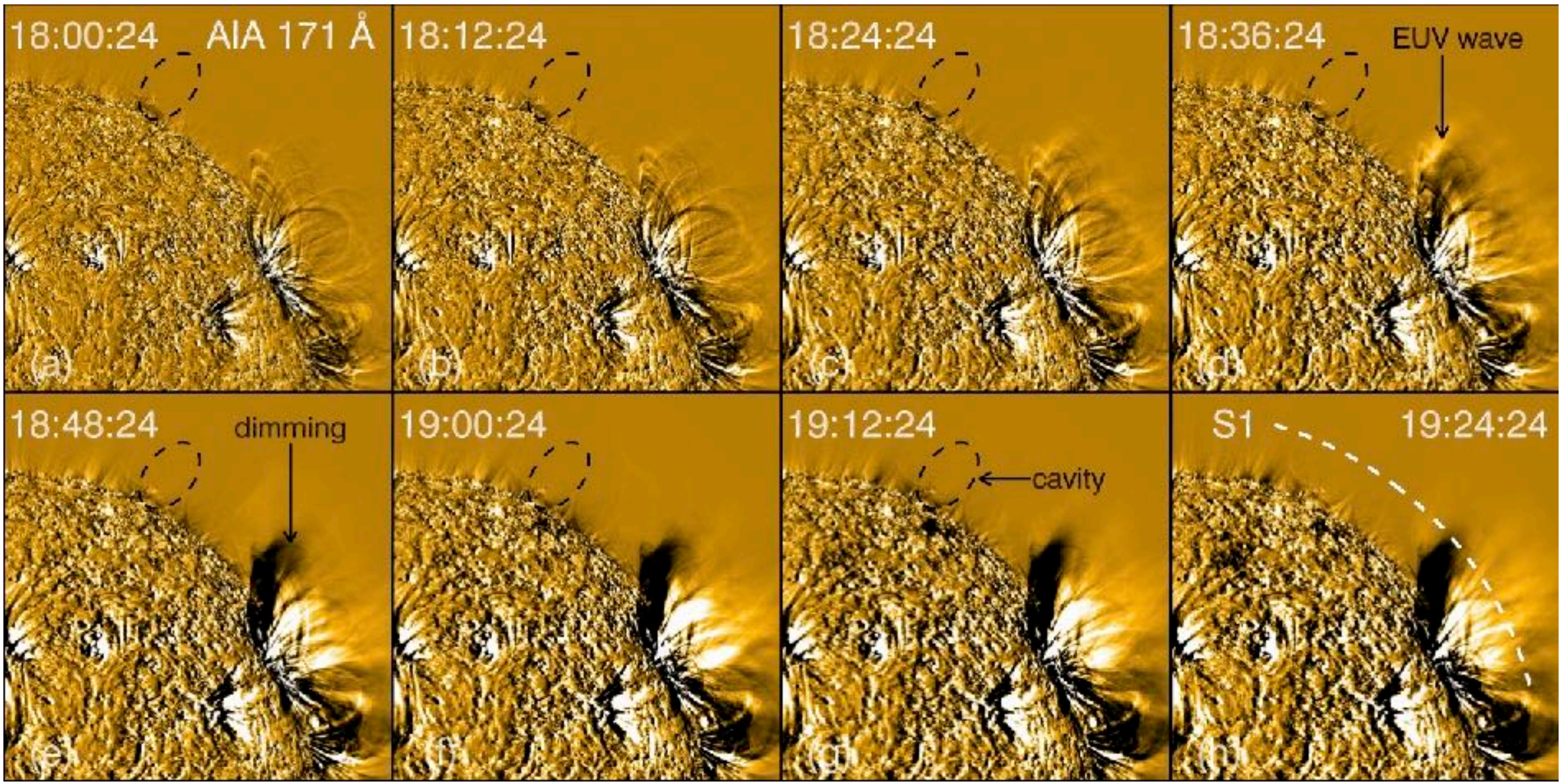

Time-slice diagrams along S1

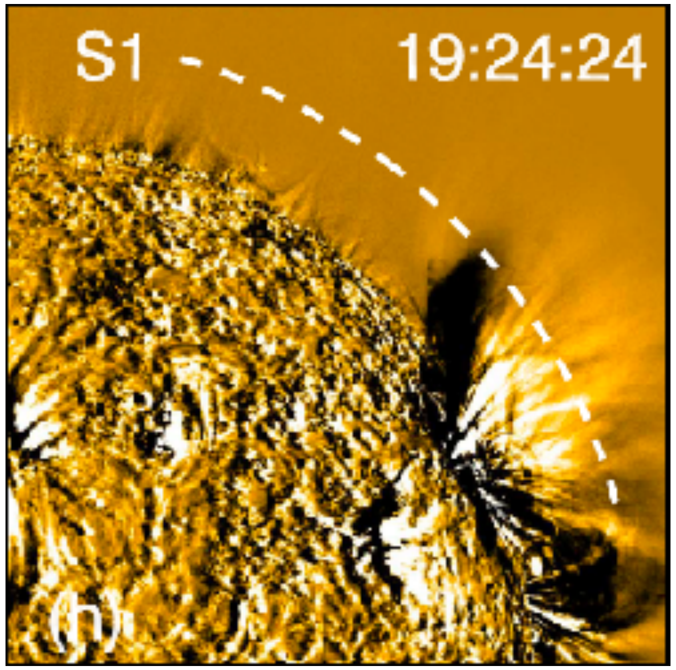

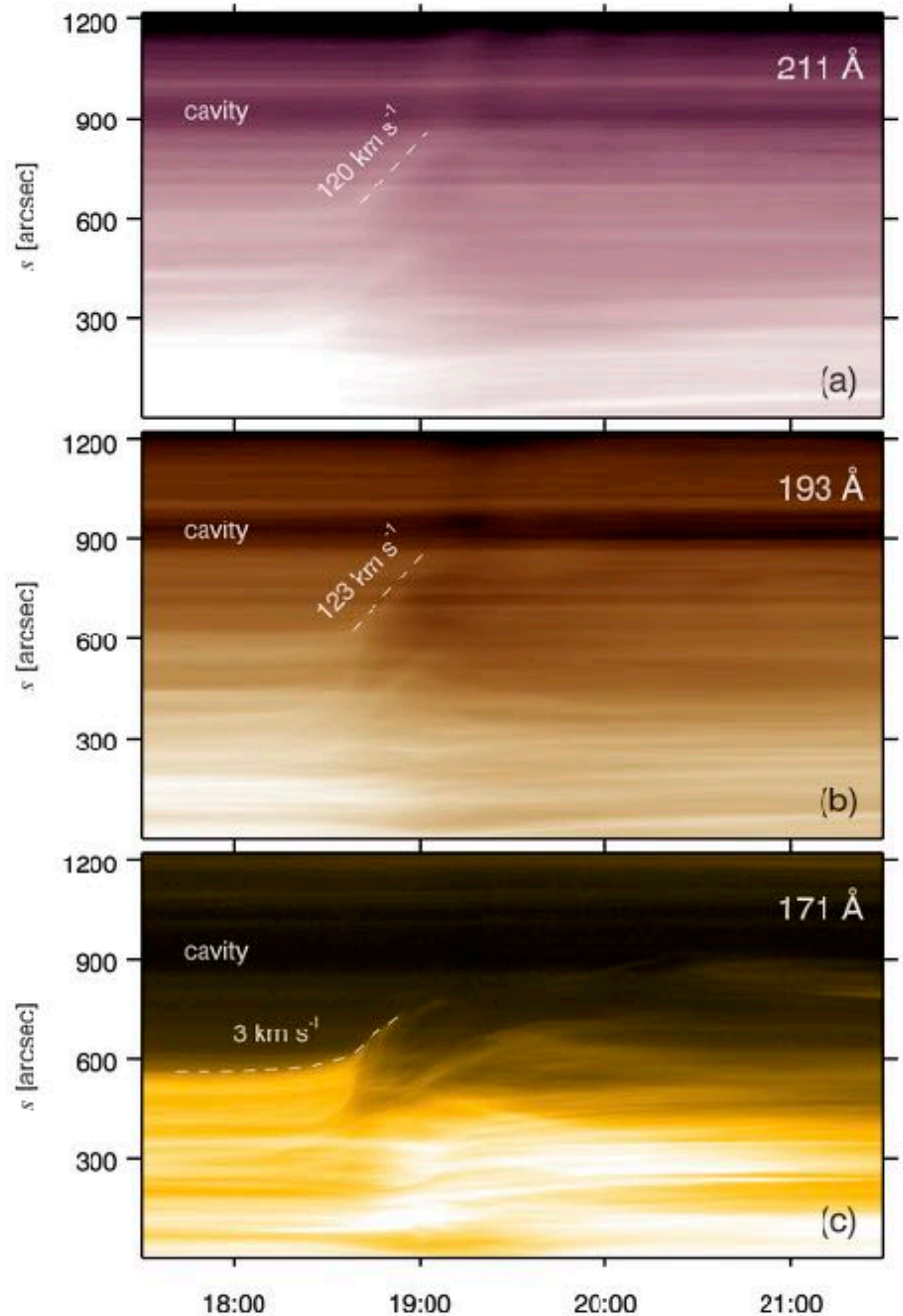

Base-differences images in EUVI 195 A

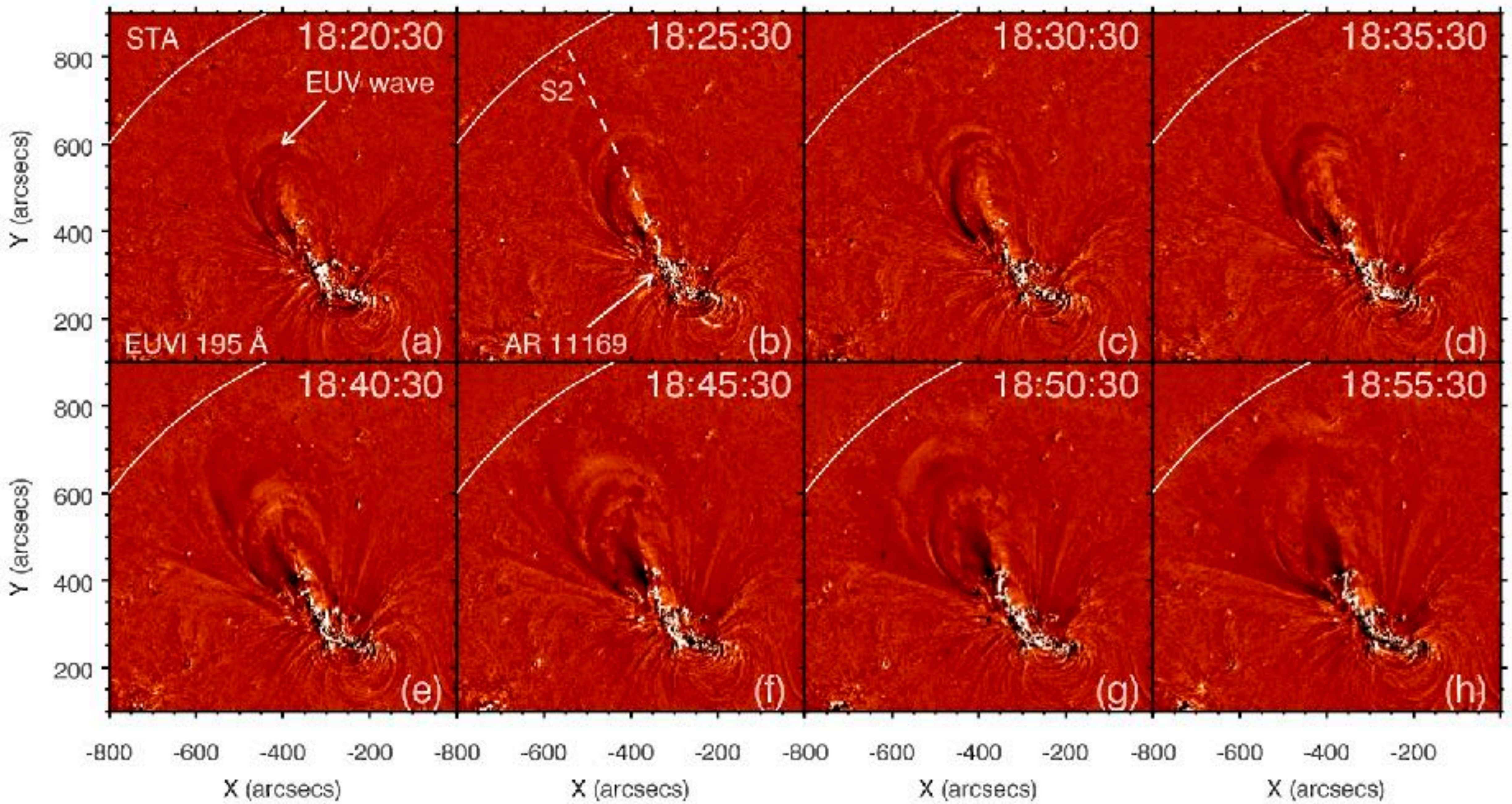

Time-slice diagrams along S2

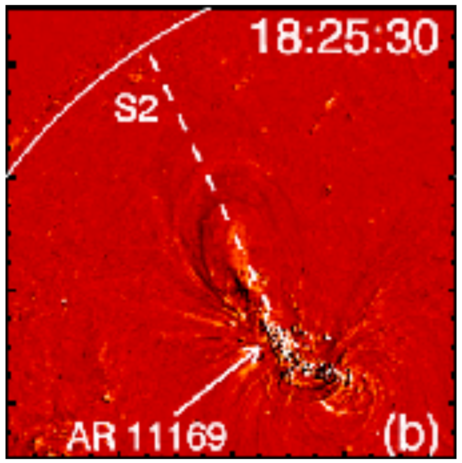

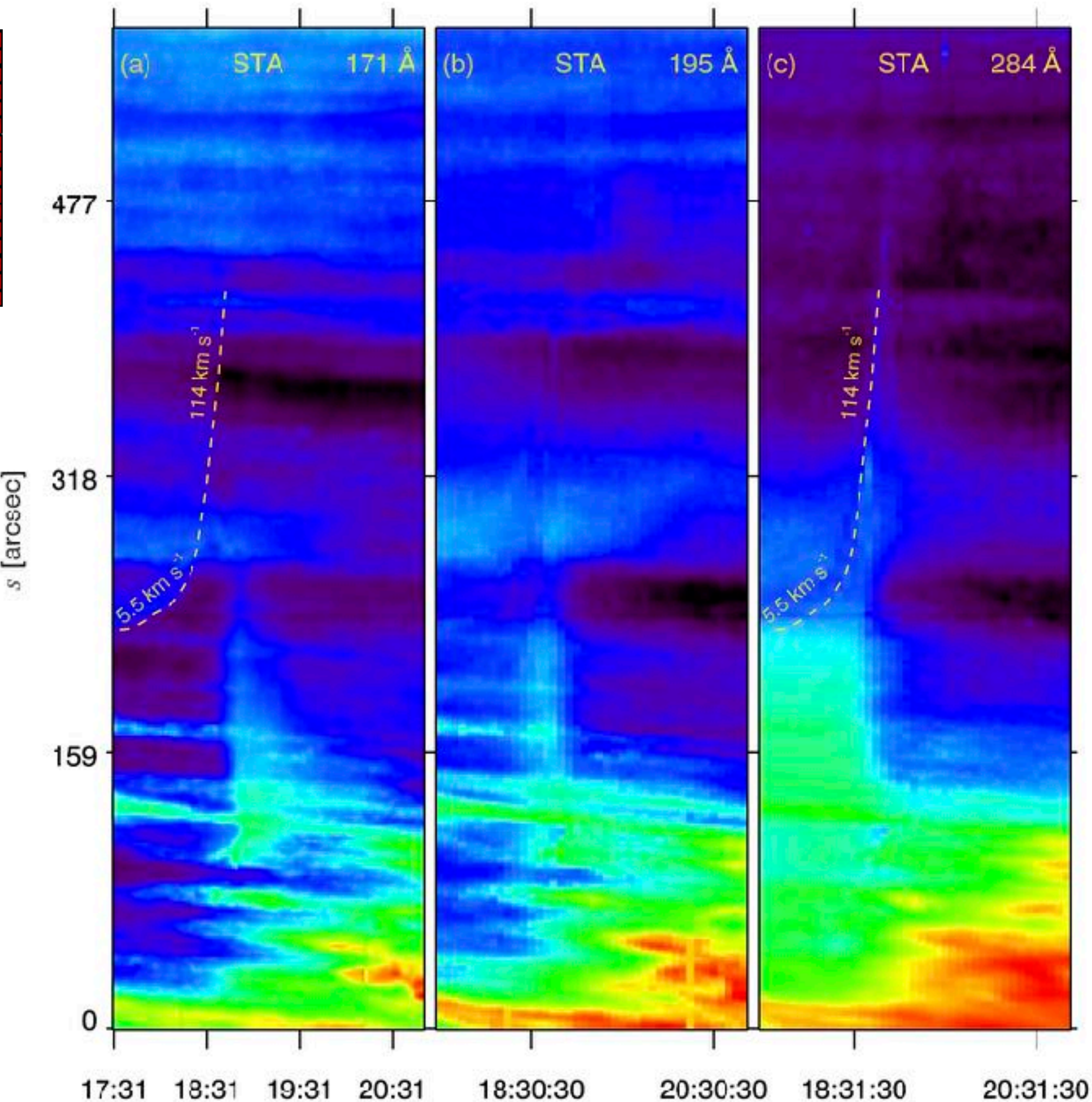

Time-slice diagrams along S3

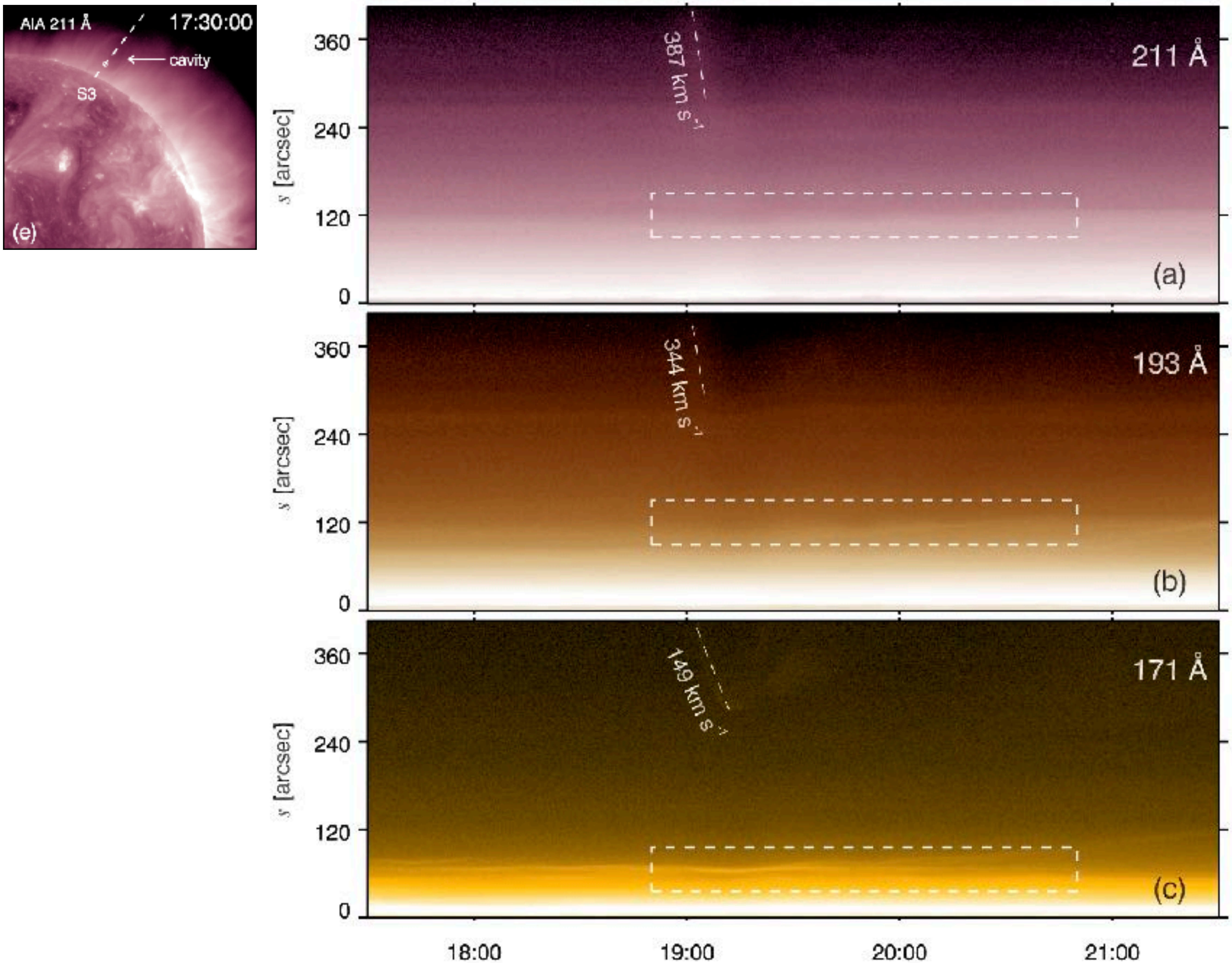

closeup of the time-slice diagrams within the boxes

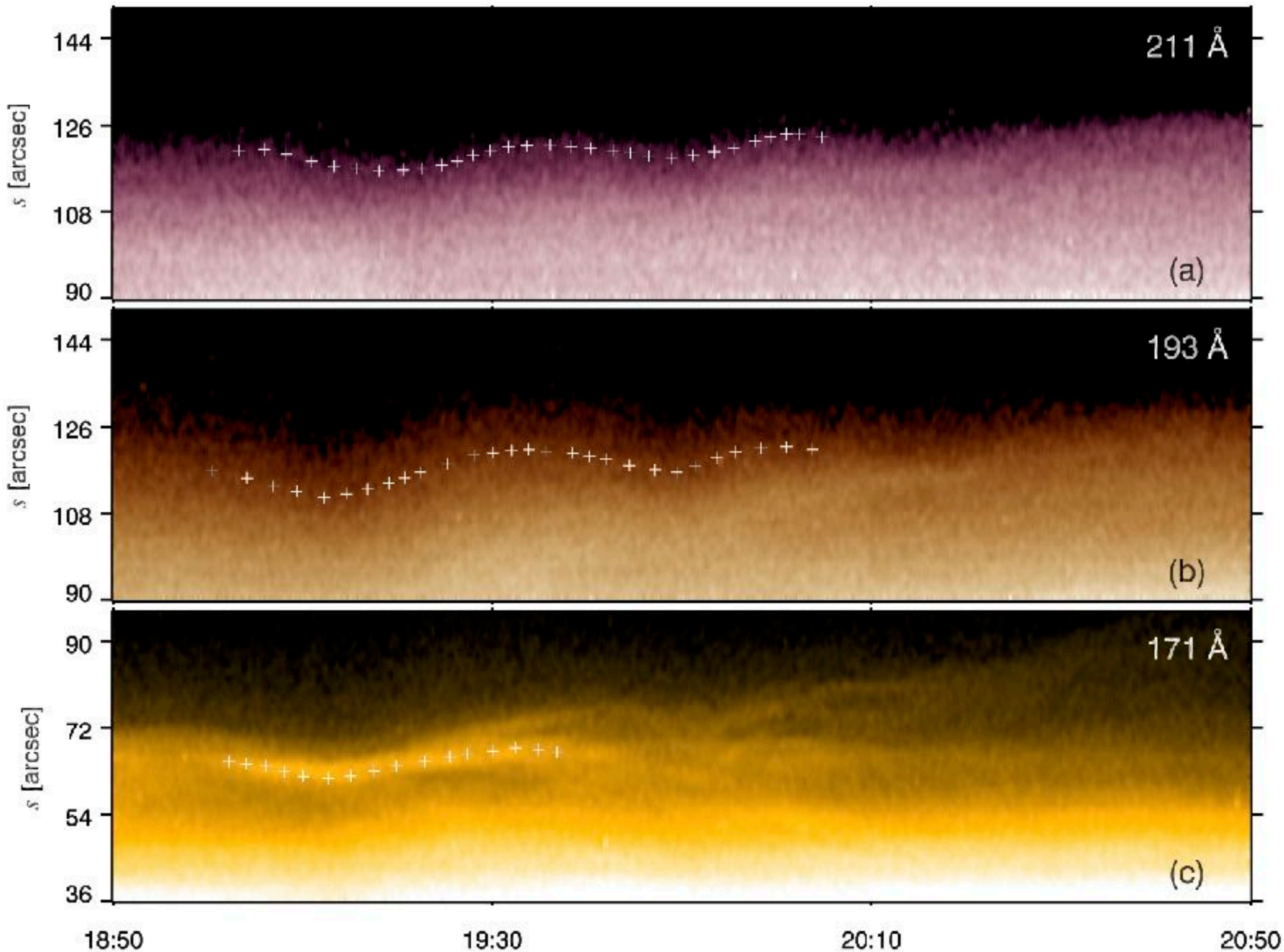

results of curve fitting $y = y_0 + bt + A_0 \sin(\frac{2\pi}{P}t + \phi_0)e^{\ t/\tau}$

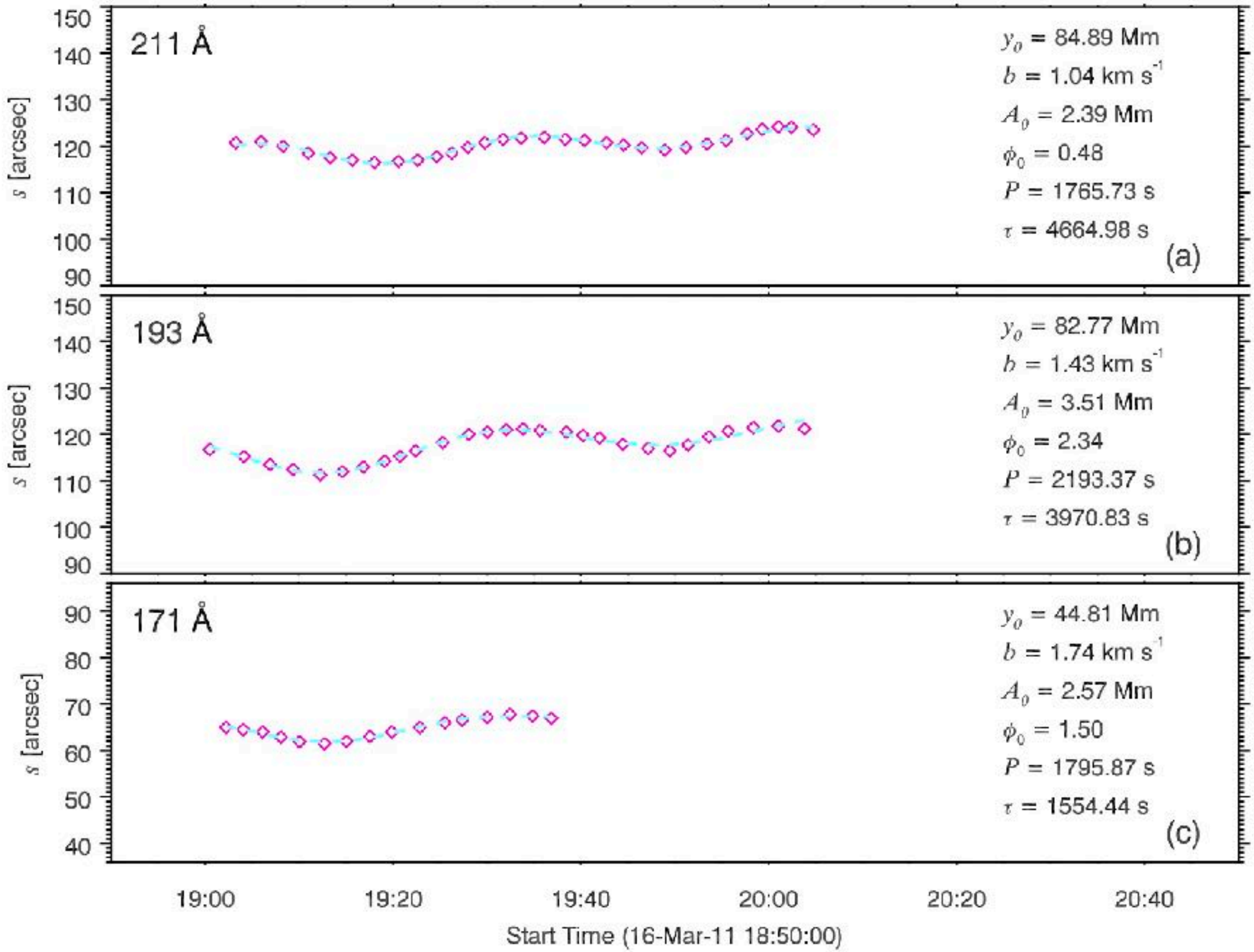

$$y = y_0 + bt + A_0 \sin(\frac{2\pi}{P}t + \phi_0)e^{-t/\tau}$$

Table 2. Fitted parameters of the vertical oscillation

λ (Å)	y_0 (Mm)	b (km s^{-1})	A_0 (Mm)	ϕ_0 (rad)	P (min)	τ (min)
211	84.89	1.04	2.39	0.48	29.4	77.8
193	82.77	1.43	3.51	2.34	36.6	66.2
171	44.81	1.74	2.57	1.50	29.9	25.9

velocity of the oscillation $v=ds/dt$

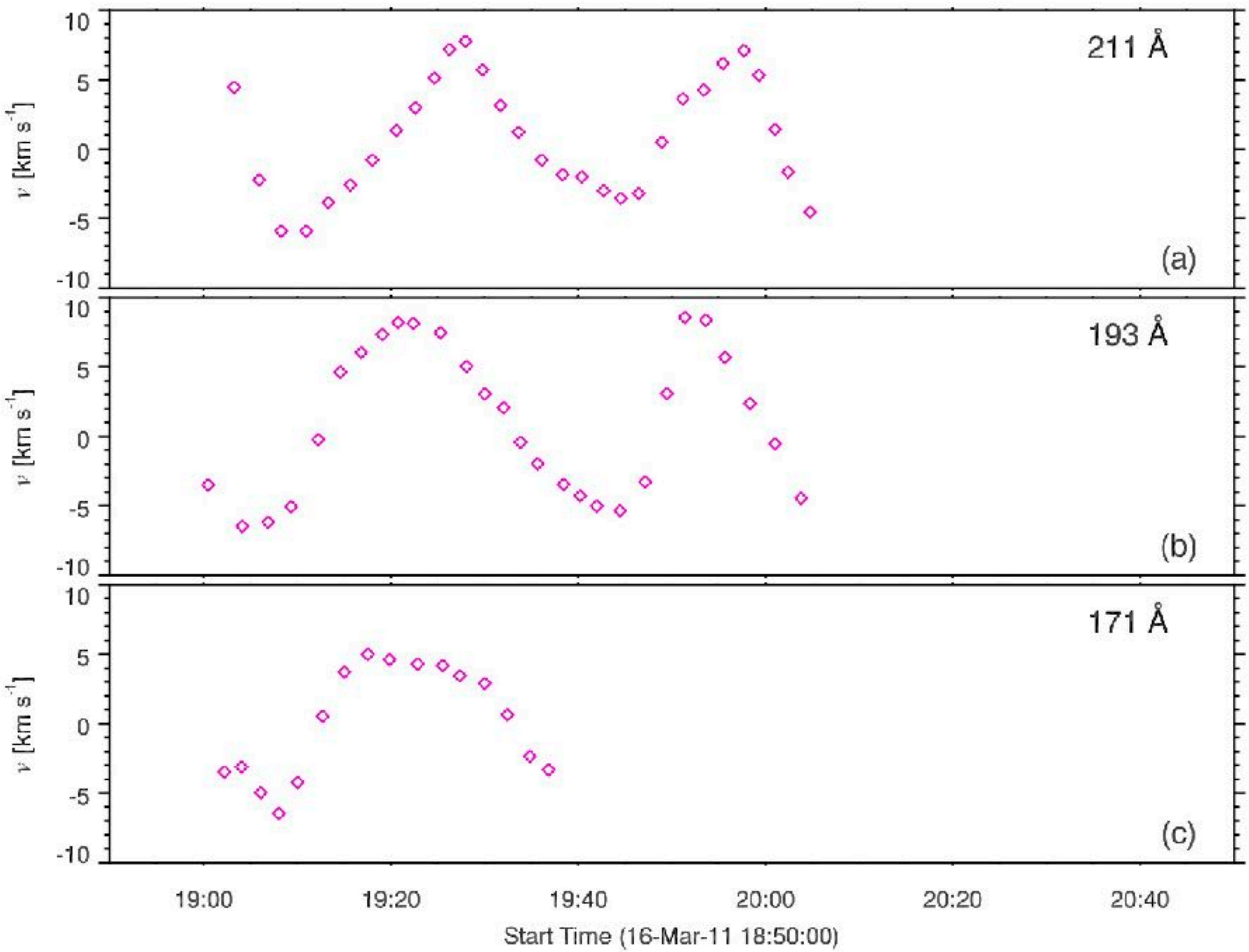

How is the oscillation triggered?

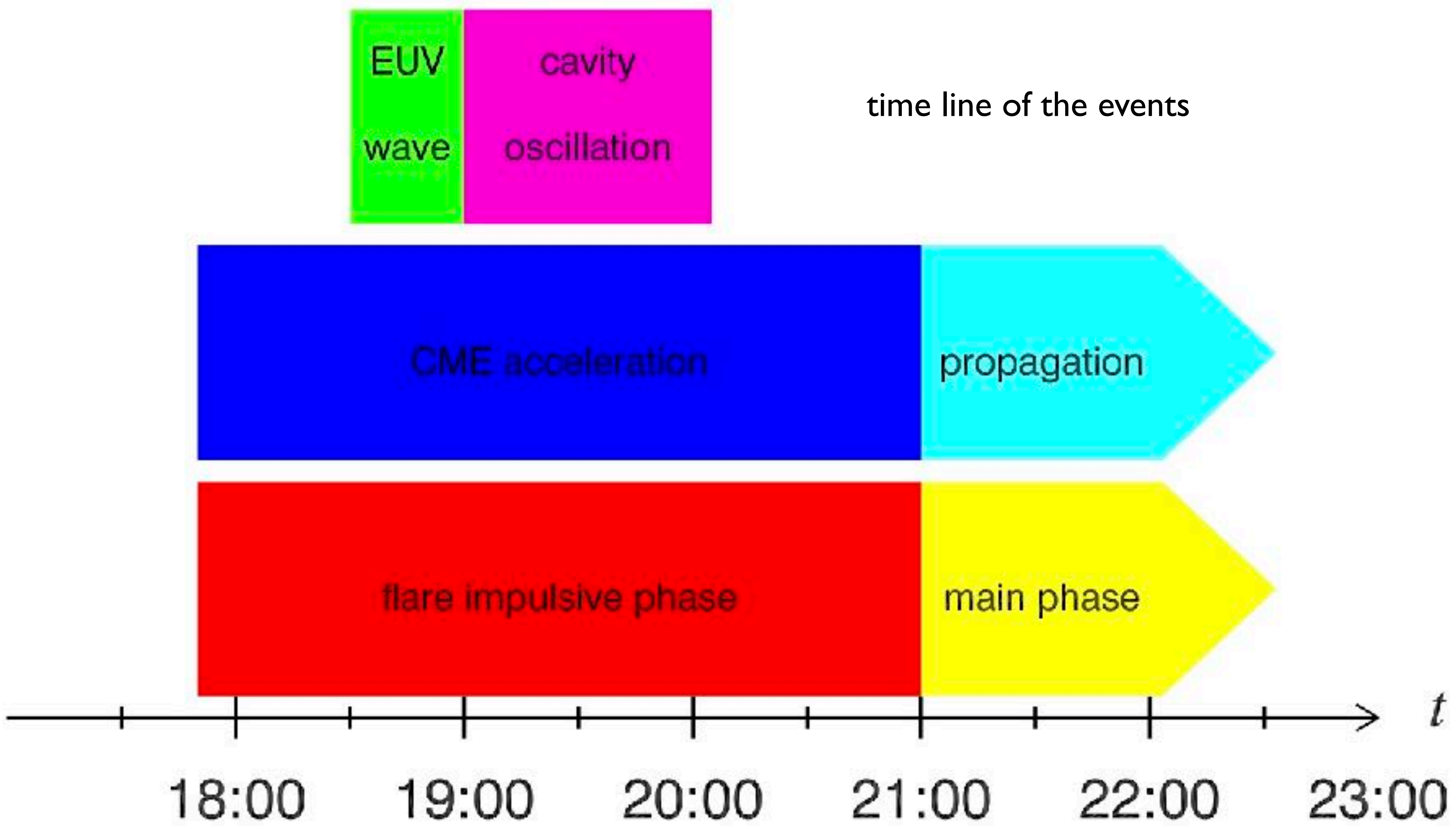

time line of the events

What is the difference?

Liu et al. 2012

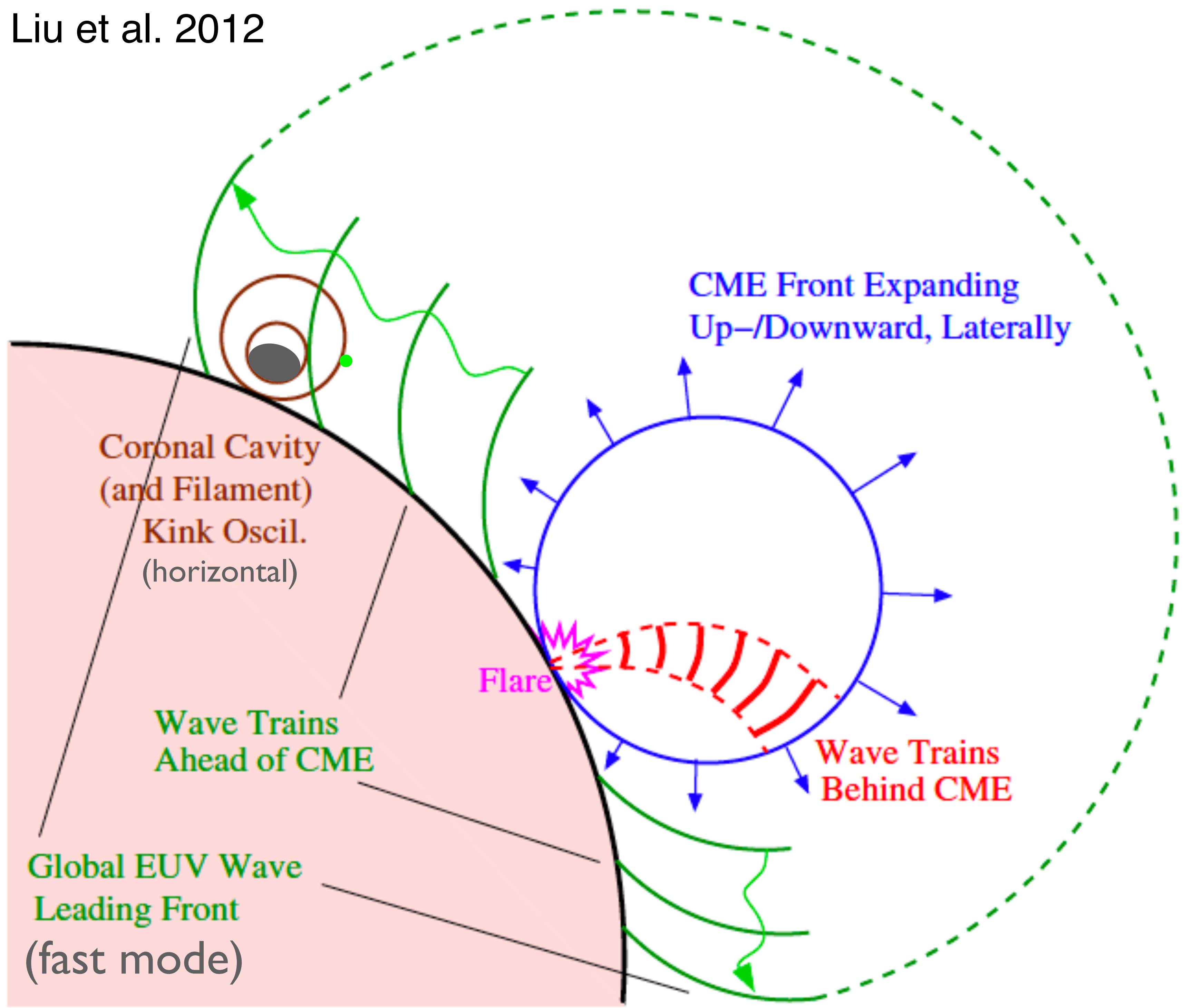

schematic cartoon

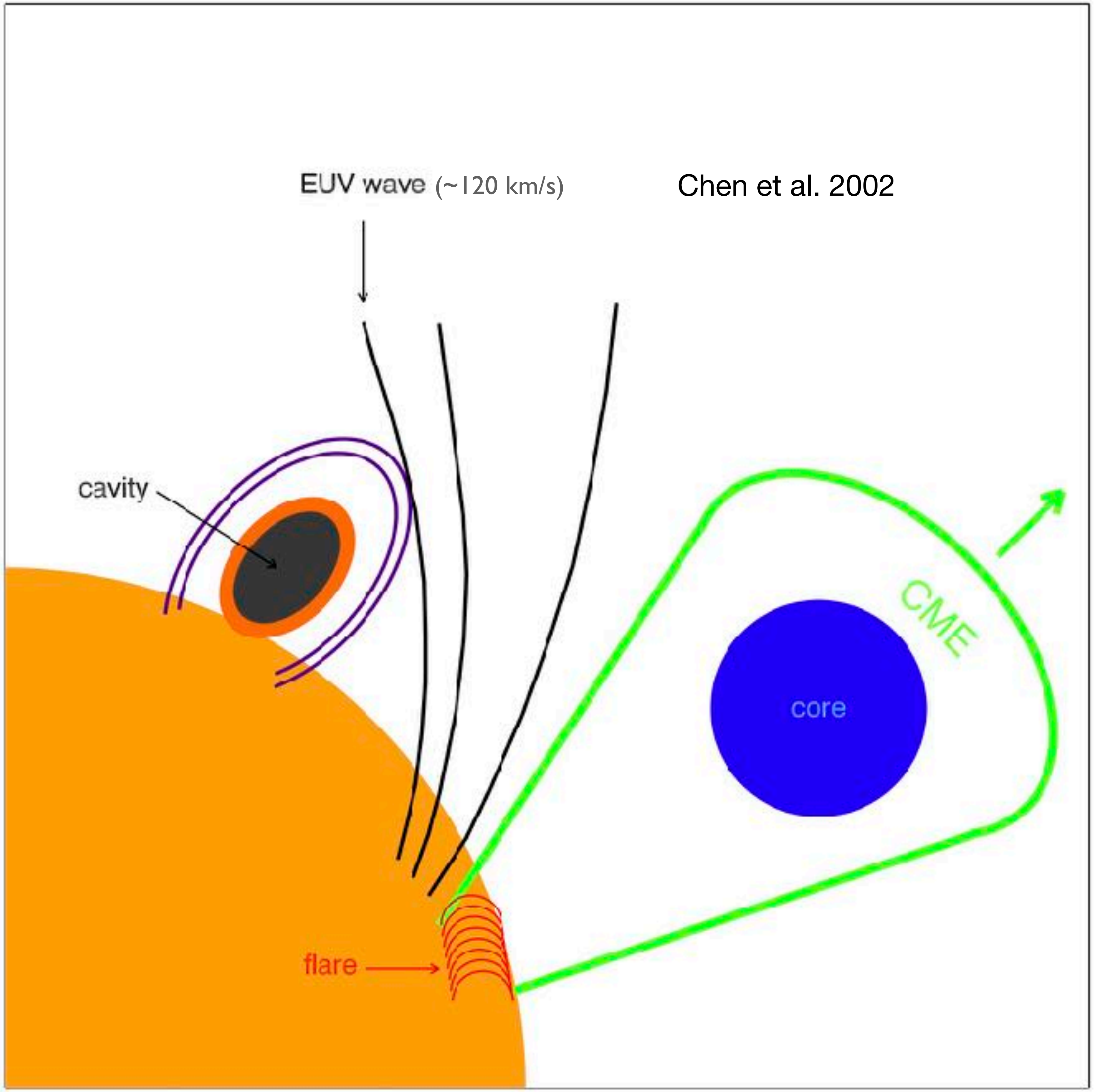

schematic cartoon

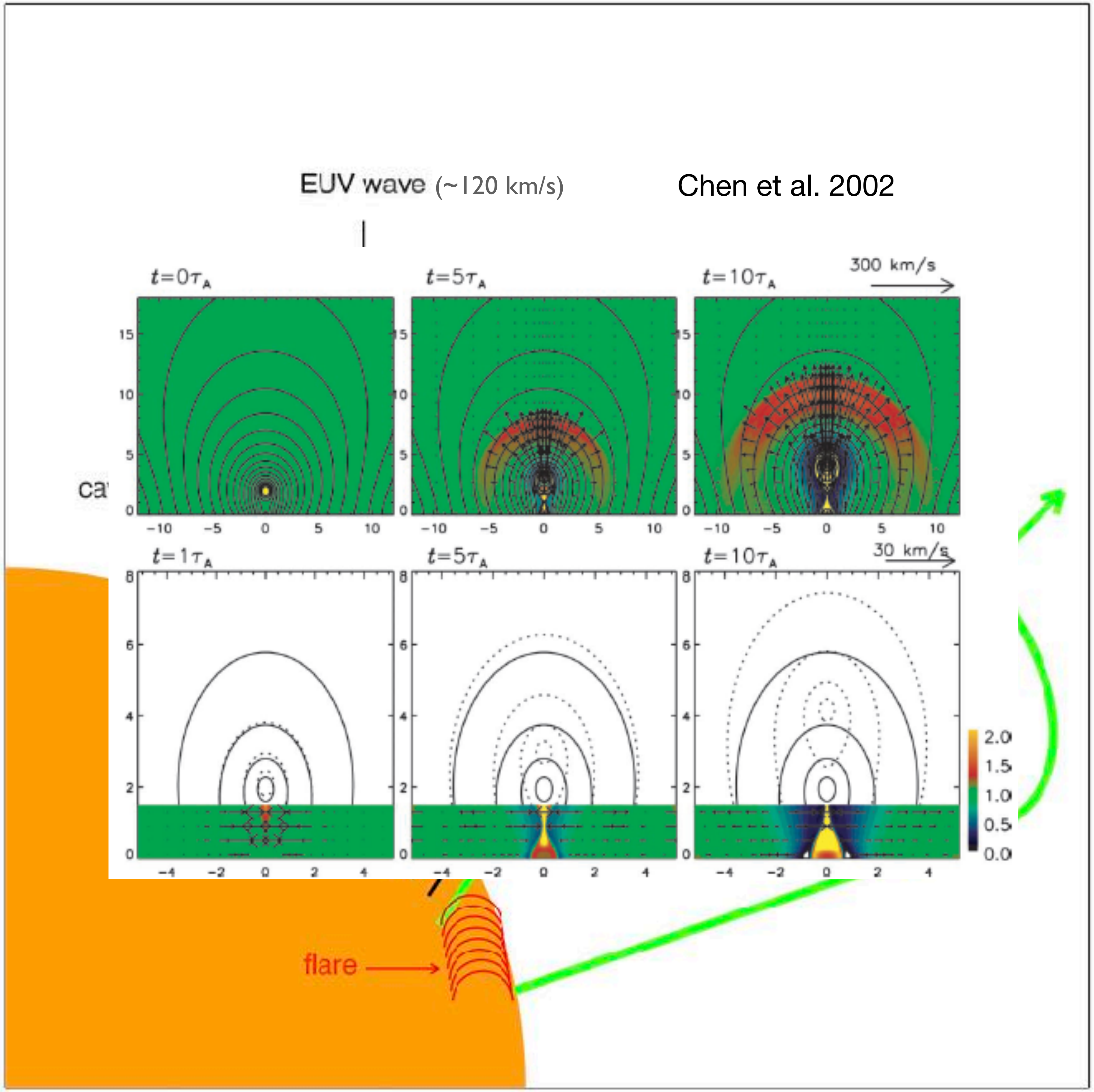

What is the magnetic field strength of the cavity?

cavity: global vertical oscillation of a fast kink mode

$$B_c = 2L_c\sqrt{4\pi\rho_c}/P,$$ (Zhou et al. 2016)

~30 min (table 2)

$$\rho_c = 1.67 \times 10^{-16} \text{ g cm}^{-3}$$

(Fuller & Gibson 2009)

0.06-2.9 Rs

(Karna et al. 2015)

What is the magnetic field strength of the cavity?

cavity: global vertical oscillation of a fast kink mode

$$B_c = 2L_c\sqrt{4\pi\rho_c}/P,$$ (Zhou et al. 2016)

B_c → 0.2-10 G

L_c → 0.06-2.9 Rs (Karna et al. 2015)

ρ_c → $\rho_c = 1.67 \times 10^{-16}$ g cm^{-3} (Fuller & Gibson 2009)

P → ~30 min (table 2)

What is the magnetic field strength of the cavity?

$$B_r^2 = \pi \rho_p r_0^2 (4\pi^2 P^{-2} + \tau^{-2})$$ (Hyder 1966)

$$\rho_p = 4 \times 10^{-14} \text{ g cm}^{-3}$$

$$r_0 = 3 \times 10^9 \text{ cm}$$

$$B_r^2 = 4.8 \times 10^{-12} r_0^2 (P^{-2} + 0.025\tau^{-2})$$ (Shen et al. 2017)

25.9 min (table 2)

~30 min (table 2)

What is the magnetic field strength of the cavity?

$$B_r^2 = \pi \rho_p r_0^2 (4\pi^2 P^{-2} + \tau^{-2})$$ (Hyder 1966)

$$\rho_p = 4 \times 10^{-14}\ \mathrm{g\ cm^{-3}}$$

$$r_0 = 3 \times 10^9\ \mathrm{cm}$$

$$B_r^2 = 4.8 \times 10^{-12} r_0^2 (P^{-2} + 0.025\tau^{-2})$$ (Shen et al. 2017)

3.8 G

~30 min (table 2)

25.9 min (table 2)

What is the magnetic field strength of the cavity?

$$B_r^2 = \pi \rho_p r_0^2 (4\pi^2 P^{-2} + \tau^{-2})$$ (Hyder 1966)

$$\rho_p = 4 \times 10^{-14} \text{ g cm}^{-3}$$

$$r_0 = 3 \times 10^9 \text{ cm}$$

$$B_r^2 = 4.8 \times 10^{-12} r_0^2 (P^{-2} + 0.025\tau^{-2})$$ (Shen et al. 2017)

3.8 G

~30 min (table 2)

25.9 min (table 2)

in brief: a few G, less than 10 G

key points

longitudinal oscillation

- trigger: velocity perturbation, micro-flares, coronal jet (Part 2, 4)
- restoring force: gravity along the dip, R (Part 2)
- damping mechanism: radiative loss, A_0 (Part 2)
- mass drainage plays an important role (Part 2, 3)

complex behavior of oscillation

- growing & damping amplitudes, implying thread-thread interaction (Part 3)
- simultaneous longitudinal & transverse oscillations (Part 4)

prominence seismology

- curvature radius of the magnetic dip (Part 3, 4)
- magnetic field strength of filament (Part 3, 4)
- magnetic field strength of cavity (Part 5)

EUV wave — filament interaction

- horizontal oscillation when interacting sideways
- vertical oscillation when interacting from the top

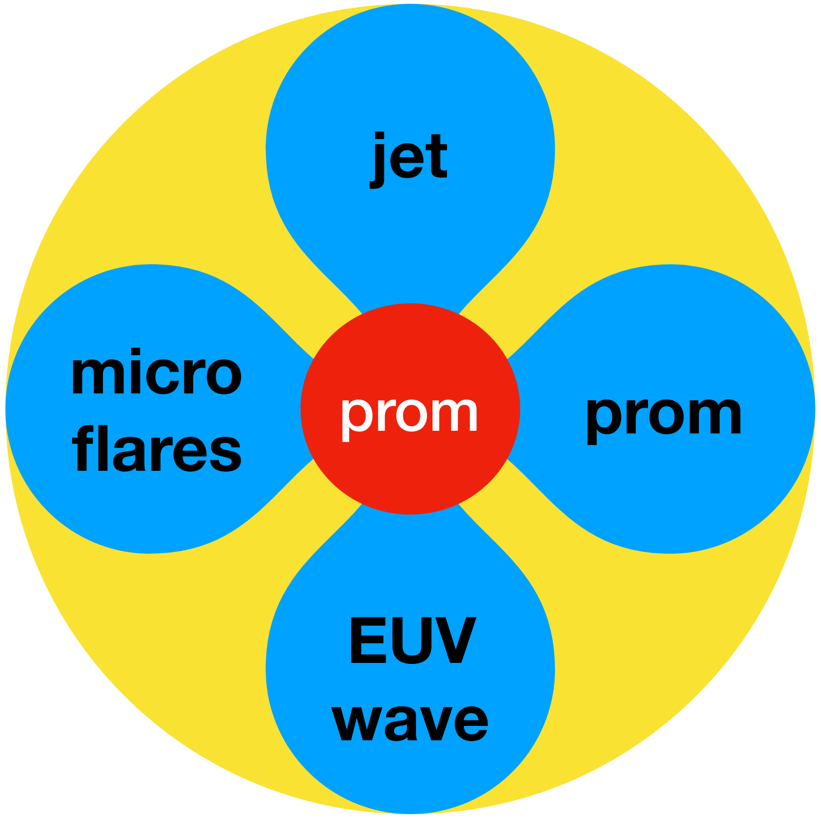

outlook

1. relationship between prominence oscillation and eruption
2. relationship between magnetic configuration and oscillation mode
3. relationship between perturbation and oscillation mode
4. causes of damping & growing amplitudes
5. prominence seismology: diagnostics with better accuracy
6. numerical simulations of interaction between filaments and jet, EUV wave
7. numerical simulations considering partial ionization

outlook

1. relationship between prominence oscillation and eruption
2. relationship between magnetic configuration and oscillation mode
3. relationship between perturbation and oscillation mode
4. causes of damping & growing amplitudes
5. prominence seismology: diagnostics with better accuracy
6. numerical simulations of interaction between filaments and jet, EUV wave
7. numerical simulations considering partial ionization